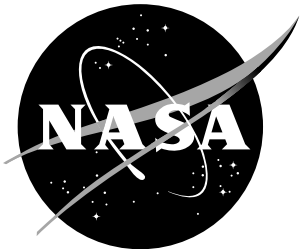


NASA/CR-1999-209002



Advanced Turbofan Duct Liner Concepts

*Gerald W. Bielak and John W. Premo
Boeing Commercial Airplane Group, Seattle, Washington*

*Alan S. Hersh
Hersh Acoustical Engineering, Inc., Westlake Village, California*

February 1999

The NASA STI Program Office ... in Profile

Since its founding, NASA has been dedicated to the advancement of aeronautics and space science. The NASA Scientific and Technical Information (STI) Program Office plays a key part in helping NASA maintain this important role.

The NASA STI Program Office is operated by Langley Research Center, the lead center for NASA's scientific and technical information. The NASA STI Program Office provides access to the NASA STI Database, the largest collection of aeronautical and space science STI in the world. The Program Office is also NASA's institutional mechanism for disseminating the results of its research and development activities. These results are published by NASA in the NASA STI Report Series, which includes the following report types:

- TECHNICAL PUBLICATION. Reports of completed research or a major significant phase of research that present the results of NASA programs and include extensive data or theoretical analysis. Includes compilations of significant scientific and technical data and information deemed to be of continuing reference value. NASA counterpart of peer-reviewed formal professional papers, but having less stringent limitations on manuscript length and extent of graphic presentations.
- TECHNICAL MEMORANDUM. Scientific and technical findings that are preliminary or of specialized interest, e.g., quick release reports, working papers, and bibliographies that contain minimal annotation. Does not contain extensive analysis.
- CONTRACTOR REPORT. Scientific and technical findings by NASA-sponsored contractors and grantees.

• CONFERENCE PUBLICATION. Collected papers from scientific and technical conferences, symposia, seminars, or other meetings sponsored or co-sponsored by NASA.

• SPECIAL PUBLICATION. Scientific, technical, or historical information from NASA programs, projects, and missions, often concerned with subjects having substantial public interest.

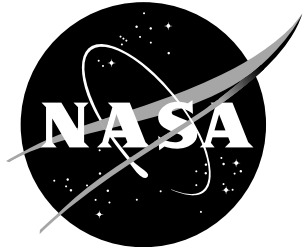
• TECHNICAL TRANSLATION. English-language translations of foreign scientific and technical material pertinent to NASA's mission.

Specialized services that complement the STI Program Office's diverse offerings include creating custom thesauri, building customized databases, organizing and publishing research results ... even providing videos.

For more information about the NASA STI Program Office, see the following:

- Access the NASA STI Program Home Page at <http://www.sti.nasa.gov>
- E-mail your question via the Internet to help@sti.nasa.gov
- Fax your question to the NASA STI Help Desk at (301) 621-0134
- Phone the NASA STI Help Desk at (301) 621-0390
- Write to:
NASA STI Help Desk
NASA Center for AeroSpace Information
7121 Standard Drive
Hanover, MD 21076-1320

NASA/CR-1999-209002



Advanced Turbofan Duct Liner Concepts

*Gerald W. Bielak and John W. Premo
Boeing Commercial Airplane Group, Seattle, Washington*

*Alan S. Hersh
Hersh Acoustical Engineering, Inc., Westlake Village, California*

National Aeronautics and
Space Administration

Langley Research Center
Hampton, Virginia 23681-2199

Prepared for Langley Research Center
under Contract NAS1-20090

February 1999

The use of trademarks or names of manufacturers in the report is for accurate reporting and does not constitute an official endorsement, either expressed or implied, of such products or manufacturers by the National Aeronautics and Space Administration.

Available from:

NASA Center for AeroSpace Information (CASI)
7121 Standard Drive
Hanover, MD 21076-1320
(301) 621-0390

National Technical Information Service (NTIS)
5285 Port Royal Road
Springfield, VA 22161-2171
(703) 605-6000

Table Of Contents

| | Page |
|---|------|
| LIST OF FIGURES | v |
| LIST OF TABLES | viii |
| 1.0 Summary | 1 |
| 2.0 Introduction | 5 |
| 2.1 Technical Approach | 5 |
| 2.2 Report Organization | 6 |
| 3.0 Passive Acoustic Liners | 8 |
| 3.1 Acoustic Liner Characteristics | 8 |
| 3.2 Summary Of Preliminary NASA/FAA Contract | |
| Investigating Broadband Liner Concepts | 8 |
| 3.3 Passive Liner Tests. | 10 |
| 3.3.1 Grazing Flow Impedance | |
| Measurement Technique | 11 |
| 3.3.2 Grazing Flow Impedance | |
| Measurements For Passive Element | |
| Liners | 12 |
| 3.3.3 Bulk Absorber Materials Study | 13 |
| 3.3.4 Linear Liners | 15 |
| 3.3.4.1 Slot Linear Liners | 16 |
| 3.3.4.2 Micro-perforate Linear | |
| Liners | 16 |
| 4.0 Adaptive Liners | 19 |
| 4.1 Introduction | 19 |
| 4.2 Bias Flow Adaptive Liner Designs | 19 |
| 4.3 High Temperature Adaptive Liner Design | 20 |
| 5.0 ADP Model Fan Acoustic Liner Design | 21 |
| 5.1 Aft Liner Depth Constraints | 21 |
| 5.2 Target ADP 22" Fan Rig Hardwall Fan Noise Spectra | 22 |
| 5.2.1 ADP Demo Hardwalled Aft Fan | |
| Spectra | 23 |
| 5.2.2 22" ADP Fan Rig Hardwalled | |
| Spectra | 23 |
| 5.3 Liner Design Points for the Aft Fan | 24 |

| | |
|---|----|
| 5.4 Source Noise Modal Energy Assumptions | 24 |
| 5.5 Optimum Liner Impedances for the Aft Fan | 25 |
| 5.6 Design Methodologies for the Aft Duct | 26 |
| 5.6.1 Optimize Lining Parameters to Match Admittance | 26 |
| 5.6.2 Optimize PNLT Attenuations (both sides the same) | 28 |
| 5.6.3 Optimize PNLT Attenuations (allow two sides to be different) | 28 |
| 5.6.4 Calculate the Cross-Performance | 28 |
| 5.7 Predicted Liner Attenuations for the AFT Fan | 28 |
| 5.8 Conclusions | 29 |
| 6.0 Evaluation of Broadband Liners for a Mid-Sized Twin Engine Airplane | 31 |
| 6.1 Program Overview | 31 |
| 6.1.1 Airplane/Engine Definition | 31 |
| 6.1.1.1 Airplane Definition | 31 |
| 6.1.1.2 Engine Definition | 32 |
| 6.1.1.3 Nacelle Definition—Inlet | 32 |
| 6.1.1.4 Nacelle Definition—Aft Duct | 32 |
| 6.1.2 Target Spectra | 32 |
| 6.1.2.1 Inlet Noise | 32 |
| 6.1.2.2 AftFan Noise | 33 |
| 6.1.3 Types of Nacelle Noise Suppression Technologies | 33 |
| 6.1.4 Linings Evaluated in the Study | 34 |
| 6.2 Inlet Trade Studies | 34 |
| 6.2.1 Technologies Evaluated | 35 |
| 6.2.2 Liner Depth Constraints | 35 |
| 6.2.3 Source Assumptions | 35 |
| 6.2.4 Optimum Liner Impedances | 35 |
| 6.2.5 Evaluation Process | 36 |
| 6.2.5.1 Optimize Lining Parameters to Match Admittance | 36 |

| | |
|---|----|
| 6.2.5.2 Run Rdiff Code to Determine Lining Attenuations | 36 |
| 6.2.5.3 Add Attenuations to Hardwall Data | 37 |
| 6.2.5.4 Extrapolate Dats to FAR 36 Condition | 37 |
| 6.2.6 Trade Study Results | 37 |
| 6.2.6.1 Impedance Trade Study | 37 |
| 6.2.6.2 Lining Area and Configuration Trade Study | 39 |
| 6.2.7 Conclusions | 40 |
| 6.3 Aft Duct Trade Studies | 41 |
| 6.3.1 Technologies Evaluated | 42 |
| 6.3.2 Liner Depth Constraints | 43 |
| 6.3.3 Source Modal Energy Assumptions | 43 |
| 6.3.4 Optimum Liner Impedances | 43 |
| 6.3.5 Evaluation Process | 44 |
| 6.3.5.1 Optimize Lining Parameters to Match Admittance | 44 |
| 6.3.5.2 Optimize PNLT Attenuations Using the YMATCH starting points | 45 |
| 6.3.5.3 Choose Best Lining Based on PNLT Attenuations | 45 |
| 6.3.5.4 Calculate the Off–Design Perfromance | 46 |
| 6.3.6 Trade Study Results | 46 |
| 6.3.6.1 Approach Design Point Impedance Study | 46 |
| 6.3.6.2 Cutback Design Point Impedance Study | 46 |
| 6.3.6.3 Off–Design Point Study | 47 |

| | |
|---|-----|
| 6.3.7 Conclusions | 47 |
| 7.0 References | 49 |
| Appendices | 111 |
| A1. "Theory And Design Of Helmholtz Resonators Constructed With Slot Perforates" Allen Hersh and Bruce Walker | |
| A2. "Theory And Design Of Helmholtz Resonators To Suppress Aircraft Engine Noise" Allen Hersh and Bruce Walker | |
| A3. "Theory And Design Of Helmholtz Resonators Constructed With Micro-Diameter Perforates" Allen Hersh, Joseph W. Celano and Bruce Walker | |
| A4. Impedance Models. | |

List of Figures

| Fig. No. | Fig. Title | Page |
|----------|---|------|
| 1. | Single Layer Acoustic Liners | 50 |
| 2. | Double & Triple Layer Acoustic Liners | 51 |
| 3. | Parallel Element Acoustic Liners | 52 |
| 4 | Double Layer Parallel Element Acoustic Liner | 53 |
| 5. | Typical Wide Chord Fan Spectrum Shape | 54 |
| 6. | Fan Duct OAPWL Attenuations | 55 |
| 7. | Inlet OAPWL Attenuations | 56 |
| 8. | Inlet Impedance and Attenuation Spectra | 57 |
| 9. | Fan Duct Impedance and Attenuation Spectra | 58 |
| 10. | Schematic of NASA Langley Standard Grazing Flow Impedance Sample | 59 |
| 11. | Passive Liner Test Designs | 60 |
| 12. | Schematic Of Wichita Grazing Flow Impedance Measurement System | 61 |
| 13. | Comparison Of NASA And Boeing Wichita Grazing Flow Resistance Test Data | 62 |
| 14. | Comparison Of NASA And Boeing Wichita Grazing Flow Reactance Test Data | 63 |
| 15. | Measured And Predicted Impedance Of The Double Layer Perforate Liner; $M=0.0, 0.33$, and 0.50 | 64 |
| 16. | Measured And Predicted Impedances Compared To Target Impedance, $M=0.33$ | 65 |
| 17. | Measured vs. Predicted Surface Impedance – Fiberglass Bulk Absorber | 66 |
| 18. | Measured Surface and Characteristic Impedance | 67 |
| 19. | Measured vs. Predicted Characteristic Impedance | 68 |
| 20. | Measured vs. Predicted Attenuation Constant | 69 |
| 21. | Measured vs. Predicted Phase Speed Ratio | 70 |
| 22. | Effect Of Orifice Number, Grazing Flow Speed and SPL on Resonator Tuned Resistance | 71 |
| 23. | Effect Of Orifice Number and Grazing Flow Speed on Resonator Face–Sheet Mass Reactance: $SPL=135$ dB | 72 |
| 24. | Comparison Of Effect Of Grazing Flow AND SPL Changes On Acoustic Resistance Of Currently Used Perforates With Micro–Perforate | 73 |
| 25. | Comparison Of Acoustic Mass Reactance For Currently Used Perforates With Micro–Perforate | 74 |

| | | |
|-----|--|-----|
| 26. | Adaptive Liner Test Designs | 75 |
| 27. | Bias Flow Impedance Changes For Test Liner | 76 |
| 28. | Comparison Of Predicted Impedance Spectra For The Bias Flow Test Liner With The Original and Updated Bias Flow Impedance Models. | 77 |
| 29 | High Temperature Liner Impedance and Attenuation | 78 |
| 30 | Cartoon of Lining Segments | 79 |
| 31 | Comparison of the Design ADP Hardwalled Data Predictions | 80 |
| 32 | Hardwall Target Spectra Based On ADP Demo Data | 81 |
| 33 | Comparison of Hardwalled 22" ADP Data | 82 |
| 34 | Hardwall Target Spectra Based On ADP Model Fan Data | 83 |
| 35 | Representation of the Fan Duct with the MELO Program | 84 |
| 36 | Optimum Lining Impedance for the ADP Fan Duct | 85 |
| 37 | Preliminary Ideal Impedance Calculations for the ADP Fan Duct | 86 |
| 38 | Ideal Impedance Calculations for the ADP Fan Duct | 87 |
| 39 | Comparison of Boundary Layer Effect on Optimum Impedances | 88 |
| 40 | Block Diagram of the Design Process | 89 |
| 41 | MELO Predicted Lining Attenuations vs the Optimum Attenuations | 90 |
| 42 | Predicted Lining Impedance vs the Optimum Impedance (1 layer) | 91 |
| 43 | Predicted Lining Impedance vs the Optimum Impedance (2 layer) | 92 |
| 44 | Conventional and Scarf Inlets | 93 |
| 45. | MELO Representation of the Fan Duct Nacelle | 94 |
| 46 | Inlet Spectra for the Approach, Cutback and Sideline Conditions | 95 |
| 47 | Aft Duct Spectra for the Approach, Cutback and Sideline Conditions | 96 |
| 48 | Examples of Linings Considered in the Trade Study | 97 |
| 49 | Block Diagram of the Evaluation Process for the Inlet | 98 |
| 50 | Results of the Impedance Study for the Inlet Component | 99 |
| 51 | Impedance of the Inlet Liners (at the approach condition) | 100 |
| 52 | Ray Acoustic Argument for Low Inlet Attenuations | 101 |
| 53 | Impedance of the Inlet Liners (at the cutback condition) | 102 |
| 54 | Comparison of Lining Area Technologies | 103 |
| 55 | Conventional and Scarf Inlet Nacelles | 104 |
| 56 | Inlet Lining Area and Configuration Study | 105 |
| 57 | MELO Predicted Ideal Impedances | 106 |
| 58 | Block Diagram of the Evaluation Process for the Aft Duct | 107 |

| | | |
|----|--|-----|
| 59 | Comparison of Aftfan PNLT Attenuations at Approach | 108 |
| 60 | Comparison of Aftfan PNLT Attenuations at Cutback | 109 |
| 61 | Comparison of Aftfan PNLT Attenuations (summed approach and cutback condition) | 110 |

List of Tables

| Table No. | Table Title | Page |
|-----------|---|------|
| 1. | Bulk Absorber Acoustic Materials Candidates Identified By Boeing Materials Technology | 12 |
| 2. | Fluid Renention Properties Of Bulk Absorber Material Candidates | 13 |
| 3. | Summary Of Micro–Diameter Resonator Geometry | 16 |
| 4 | Preliminary 22" Fan Rig Lining Depth Constraints | 20 |
| 5 | Definition of the ADP Demo Aft Liner | 22 |
| 6 | Frequency Weightings Used for YMATCH by Band Number | 26 |
| 7 | Single Layer/ Single Layer Final Designs | 27 |
| 8 | Double Layer/ Double Layer Final Designs | 27 |
| 9. | FAR 36 Operating Conditions for Trade Study Airplane | 31 |
| 10. | YMATCH Frequency Weightings for the Inlet | 35 |
| 11. | Results of the Impedance Study for the Inlet Component | 36 |
| 12. | Results of the Lining Area and Configuration Study for the Inlet Component | 39 |
| 13. | Frequency Weightings Used for the Narrow Chord Fan at Approach | 43 |
| 14. | Frequency Weightings Used for the Narrow Chord Fan at Cutback | 43 |
| 15. | Frequency Weightings Used for the Wide Chord Fan at Approach | 43 |
| 16. | Frequency Weightings Used for the Wide Chord Fan at Cutback | 44 |
| 17. | Results of the Impedance Study for the Aft Component at Approach | 45 |
| 18. | Results of the Impedance Study for the Aft Component at Cutback | 46 |

1. Summary

The Advanced Subsonic Technology (AST) Noise Reduction Program goal is to reduce aircraft noise by 10 EPNdB by the year 2000, relative to 1992 technology. Interim goals have been established which include a goal to validate concepts to improve nacelle duct treatment effectiveness by 25% relative to 1992 technology by the second quarter of fiscal year 1997. The Advanced Turbofan Duct Liner Concepts Task (Task 1 NAS-20090) work by Boeing was supporting this goal. The duration of this contract was February 1994 to September 1996.

The technical approach was to investigate methods for increasing the attenuation bandwidth of nacelle acoustic linings. The primary motivation for this approach is the character of the fan noise spectrum generated by modern wide chord fan engines. The wide chord fans have approximately 50% fewer blades and run at slightly reduced tip speeds compared to older narrow chord fans. As a result, the fan blade passing harmonic frequencies are significantly lower than for narrow chord fans. For example, blade passing frequency (BPF) at landing for the engines powering the Boeing 777 airplane is in the 630 to 800 Hz 1/3 octave band range. The broadband fan noise spectrum however is very similar for the narrow and wide chord fans with the peak Noy weighted levels in the 3 kHz to 4 kHz region. Therefore, for effective PNLT attenuation, approximately 3 octave bandwidth lining attenuation is required for wide chord fans in order to attenuate the peak NOY region of the spectrum and reduce the tone correction resulting from the BPF.

The basis for the technical approach was a Boeing study conducted in 1993-94 under NASA/FAA contract NAS1-19349, Task 6 investigating broadband acoustic liner concepts. As a result of this work, it was recommended that linear double layer, linear and perforate triple layer, parallel element, and bulk absorber liners be further investigated to improve nacelle attenuations. NASA Langley also suggested that "adaptive" liner concepts, which would allow "in-situ" acoustic impedance control, be considered. As a result, bias flow and high temperature liner concepts were added to the investigation. The following summarizes the specific studies conducted for Task1 NAS-20090:

1. **Passive Acoustic Liners.** This study investigated liner designs with increased degrees-of-freedom such as double layer, triple layer and parallel element liners; liners with linear resistance elements such as the currently used woven wire as well as new concepts such as slots and micro-perforates; and bulk absorber materials such as fiberglass, kevlar felts and ceramic foam. Subcontracts were given to Hersh Acoustical Engineering (HAE) to study the linear liner concepts of narrow slots and micro-perforates.

Analysis of the grazing flow impedance test data gathered to verify the impedance models used for the analytical study of the passive and adaptive liners was not complete at the time this contract concluded. However, passive liner concepts, which included triple layer and parallel element liners designed for fan duct application, were tested and preliminary data analysis was completed. This data indicated that the liners may be slightly better than predicted, but there was sufficient scatter in the data that its accuracy, particularly at grazing flow Mach numbers greater than 0.3, is questionable.

Boeing does not use woven wire resistance elements in the nacelles it

- builds because of a number of concerns associated with manufacturing and in-service durability. However, the above studies showed important potential acoustic benefits from use of linear materials. The slot concept proposed by Hersh Acoustical Engineering showed good acoustic properties, but it was concluded that slots had strength and manufacturing efficiency difficulties which would result in very heavy liners. Therefore, their development was terminated in favor of micro-perforates. Initial acoustic testing with micro-perforates with hole sizes down to .004 in. laser drilled into .040 in. thick titanium plate showed acoustic characteristics very similar to currently used woven wire. As a result, further work with micro-perforate liners is planned for follow on work. Although a number of bulk absorber materials were found with good acoustic characteristics, none were considered usable in aircraft engines because fluid absorption testing showed a strong tendency to absorb hydrocarbons such as jet fuel and hydraulic fluid. Further bulk absorber investigations were therefore terminated.
2. **Adaptive Acoustic Liners.** Two concepts were chosen for investigation. The first was a bias flow concept which uses a steady bias flow (blowing or suction) through the liner to modify the acoustic properties of the liner. The second concept involved increasing the temperature of the liner to modify its acoustic properties. The design application investigated for bias flow was to design a non-linear liner for the high engine power condition (high local SPL) and use bias flow to maintain the desired acoustic resistance at low engine powers (low local SPL). Although grazing flow impedance tests were completed the data analysis has not been completed for the adaptive liner concepts.
 3. **ADP Model Fan Acoustic Liner Design.** This was the first of two airplane nacelle design studies conducted. It was a joint study to design and build acoustic liners for testing on the NASA Lewis 22 inch Advanced Ducted Propeller (ADP) model scale fan. The airplane application was assumed to be a Boeing 747 derivative powered by ADP engines. The scale factor assumed was 5.91. Boeing had responsibility for design of the fan duct liners, PW had responsibility for designing the inlet liners, Rohr manufactured the liners and NASA Lewis performed the testing in their 9x15 acoustic wind tunnel. NASA Langley served as consultant and coordinator for the lining design work. There was a great deal of interaction among the participants during the design phase to insure that the best technology available was being applied. Preliminary analysis of the model scale ADP acoustic lining data indicates that the fan duct liners were behaving as predicted, but a detailed analysis with narrow band data is planned in the follow on work.
 4. **Medium Sized Twin-Engine Airplane Liner Study.** The purpose of this design study was to apply the design concepts developed from the above work to engines representing 1992 technology powering a mid-sized, twin-engine, commercial airplane. The Boeing 767 airplane was used to represent this class of airplane. Both inlet and fan duct lining

studies were conducted. For the inlet, the effect of increasing the lining area by improvements in manufacturing and structural design, as well as increasing the inlet length, were examined in addition to lining acoustic impedance improvements. Also, the impact of a scarf inlet concept, which uses the inlet shape to direct noise upward above the airplane while reducing energy propagating to the ground, was examined.

The major conclusion from the above studies is that improvements in nacelle liner average impedance characteristics alone will not result in 25% increased nacelle noise attenuation improvements relative to 1992 technology. (The liner assumed for 1992 technology was a double layer, perforate liner using the Boeing buried septum technology.) Optimum uniform liners, i.e. imaginary liners with optimum impedance at each frequency, were predicted to result in improvements of approximately 10% for inlets and 15% for fan ducts at the airplane landing condition. Liners with increased degrees-of-freedom such as triple layer perforates were estimated to offer only 2% – 3% improvement for inlets and 6% – 10% improvement for fan ducts. Liners with linear resistance elements such as linear double and linear triple layer liners were estimated to offer 6% – 7% improvement for inlets and 7% – 10% for fan ducts.

The effects of varying liner impedance within the nacelle was not evaluated in detail in this study. A previous inlet study using an early version of the ray tracing code used here found only a small benefit for varying liner impedance in the inlet. For the fan duct, the duct wave propagation code used only applies to ducts with constant geometry, lining and flow conditions. An approximate calculation indicated that varying liner impedance axially in a constant geometry fan duct gives approximately the same attenuation bandwidth as calculated for the uniform impedance spectrum of parallel element liners.

One aspect of varying liner impedance which may be particularly beneficial for fan ducts is modal scattering. This could not be analytically evaluated with the code used in the present study however. For typical length fan ducts the duct propagation studies indicated that the attenuation was limited by the modest attenuation of low order modes. This suggests a concept where the initial fan duct lining is used to attenuate the higher order modes; which is then directly followed by a mode scattering device (such as an impedance discontinuity) used to scatter the energy in the remaining low order modes into high order modes that the following lining can more effectively attenuate. Inlet broadband noise is composed of a large number of cut-on modes, so scattering would not be expected to do anything more than re-mix the modal energy distribution.

The possibility of taking advantage of the 3-D geometry of fan ducts has also been suggested for improving fan duct attenuation. The rectangular/circular/annular duct code used for the present fan duct studies did not allow anything but idealized geometries. The fan duct scattering and 3D geometry concepts will be evaluated later with a new code being developed at Boeing under AST contract.

Additional nacelle advancements such as liner structural design improvements to allow reduction in panel area used for fasteners and strength reinforcement are presently being studied with internal funds at Boeing. Additionally, the effects of liners on the boundary layer in the inlet throat region are being studied which may allow lining forward of the throat. These nacelle design advancements are expected to add 20% to 40% more active acoustic lining area in current inlets which is predicted to result in a 40% – 80% attenuation improvement. Similar advancements are expected to allow 10% to 30% more acoustic lining in current fan ducts with 10% to 30% more attenuation expected. In addition, Boeing is currently developing a scarf inlet

concept which is expected to give an additional 40% to 80% attenuation improvement for an equivalent lining area.

2. Introduction

The Advanced Subsonic Technology Noise Reduction Program (AST) goal is to develop technology by the year 2000 to reduce aircraft noise by 10 EPNdB relative to 1992 technology. The technology development strategy is a coordinated effort among government, industry and academia addressing engine source understanding and reduction, nacelle aero-acoustics, engine/airframe integration and flight procedures. Interim goals have been established which includes a goal to validate concepts to improve nacelle duct treatment effectiveness by 25% relative to 1992 technology by the second quarter of fiscal year 1997 (FY '97).

The Advanced Turbofan Duct Liner Concepts Task (Task 1 NAS1-20090) reported here was assigned to pursue the above goals. The basis for the technical approach was a Boeing study conducted in 1993-94 under NASA/FAA contract NAS1-19349, Task 6 investigating broadband acoustic liner concepts. As a result of this work, it was recommended that linear double layer, linear and perforate triple layer, parallel element, and bulk absorber liners be further investigated to improve nacelle liners. NASA Langley also suggested that "adaptive" liner concepts which would allow "in-situ" acoustic impedance control also be considered. As a result, bias flow and heated core liner concepts were added to the investigation.

The purpose of this report is to communicate the work done under contract NAS1-20090, Task #1, "Advanced Turbofan Duct Liner Concepts." This report represents a fulfillment of deliverable items specified in the contract.

2.1 Technical Approach

Using Boeing design tools and experience with parallel element, double layer and triple layer liners, a complement of linings was designed for improved fan duct broadband attenuation. These design studies were guided by the results of a Boeing study conducted in 1993-94 under NASA/FAA contract NAS1-19349, Task 6 investigating broadband acoustic liner concepts. Panels using these designs were then manufactured for testing in Boeing's grazing flow impedance measurement facility. This facility propagates the fundamental mode over the acoustic liner with a flow Mach number up to $M=0.5$ and determines the effective liner impedance from the measurement of the complex acoustic pressure pattern over the length of the liner. The purpose of the testing was to verify the designed impedance spectrum of the liners with a grazing flow and a noise environment representative of an engine fan duct at typical landing and takeoff conditions.

The Boeing Materials Engineering group completed a survey of potential bulk absorber materials and together with Noise Engineering selected five materials for further investigation: Manville Fiberglass batting, Osaka Gas (ANA) Carbon fiber batting, Tex Tech Kevlar felt, Tex Tech Polyimide felt and Lockheed Ceramic fiber. Acoustic impedance testing, including measurement of the characteristic impedances and propagation constants, and fluid absorption tests were conducted on the five selected materials. While all five of the materials tested showed good acoustic characteristics, they all showed unacceptable hydrocarbon fluid wicking. As a result the bulk absorber investigation was essentially terminated. One supplier, Osaka Gas, said they would study ways to correct this problem on a very low priority level.

Under subcontract to Boeing, Hersh Acoustical Engineering (HAE), in conjunction with testing at NASA Langley, developed verification and modeling data demonstrating the nonlinearity and grazing flow independence of their slotted liner concept. However, Boeing structural design

personnel concluded that the concept posed serious structural and manufacturing difficulties for nacelle application. As a result, development of this concept did not continue beyond 1995. In 1996 HAE began an investigation of the impedance properties of micro-perforate sheets to develop acoustic data which could be used to evaluate their feasibility for linear liner systems. HAE developed both circular and slotted orifice semi-empirical acoustic impedance models using the data from these tasks as well as past HAE work.

Boeing participated with P&W, Rohr, NASA Langley and NASA Lewis to design acoustic liners for the 22 in. model scale ADP fan to be tested at NASA Lewis in 1996. Boeing had prime responsibility for the fan duct liner design and P&W had prime responsibility for the inlet and fan case liner designs. This division of responsibility was somewhat arbitrary. Initially it was envisioned that both Boeing and PW would be strongly involved in the design of all of the liners (even doing independent designs for the same part) but in the end there was only time for each company to review the others progress during the design period. The objective was to demonstrate advanced liner design and analysis concepts and show a 25% attenuation improvement relative to the baseline liner which was scaled from the Advanced Ducted Propeller (ADP) demonstrator engine test in 1992.

An analytical evaluation study was conducted applying the design concepts developed from the above work to engines representative of 1992 technology powering a medium twin commercial airplane. The objective of this study was to design liners which would be predicted to give at least 25% attenuation improvement relative to a 1992 technology engine nacelle. Both narrow chord and wide chord fan engine representations were evaluated. A major element of this study was to be the choice of mode energy distribution assumed for the tones. It was expected that the mode predictions and measurements made for the 22" ADP model would influence this choice. Unfortunately the modal data was not available in time to be used. Therefore, the standard Boeing assumption of nearly equal energy in each propagating mode was used. For the inlet, ray acoustics was used, which is equivalent to assuming a very large number of modes with equal energy. For the fan duct, a rectangular duct model was used with the mode energies being approximately equal except near cut-off where the assumed energies drop off significantly.

2.2 Report Organization

This report is organized in sections which describe the details of the work conducted for the above investigations. The report is a composite of mini-reports on all of the studies conducted over the term of the contract. The sections are somewhat chronological, but there is also a logical flow moving from investigation of lining design concepts to application of these concepts to a specific airplane noise reduction study. Section 3 describes the passive liner investigations including the grazing flow impedance tests, the bulk absorber materials investigations and the linear materials investigations. Reports from Hersh Acoustical Engineering on the slot liner development, the single orifice impedance modeling and the preliminary micro-perforate investigation are contained in Appendices 1, 2 and 3 respectively. A brief summary of the preliminary analytical passive liner studies conducted in 1993–94 under NASA/FAA contract is contained in this section for completeness since this work formed the basis for all of the follow on passive liner studies. Although the NASA/FAA contract studies were somewhat idealized in that specific airplane noise design and attenuation metrics were not used, we felt the results apply to the airplane design and the community noise evaluation metrics generally used (EPNdB).

Section 4 describes the adaptive liner work status at this point, but is not yet complete since the measured impedance data has not yet been analyzed.

Section 5 describes the details of the ADP fan duct liner and design process including the predicted attenuations for the ADP model scale fan test.

Finally, the analytical evaluation of the passive liners applied to the nacelles on a medium twin airplane powered by narrow chord and wide chord fan engines is contained in Section 6. This work used the design tools and experience developed from the above work and analytically evaluated the primary passive liner design concepts of single, double and triple layer perforate and linear liners considering the specific constraints, noise characteristics, aerodynamics and certification metrics of a medium sized, twin engine airplane. In addition, the acoustic benefits of new nacelle manufacturing concepts allowing more acoustic lining within the current nacelle envelope and a new inlet geometry (scarf inlet) were analytically evaluated for comparison.

Appendix 4 is a listing of the lumped element acoustic impedance models developed under this contract and coded into the Boeing impedance library. These models were used in the calculation of liner acoustic impedances.

3. Passive Acoustic Liners

3.1 Acoustic Liner Characteristics

The following discussion is intended to introduce the reader to the nomenclature of acoustic linings which is utilized in the later sections.

A typical single layer acoustic lining, shown in Figure 1, is composed of a face sheet and honeycomb core with an impervious backing sheet. Face sheets are usually composed of a perforated plate or woven wire/perforated plate sandwich. The honeycomb core is composed of cells which, when bonded to the face sheet, create cavities behind the face sheet. The attachment of an impervious backing sheet to the honeycomb core seals the honeycomb so that each cavity is isolated from its neighbors. This creates a single-layer resonator, whose impedance (Z) is characterized by a resistive (R) real part and reactive (X) imaginary part, $Z = R + iX$. The resistive impedance is only a function of the face sheet configuration. The reactive impedance is a function of the face sheet configuration and the cavity depth behind the face sheet.

Characterizing the impedance in such a way as to isolate the effect of the cavity reactance, leads to

$$Z = Z_{\text{face sheet}} - i \cot(kd) . \quad (+ i\omega t \text{ convention})$$

The cavity reactance, $-i \cot(kd)$, strongly influences the frequency response characteristics of the liner. As frequencies increase above the first resonance ($X=0$, approximately where the attenuation is maximum), the reactance approaches positive infinity. At frequencies below the resonance frequency, the reactance approaches negative infinity. There are several methods to modify this behavior. One method is to create multiple layer liners as shown in Figure 2. Another method is to create a multi-segment parallel element liner, shown in Figure 3.

Figure 4 is a diagram of the two parallel element, double perforate layer liner to aid in understanding of the nomenclature.

3.2 Summary Of Preliminary NASA/FAA Contract Investigating Broadband Acoustic Liner Concepts

This section summarizes the results of a Boeing analytical study conducted in 1993–94 under NASA/FAA contract NAS1–19349, Task 6 investigating broadband acoustic liner concepts. The results of this work formed the basis for the passive liner work conducted under the present AST contract. The main objective of this study was to investigate acoustic linings which have increased bandwidth attenuation compared to conventional nacelle liners. Broad bandwidth liner attenuation was believed necessary for new turbofan engines which use wide chord fan blades. The number of fan blades for these engines is much fewer than in the past. These fans therefore generate much lower frequency blade passing tone noise (of the order of 800 Hertz at approach power). The broadband fan noise spectrum however, is very similar for the narrow and wide chord fans with the peak NOY weighted levels in the 3 kHz to 4 kHz region (see Figure 5). Therefore, for effective PNLT attenuation, approximately 3 octave bandwidth lining attenuation is required for wide chord fans in order to attenuate the peak NOY region of the spectrum and reduce the tone correction resulting from the BPF.

There are several techniques for achieving increased bandwidth attenuation with acoustic liners. This study concentrated on liners with distributions of parallel elements while examining other

designs for comparison. Although the impedance of the individual elements of the parallel element liner was allowed to vary, an effective uniform impedance was assumed to determine its effect on sound propagation. Therefore, all of the liner designs (except for the two segment series duct configuration) were studied as constant impedance liners.

Candidate lining concepts were evaluated using Boeing lining design optimization tools. Two different approaches were applied for the design and evaluation of the lining concepts. The first was a “plane wave” approach and the second a “mode” approach. Most of the attenuation trends concluded from the plane wave reflection design optimizations were also observed for the duct propagation design optimizations although not as strongly. The following are the primary conclusions for nacelle liner design for broadband attenuation from this study:

1. Maximum attenuation was attained with the triple layer and bulk absorber liners.
2. Triple layer liner attenuation was greater than double layer liner attenuation which was greater than single layer liner attenuation
3. The parallel element liners resulted in superior attenuation compared to the constant geometry liners.
4. The two segment series duct version of the parallel element double layer liner gave nearly identical attenuation as the parallel element liner for aft duct propagation.
5. Linear liner face sheets and septa did not show as large a benefit for the duct propagation analysis as seen for the plane wave analysis, but still generally resulted in attenuation improvements.

The above results are summarized in figures 6 and 7. Figure 6 is a plot of the estimated OAPWL attenuation of a given liner in an engine fan duct vs. the number of parameters which could be varied to optimize the liner design (DOF—degrees of freedom). For example a double layer perforate liner is shown to have 4 DOF since the face sheet and septum open areas and the top and lower depths were optimized. Figure 7 shows the same results for engine inlet liners. Impedance and attenuation spectra for perforate single, double and triple layer fan duct and inlet liners are shown in figures 8 and 9.

Comparison of the predicted maximum attenuation attainable from a uniform “ideal” liner impedance with the predicted attenuation of the current production perforate double layer liner concept indicates that the potential for improvement with uniform impedance is approximately 30% (overall power level (OAPWL) dB improvement) for the inlet and 60% for the fan duct. The best liner designs developed in the above study are predicted to attain approximately 25% improvement (both inlet and fan duct) relative to that attainable with the current perforate double layer liner concept, using the broadband OAPWL noise metric for comparison.

The bulk absorber liners are predicted to give the most attenuation of all of the liners studied followed closely by the triple layer liner. The application of bulk absorbers for turbofan engine nacelle application has not been pursued in the past because of structural and maintainability concerns. Several new bulk absorber materials have become available which were recommended for examination. These materials included polyimide foam, ceramic felt and metal matrix foam. It was recommended that the examination include acoustic characterization and consideration of the structural, weight and other mechanical issues associated with their use.

“Linear” acoustic materials clearly showed predicted acoustic advantages with the plane wave evaluation but the duct propagation analysis showed less and somewhat inconsistent benefits. At the design engine power condition a “linear” liner gives greater attenuation bandwidth compared to a perforate liner because of the lower mass reactance of the linear liner. Consideration of the acoustic performance of “linear” vs. perforate liners at higher engine power conditions (off design), where the liner is exposed to higher grazing flow Mach numbers and higher sound levels, showed higher OAPWL attenuation for the linear liner compared to the perforate liner, for both fan duct and inlet models. “Linear” materials such as woven wire over aluminum, woven wire over composite, laser drilled thermoplastic, laser drilled graphite epoxy composite and pre-preg polyimide were recommended for study. Again, consideration of the structural, weight and other mechanical issues associated with “linear” materials as well as the acoustic characteristics (impedance) was recommended.

The effects of varying liner impedance within the nacelle or varying nacelle geometry were not evaluated in detail in this study. However, an approximate calculation indicated that varying liner impedance in a constant geometry fan duct gives approximately the same attenuation bandwidth as calculated for the uniform impedance spectrum of parallel element liners. One aspect of varying liner impedance, which may be particularly beneficial for fan ducts, is modal scattering. Scattering could not be analytically evaluated with the code used in the present study however. For typical length fan ducts, the duct propagation studies indicated that the attenuation was limited by the modest attenuation of low order modes. A concept is therefore suggested whereby the initial fan duct lining is used to attenuate the higher order modes and is followed by a mode scattering device (such as an impedance discontinuity) to scatter the energy in the remaining low order modes into high order modes so that the following lining can more effectively attenuate the remaining noise.

The results from the study of the application of advanced liners to a medium twin airplane discussed in section 6 showed approximately 1/4 of the improvements relative to 1992 perforate double layer liner technology found in the FAA study. The primary reasons for this discrepancy are the differences in the source noise spectral characteristics assumed and the evaluation metric used. For the NASA/FAA study the assumed source spectrum was a 1/3 octave spectrum with constant SPL from 500 Hz to 4000 Hz. The evaluation metric was overall power level (OAPWL). For the medium twin study, the evaluation metric was fan component peak flyover PNLT, where the source spectrum had maximum NOY weighting in the frequency range of 2 to 5 kHz. The maximum attainable attenuation in this frequency range is significantly lower than in the lower frequencies because of the beaming effect of higher frequency modes. Also, attenuation bandwidth was not as important for the airplane study as it was for the 500 Hz to 4 kHz power level attenuation study. This was even the case for the wide chord fan which had a relatively low frequency BPF at approach (630 Hz band), with a resulting 2.2 dB tone correction. Attenuation of noise in the BPF frequency region in this case had only a small contribution to PNLT attenuation since the tone correction did not change very much. In reality the masking effect of other noise sources such as airframe noise would probably cause the tone correction to be reduced as the inlet radiated fan noise is reduced in the BPF region. This effect however was not accounted for in the airplane study.

3.3 Passive Liner Tests

The above analytical studies made use of Boeing semi-empirical models for predicting the acoustic impedance of the elements of a liner and a transmission line analogy analysis tool for

calculating the impedance of the arrangement of the elements to form a liner design. In order to verify the calculated impedances, measurements were made at the Boeing Wichita facility. The objectives of these measurements were:

1. Measure the “standard sample” from NASA Langley for comparison of measurement processes.
2. Measure no flow impedance (Z) in a normal incidence impedance tube.
3. Measure no flow and with flow Z in Wichita grazing flow Z duct for comparison to predictions and targets. (Grazing flow effects and parallel element assumption investigated).
4. Measure Hersh slot resistance elements sample in grazing flow to compare with data taken at NASA Langley and to expand Mach number range if possible.

The liners chosen for testing were (See Figure 11):

1. NASA Langley standard sample.
2. Perforate double layer (for reference –1992 technology).
3. 5 element parallel element linear double layer.
4. 2 element parallel element double / triple layer – perforate.
5. Triple layer– perforate.
6. Hersh slotted face sheet single layer liner.

Figure 10 is a schematic of the NASA Langley “standard sample.” This sample was borrowed from NASA to develop confidence in the accuracy of the Langley and Wichita grazing flow impedance measurement facilities. The Boeing liner designs tested are shown schematically in Figure 11. These designs were optimized for fan duct broadband acoustic attenuation application. However, the designs are thicker (3 in. to 4 in.) than those allowed in todays fan ducts. Even todays largest engines limit the fan duct liner thickness to approximately 2 in. Liner thickness is not as severely limited for the engine inlet application where 3 to 4 inch deep liners are feasible.

3.3.1 Grazing Flow Impedance Measurement Technique

The technique used at the Boeing Wichita facility to measure liner impedance in the presence of grazing flow is called the “waveguide” technique. The waveguide method involves measuring sound attenuation properties in an acoustically lined flow duct. One wall of the duct contains the acoustic liner being evaluated. A wall mounted traversing microphone on the opposite hard wall is used to measure the attenuation and phase variation down the duct. These data are used in conjunction with the convected wave equation for establishing the acoustic liner impedance. Figure 12 is a schematic of the measurement system. The test section used for the measurements had a 2 x 2 in. cross section and was 16 inches in length. The resulting frequency range for the system is 1000 to 6000 Hz and the Mach number range is up to $M=0.5$. Sound levels over the lining can be as high as 150 dB OASPL. Data analysis consists of using an optimization technique to find the liner impedance which will give the “best” match of the analytically calculated pressure and phase to the measured data. The analytical calculation allows for segmentation of the duct to account for reflection effects at impedance discontinuities and impedance variation with non-linear liners, but assumes plug flow.

3.3.2 Grazing Flow Impedance Measurements For Passive Element Liners

Boeing borrowed the NASA Langley “standard” grazing flow test sample and tested it in the Wichita facility. The NASA “standard” sample is a porous ceramic 3.25 in. thick. The pores are nearly cylindrical with a diameter of approximately .025 in. extending the entire thickness of the material. The surface open area is approximately 60%. NASA has shown that the standard liner impedance is linear and minimally affected by grazing flow. The liner is of such depth that the frequency range from 0.5 kHz to 3.0 kHz encompasses two resonance frequencies and one anti-resonance, so that the measurement procedure gets exercised across a significant range of resistance and reactance. Langley data are generally consistent for both downstream and upstream propagation except where an anti-resonance has a pronounced effect on the measurement uncertainty.

The Boeing measured resistances and reactances for the NASA Langley standard sample are compared with NASA data (Ref. 1) in Figures 13 and 14 respectfully. The agreement with the NASA data is reasonably good for $M=0.0$ and 0.3 , but the Boeing resistances for $M=0.5$ are lower than the Langley results. Even for $M=0.0$ and 0.3 , the Boeing data deviates significantly from the NASA data near 2 kHz. Given the expectation that the standard sample should show little grazing flow dependence, the Boeing data appears inconsistent at this frequency. NASA shows the largest deviation of their upstream vs. downstream propagation data near 2 kHz as well. In Ref.12 they describe a procedure for estimating measurement accuracy and find that near anti-resonance the measurement accuracy is poor for the wave guide impedance measurement procedure.

Figure 15 compares Boeing measured and predicted impedance results for the double layer liner shown in Figure 11, at grazing flow Mach numbers of 0, 0.33 and 0.50. While the agreement is fairly good at $M=0$, it is seen that it gets poorer as Mach number increases. Generally, it was found that the $M=0.5$ results seemed highly suspect. Note that the $M=0.5$ measured resistances are lower than those at $M=0.33$. The measured data also showed lower reactances than the predictions at $M=0.33$ and 0.5 . At the 5 kHz predicted anti-resonance, the measured data agrees poorly with the predictions. This even happens for the $M=0.0$ case. Figure 16 compares predicted and measured impedances with the design target impedance spectra at $M=0.33$ for all four liners tested (Figure 11). It is interesting to note that all of the liners showed measured impedances which better matched the target impedance spectra (fan duct propagation target) than was predicted for $500 \text{ Hz} \leq \text{frequency} \leq 3150 \text{ Hz}$. It was estimated that the measured impedance spectrum for the double layer liner would result in 2 – 5 dB better attenuation for the fan duct geometry assumed for Figure 6 than with the predicted impedance spectrum. Much of this benefit is probably due to the lower than predicted reactance in the 1–4 kHz region. Unfortunately, the measured resistance data at grazing flow Mach number of .5 is sufficiently suspect to cause one to question the validity of the $M=.3$ results as well. Therefore, the Boeing impedance models were not modified to reflect the reactance effect of grazing flow observed in this data. In addition this data was not available prior to beginning the mid-sized twin lining design study discussed in section 6. A new AST initiative, led by NASA Langley, is planned to define the lining impedance changes caused by grazing flow. Measurements will be made by NASA Langley, GE, Boeing and BF Goodrich (Rohr) with different perforate geometries, both in order to define the relative merits of the different measurement techniques, as well as to define the parametric dependencies.

The following conclusions were drawn from the grazing flow impedance test results:

1. Predicted and measured impedance agreed fairly well at zero grazing flow but agreement was poor with grazing flow.
2. The accuracy of the grazing flow impedance measurement needs to be quantified.
3. The triple layer and triple/double layer liners showed similar impedance characteristics.
4. The measured data showed better agreement with the target impedance spectrum than was predicted.

3.3.3 Bulk Absorber Materials Study

The following is the list of bulk absorber material candidates identified as having potential for nacelle application developed by Boeing noise and materials engineering personnel:

Table 1: Bulk Absorber Acoustic Material Candidates Identified by Boeing Material Technology

| MATERIAL TYPE | SUPPLIER | COMMENTS |
|---|--|--|
| Carbon fiber batting | Osaka Gas (ANA Trading Corp.) | Very low density, 0.3 pcf. Osaka seems to understand the problem. Aggressive marketing from ANA. |
| Kevlar,Nomex Polyimide etc. (Needle felting) | Tex Tech Industries | Wide range of materials. Require water repellent. Suggested Zonyl |
| Ceramic batting | Carborundum Hi Temp Insulation Cotronics Corp. Zircor Products Orcon Corp. | Must have water repellent |
| Pyroloft AA-fiberglass batt Pyropel – polyimide felt | A.L. International L.P. | |
| Polyurethane foam | General Plastics | Requires sealing foam or hydrophobic coating |
| Polyimide foam | Imi-Tech | Requires sealing foam or hydrophobic coating |
| Ceramic tiles (aluminum oxide and silicon dioxide) | Lockheed | In development stage. Approx 4 pcf |
| Polyurethane and polyester foams | Illbruck | Requires sealing foam or hydrophobic coating |
| Copper and nickle foam metals | Hogen Industries | High cost |
| Aluminum and ceramic open cell foams | ERG, Inc. Astro Met, Inc | High cost (\$100 per cubic inch) |
| Silicon rubber based systems | CHR Div. of Furon Co. | Heavy |
| Fiberglass | Manville | Fluid absorption and sonic fatigue concerns |

From this list the following materials were chosen for normal incidence impedance tube and fluid retention testing:

Manville Fiberglass batt, Osaka Gas (ANA) Carbon fiber batt, Tex Tech Kevlar felt, Tex Tech Polyimide felt and Lockheed Ceramic fiber.

The fluid retention testing consisted of “ground–air–ground” simulation of a complete mission including takeoff, cruise and landing as well as fluid wicking testing. The ground–air–ground simulation consisted of 100 simulated flight cycles of temperature, pressure and humidity. The fluid wicking testing measured the weight gain after samples of the material floated on the surface of water, jet fuel and hydraulic fluid for 24 hours. The results were as follows:

Table 2: Fluid Retention Properties of Bulk Absorber Material Candidates

| MATERIAL | % WEIGHT GAIN | | | |
|--------------------------------------|-------------------------|---------|----------|-------------------------|
| | GROUND AIR GROUND | WICKING | | |
| | | WATER | JET FUEL | HY- DRAULIC FLUID |
| Fiberglass 1, .6 lb/ft ³ | 9.34 | 11 | 3620 | 7810 |
| Fiberglass 2, .4 lb/ft ³ | 7.03 | -2 | 4310 | 6460 |
| Fiberglass 2, 1.5 lb/ft ³ | 2.49 | 4 | 3540 | 4870 |
| ANA Carbon .44 lb/ft ³ | 1.09 | 2 | 6550 | 9290 |
| ANA Carbon 1.33 lb/ft ³ | 1.13 | 82 | 3950 | 5430 |
| Lockheed #13–031 | 0.27 | 1630 | 1020 | 1460 |
| Lockheed #11–107 | -0.15 | 1370 | 1050 | 1380 |
| Kevlar Style 4681 | 0.99 | 1910 | 1180 | 2510 |
| P84 Polyimide Style 4682 | 1.15 | 1760 | 9940 | 1580 |

Normal incidence impedance tube measurements before and after the ground–air ground cycling did not show any significant changes for any of the materials.

Normal incidence surface impedance and characteristic impedance measurements were made with a nominal material thickness of 3 in. for a frequency range of 200 to 6000 Hz. for the above materials. The characteristic impedance calculation followed the equations in Ref. 2 and Ref. 3 requiring measurements of surface impedance using two backing cavity depths. This is a new procedure at Boeing, but was easily implemented since our surface impedance measurement process automatically measures data either with zero depth backing cavity or 1/4 wavelength backing cavity depth (one tone frequency at a time).

The measured impedances were compared with the Delaney and Bazley (Ref.4) and the Voronina (Ref.5) impedance models. Figure 17 shows comparisons of the measured surface impedance with predictions using the above procedures for fiberglass with a nominal density of 0.44 lb/ft³. The Delaney and Bazley (D&B) prediction model requires input of bulk absorber resistivity and lining depth. For this prediction, the resistivity was calculated from an estimate of the fiber diameter and bulk density using the equation (Ref. 6):

$$R = (1.273 \cdot 10^{-3}) \rho^{1.53} / d_f^2 \quad (\text{cgs units})$$

(A nominal measured value of 18 cgs R/cm was also used for the D&B prediction of the 0.44 lb/ft³ material).

The Voronina (V) model requires input of material density, fiber diameter, fiber length and material thickness. Through experimentation it was found that the V model predictions were not very sensitive to the fiber length parameter, so a nominal value of 4 cm was used for all predictions. Both prediction procedures gave similar results for higher frequencies but the Voronina procedure appeared superior below 1000 Hz., particularly at higher densities.

The next set of figures compare measurements of characteristic impedance and propagation constant with predictions for the 0.44 lb/ft³ density fiberglass. Figure 18 shows measurements of both the surface impedance (8.5 cm thick material) and the characteristic impedance. The high frequency surface impedance data matches the characteristic impedance data as expected because of the large material thickness. Figure 19 shows measured and predicted characteristic impedance. Figure 20 shows the measured vs. predicted attenuation constant in dB/cm and Figure 21 shows the propagation speed to air propagation speed ratio vs. frequency. There were cases for which the agreement between the V model predicted trends and measurements were not as good as those shown in figures 18 – 21 and the reasons for these discrepancies have not been thoroughly pursued. The equation used to calculate the propagation constant from measured data is probably subject to large error when the characteristic impedance and measurement surface impedance are nearly equal. This suggests that thinner material samples may give better results for propagation constant at higher frequencies. Also, material fit within the impedance tube and methods for holding the material in place were found to be important elements in obtaining good data.

The above described acoustic and fluid retention testing led to the conclusion that all of the materials showed good acoustic attenuation properties for nacelle application, but the fluid absorption affinity is a major problem. The fiberglass and carbon fiber materials showed good results for water wicking and perhaps a fiber coating could be found to reduce hydrocarbon wicking. The manufacturer of the carbon fiber material, Osaka Gas, has been asked to investigate methods to reduce hydrocarbon wicking.

Osaka Gas has been responsive to helping develop nacelle application capability for their material to date. They recently experimented with methods for inserting the carbon fiber material into honeycomb core and returned samples to Boeing which are planned to be used for normal incidence impedance testing, with a full panel impedance meter now under development.

3.3.4 Linear Liners

Linear liners refer to liners with resistance elements whose resistance shows a small dependence on the SPL level of the sound incident on them. Fiber metal mesh and woven wire, usually overlaid on perforate plate for face sheets and without perforated plate for septa, are commonly used examples of linear materials. These materials usually have the additional properties of being insensitive to grazing flow variations and having mass reactances significantly lower than for perforates. The smaller mass reactance results in increased attenuation bandwidth. The

insensitivity to SPL and Mach number variations makes it possible to maintain liner impedance closer to desired values over the length of the liner while the sound levels are changing due to attenuation and the Mach numbers are changing due to duct cross sectional area changes. Also, increases in engine power setting result in SPL and Mach number increases. For the fan duct, uniform lining optimum impedances do not change with engine power setting, giving linear liners an advantage. For the inlet, the small increase in resistance which occurs with woven wire linear materials when SPL changes very nearly matches the increase in uniform lining optimum resistance as engine power is increased. While the woven wire and felted metal materials offer very good acoustic characteristics, problems with in-service maintainability has resulted in a strong resistance to their use. Non-Boeing manufactured nacelles and engine treatment sections have commonly utilized these materials in a single layer liner application but it is becoming increasingly common to see there use discontinued as repair becomes necessary. For these reasons, effort is being made to find alternative linear materials which can meet the multi-discipline requirements of noise, structures, maintenance, etc.

3.3.4.1 Slot Linear Liners

Under an AST subcontract to Boeing, Hersh Acoustical Engineering (HAE) developed an impedance data base for slotted perforates incorporating both normal incidence and grazing flow impedance data measured at NASA Langley. While there were some difficulties with the data, HAE concluded that the data was consistent with their in-house testing, showing good linearity and low sensitivity to grazing flow. Hersh also manufactured two test liners for grazing flow testing at the Boeing Wichita grazing flow test facility. Testing has been completed with the 0.002 in. width slot liner for the frequency range 1 to 6 kHz, SPL range of approximately 130 to 150 dB and grazing flow Mach number range of 0 to 0.50. Unfortunately there appears to be problems with the data. The 0.004 in. slot width liner was damaged in shipment and was not tested.

HAE consulted with Boeing nacelle structural design and manufacturing personnel with the objective of defining a method of manufacturing slotted perforates which meets nacelle structural and manufacturing requirements. HAE proposed a concept which, after preliminary study, was judged to only be suitable for non-load carrying designs and would be significantly heavier than current liners.

HAE has developed preliminary computer impedance models for both slotted and circular perforates under the AST contract. The circular perforate impedance models are for single orifices with thickness to hole diameter ratios of the order of 1. HAE reports on the orifice and slot impedance measurement and impedance modeling are contained as Appendices A1 and A2.

3.3.4.2 Micro-perforate Linear Liners

It is well known that as the airflow passages of the resistance element of the acoustic liner get smaller, the material gets more linear due to the increased importance of viscous losses compared to inertial losses. For this reason, it was decided to obtain data to quantify the relationship of small perforate geometry to acoustic impedance. Most of the data available was for perforates with hole diameters in the range of 0.050 in. whereas hole sizes of the order of .001 in. were believed to be necessary for linearity similar to woven wire materials. HAE therefore was given a subcontract to investigate the impedance properties of micro-perforate materials. The objectives of this work were:

1. Measure the acoustic impedance properties of micro-diameter perforates with and without grazing flow.
2. Develop a semi-empirical model for predicting the acoustic impedance of micro-diameter perforates.
3. Compare the acoustic properties of micro-diameter perforates with currently used perforates such as punched aluminum, woven wire and laser drilled thermoplastic.
4. Determine the advantages and disadvantages of using micro-diameter perforates for nacelle acoustic lining applications in place of current perforates.

HAE constructed resonators with face sheet orifice hole diameters ranging from .079 in. down to approximately .004 in. for acoustic impedance testing in the HAE wind tunnel. A brief description of the HAE Subsonic Wind Tunnel facility is contained in Appendix A2. Table 3 lists the geometry of the laser drilled micro-diameter resonators for which impedance data was measured by HAE. The schematic below defines the parameters listed in the table.

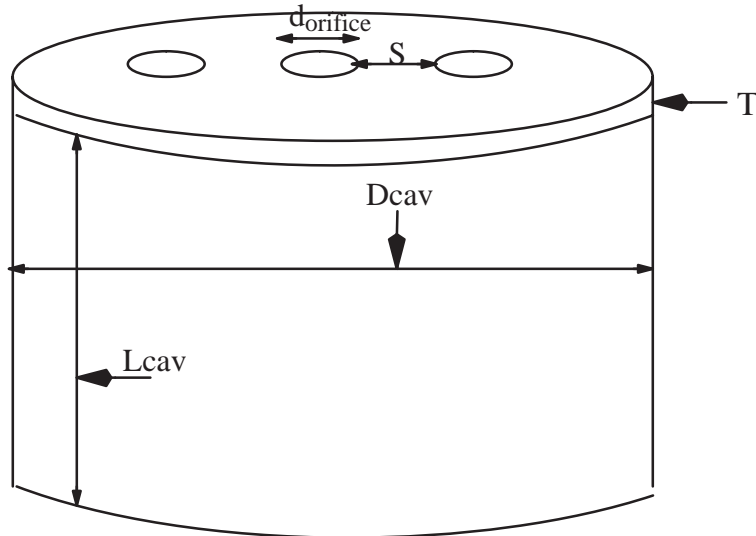


Table 3: Summary Of Micro-Diameter Resonator Geometry

| N, # of holes | d _{orifice} (inches) | S (inches) | S/d _{orifice} | Open area ratio | D _{cav} (inches) | L _{cav} (inches) | T (inches) | T/d _{orifice} |
|---------------|-------------------------------|------------|------------------------|-----------------|---------------------------|---------------------------|------------|------------------------|
| | | | | | | | | |
| 1 | 0.079 | | | 0.0343 | 0.3906 | 4.0 | 0.040 | 0.506 |
| | | | | | | | | |
| 4 | 0.0380 | 0.06 | 1.58 | 0.0379 | 0.3906 | 4.0 | 0.040 | 1.053 |
| | 0.0385 | 0.08 | 2.08 | 0.0389 | 0.3906 | 4.0 | 0.040 | 1.039 |
| | 0.0373 | 0.10 | 2.68 | 0.0364 | 0.3906 | 4.0 | 0.040 | 1.072 |

| | | | | | | | | |
|-----|--------|-------|------|--------|--------|-----|-------|--------|
| | | | | | | | | |
| 16 | 0.0210 | 0.03 | 1.43 | 0.0461 | 0.3906 | 4.0 | 0.040 | 1.905 |
| | 0.0213 | 0.04 | 1.88 | 0.0476 | 0.3906 | 4.0 | 0.040 | 1.878 |
| | 0.0213 | 0.05 | 2.34 | 0.0478 | 0.3906 | 4.0 | 0.040 | 1.878 |
| | | | | | | | | |
| 100 | 0.0063 | 0.012 | 1.91 | 0.0258 | 0.3906 | 4.0 | 0.040 | 6.349 |
| | 0.0061 | 0.013 | 2.64 | 0.0240 | 0.3906 | 4.0 | 0.040 | 6.557 |
| | 0.0063 | 0.020 | 3.18 | 0.0259 | 0.3906 | 4.0 | 0.040 | 6.349 |
| | | | | | | | | |
| 400 | 0.0035 | 0.008 | 2.32 | 0.0314 | 0.3906 | 4.0 | 0.040 | 11.429 |
| | 0.0031 | 0.010 | 3.21 | 0.0255 | 0.3906 | 4.0 | 0.040 | 12.903 |

Normalized acoustic resistance data for the resonators is shown in Figure 22 showing the dependence on sound pressure and grazing flow velocity. It is clearly seen that, as the orifice diameter decreases, the resonators become less sensitive to both of these parameters. Figure 23 shows the effect of grazing flow on the normalized acoustic mass reactance of the orifice system. At a grazing flow velocity of 77 m/s ($M=0.23$), the smallest orifice tested (approx. 0.004 in.) only reduces the mass reactance by a small amount. Unfortunately, the frequency limit of the HAE facility does not permit data to be taken above 1 kHz where the mass reactance for perforates can get very large. Reactance data is only shown for one SPL level since reactance did not vary strongly with SPL.

HAE has constructed a preliminary, semi-empirical impedance model for large T/d_{orifice} perforates based on the data collected in this effort. This work is contained in Appendix A3. Close examination of the tested orifice shapes under a microscope revealed that the hole shapes were somewhat irregular. HAE is therefore planning to make new samples using machine drilled perforates in thick face-sheets to provide the same range of T/d_{orifice} tested above. A data base will be generated including the effects of T/d_{orifice} , S/d_{orifice} , SPL, frequency, grazing flow velocity and boundary layer thickness.

Figure 24 compares the above measured resistance data from the $d_{\text{orifice}}=.0035$ in. sample with estimates of the resistance properties of currently used liner resistance materials. These include punched perforates with d_{orifice} and T approximately equal to .040 in., Boeing laser drilled septum material and woven wire overlaid over perforate plate. These materials were all chosen so as to have a normalized resistance of approximately $2q_c$ at SPL=135dB and grazing flow velocity of 70 m/s (the grazing flow velocity is 0 for the laser drilled septum). It is seen that the micro-diameter material behaved very similarly to the woven wire material showing much smaller dependence on SPL and grazing flow compared to the laser drilled septum and punched perforate used by Boeing today. A similar comparison is shown in Figure 25 for the mass reactance. Although data was measured for only a very limited frequency range, it appears that the micro-diameter material has less mass reactance than the punched perforate, but it is not as good as the woven wire material. The attenuation consequence of this will require higher frequency data but it probably would result in a lower attenuation bandwidth than that possible with the woven wire material.

4. Adaptive Acoustic Liners

4.1 Introduction

Two “adaptive” acoustic liner concepts were chosen for investigation. The first is a concept, discussed by P. Dean in 1976 (Ref. 7), uses a steady bias flow through the liner resistive elements to control the acoustic resistance. The second concept uses heating to increase the liner temperature which reduces the acoustic resistance by changing the local density. Both concepts are expected to change the acoustic reactance of the liners as well. The approach used to study the application of these concepts for nacelle acoustic liners was to study their effect on acoustic impedance with the Boeing lumped element liner impedance computer program (YMOD). This program uses a transmission line electrical analogy with lumped elements representing the elements of an acoustic liner. Existing semi-empirical models for perforated sheet and cavities with temperature dependence were used for the temperature variation calculations. The bias flow calculations were done using the Hersh orifice impedance model in Ref. 8 and Ref. 9 with the modifications suggested by Dean in Ref. 7. Using these element impedance models, liner impedance studies were conducted to define liners to be tested in the Boeing grazing flow impedance testing facility.

4.2 Bias Flow Adaptive Liner Design

Figure 26 shows the designs of the two adaptive liners manufactured for grazing flow impedance testing. The design objective for the bias flow liner was to have a double layer lining with a nonlinear perforate face sheet and septum which would have good impedance properties for a fan duct application when the local sound levels are high (as for takeoff), and use bias flow to maintain good fan duct impedance properties when the local sound levels are low (as for landing). Figure 27 shows the predicted behavior of the grazing flow test bias flow liner design as bias flow is increased at the landing condition local sound level condition (OASPL at lining approximately 130 dB, grazing flow $M=0.3$). At the time of this writing the test liner has been fabricated and tested in the Wichita grazing flow impedance measurement facility but the data has not been analyzed. The maximum mean Mach number attainable for this test data was 0.004.

Two significant effects of a bias flow mean Mach number of 0.002 are predicted for the test liner as shown in Figure 28. They are the removal of the strong anti-resonance around 2 kHz. and the increased resistance in the higher frequencies. Unfortunately, an error has been recently found in the perforate impedance model constructed from the above Refs. 8 and 9. The error involved using the bias flow velocity to modify the orifice unsteady velocity as well as including an additive resistance term proportional to the bias flow Mach number as recommended by Dean. When this error was corrected the anti-resonance at 2 kHz. does not disappear with bias flow. This prediction implies that the bias flow liner design chosen for testing will not fulfill the design objective.

Ingard and Ising (Ref. 10) recommend a resistance bias flow Mach number dependence similar to Dean for low SPLs but appear to conclude that bias flow will not strongly affect orifice resistance at high SPL. If this is the case the concept may not be applicable to aero-engine nacelles since the SPL’s even at landing within the nacelle are of the order of 140 dB. It is hoped that the test data will give some insight into the SPL dependence.

4.3 High Temperature Adaptive Liner Design

The high temperature liner design objective was to design a double layer lining with nonlinear perforate face sheet and septum which would have good fan duct impedance properties when the local sound levels were low and use heating to maintain good fan duct impedance properties when the local sound levels are high. Figure 29 shows the predicted behavior of the high temperature liner at takeoff for an assumed fan duct lining application. Note that this liner design is the same as the double layer liner tested in the passive liner program described above (Figure 11).

This liner was designed for a fan duct application at the airplane landing condition. At takeoff engine power, the liner is predicted to have a relatively high resistance due to a combination of the high grazing flow speed and duct OASPL. The strongest predicted effect of increased temperature within the lining appears to be a decreased resistance. In the non-linear region Ingard (Ref. 10) shows that the resistance of an orifice goes as Qv_{orifice} . Therefore, the reduction in density associated with an increased temperature should reduce the resistance. This analysis assumes that the liner temperature jumps discontinuously from the duct temperature. In reality this is not the case. In fact the grazing flow will act to cool the liner face sheet relative to the internal elements resulting in a relatively strong temperature gradient. Test data was measured in the Boeing Wichita grazing flow impedance with lining core temperatures to approximately 250 °F. This data has not yet been fully analyzed yet.

5. ADP Model Fan Acoustic Liner Design

In 1994 Boeing had recently completed a trade study ascertaining the value of advanced lining concepts for a broad-band spectra under a NASA/FAA contract. At this time PW and NASA decided to design, build, and test linings for the 22" Advanced Ducted Propulsor (ADP) fan rig to be tested at NASA LeRC. It was decided to have Boeing join the lining design/build team to offer expertise in the development of advanced lining concepts drawing on the earlier NASA/FAA study. Also, Boeing was asked to help determine the suitability of the ADP for a product including defining thrust and airplane performance for noise evaluation.

It was thought that the ADP engine would benefit from advanced (broadband) linings because it is a wide-chord fan engine with reduced tip speeds. This moves the BPF and harmonics down in frequency while the higher rotor/stator spacing and higher stator to rotor numbers help reduce the tone levels. The broadband noise still persists at higher frequencies and creates a situation where a broadband lining is required to attenuate both the tones and the higher frequency broadband noise.

The 22" ADP fan rig aft fan lining design was a joint effort with Boeing, Pratt and Whitney (P&W), Rohr, NASA LeRC, and NASA LaRC participating. Boeing had primary responsibility for the aft fan lining design with P&W providing consultation, Rohr had manufacturing responsibility, NASA LeRC provided the induct and far-field acoustic data for the design, and NASA LaRC provided overall program guidance and scheduling. The objective of the design was to demonstrate at least a 25% lining attenuations improvement relative to the previously tested "baseline" single layer linear design built by DEI and tested in 1995.

This report covers the design of the aft duct (fan-duct) liner for the 22" ADP fan rig. Each step of the process that was used to develop the final designs is described.

5.1 Aft Liner Depth Constraints

Initial depth constraints were defined by Pratt and Whitney and are shown in Table 4. Figure 30 shows the location of each liner segment. The lining segments C–H are in the aft duct.

Table 4: Preliminary 22" Fan Rig Lining Depth Constraints

| Liner Segment | | Max. Depth (in) | |
|--|-----------------------|-----------------|------------|
| Tag | Name | Model | Full Scale |
| A | Inlet | 0.70 | 4.14 |
| B | Aft OD Fan Case | 0.60 | 3.55 |
| C | Aft OD Aft Nacelle | 0.60 | 3.55 |
| D | Aft OD Forward Nozzle | 0.50 | 2.95 |
| E | Aft OD Aft Nozzle | 0.38(0.20) | 2.26(1.18) |
| F | Aft ID Aft Cowl | 0.38 | 2.26 |
| G | Aft ID Mid Cowl | 0.75 | 4.43 |
| H | Aft ID Aft Cowl | 0.38(0.20) | 2.26(1.18) |
| (x.xx) depth at minimum point – liner requires taper | | | |

The depth constraints for the aft duct basically fall into two categories: relatively thick constraints like Segments C, D, and G and thin constraints like Segments E, F, and H. Also, the thick lining depth constraints are generally opposite a thin lining depth constraint. This is important because it suggested the simplifying assumption of using lining with one depth on one side and another lining with a different depth on the other side of a rectangular duct model when using the Boeing rectangular duct propagation computer code for designing the model ADP fan duct linings.

After Rohr published the preliminary assembly drawings in early November 1996, it was noticed that the thin double layer liner design was too thick to fit into Sections E, F, and H at all places. In these sections the drawings showed the linings tapered in places by reducing the honeycomb core depth under the septum so that the lining would fit into the cavity.

Boeing decided to re-optimize the double layer lining design with a more severe lining depth constraint. This was done because we ultimately wanted to compare our predictions, based on the design impedance, to the measured data. The preliminary designs required enough liner area to be tapered that a significant proportion of the lining area would have a different impedance affected by the depth constraint and the predictions would not be valid. Discussions between Rohr and Boeing led to an updated maximum lining depth constraint of 0.285 inches compared to the 0.380 inches used initially. This minimized the lining area that was tapered to approximately 10% and only affected the double layer lining design. The single layer optimum designs could fit within the reduced depth constraint. The new, thinner lining constraint lowered the double layer sum PNLT attenuation (defined in section 5.4) by 0.6 dB from the value we had calculated with the older constraint.

5.2 Target ADP 22" Fan Rig Hardwall Fan Aft Fan Noise Spectra

A liner design is dependent on duct and lining geometry, modal assumptions, and far-field hardwalled spectra. In the 22" Fan Rig aft liner design, two different sets of far-field hardwalled spectra were used. The first set of spectra used were generated from the full-scale ADP Demo Engine data and were used to generate a preliminary liner design. Meanwhile, some preliminary hardwalled spectral data was taken with the 22" ADP Fan Rig with the composite blades. This data set was used to generate new target hardwall spectra which were used later in the program to refine the liner designs.

The metric used in certifying airplanes to the FAR 36 flight conditions is Effective Perceived Noise Level (EPNL), which is a time weighted sum of the tone corrected Perceived Noise Level (PNLT) calculated at 0.5 sec intervals as the airplane flies by the measurement point. Aft fan noise levels are important for all three of the FAR 36 flight conditions of approach, cutback, and sideline. Therefore, it was decided to evaluate a given lining design at all three conditions.

Since the EPNL metric is essentially the integration of the PNLT metric over time, we decided to choose hardwall design spectra representative of the peak PNLT levels. Examination of the PNLT versus emission angle showed that the peak PNLT for aft fan noise occurs near a 120 degree emission angle for all three FAR conditions; however, the tones in these spectra changed dramatically from angle to angle. It was decided to average two angles near 120 degrees to average out the tone level changes. A description of how each of the two sets of hardwalled design spectra were obtained follow in the next two sections.

5.2.1 ADP Demo Hardwalled Aft Fan Spectra

The first set of hardwall design spectra were generated from full scale ADP Demo data measured in 1992. This data set was for different geometry and Mach number than the FAR 36 operating conditions defined for the chosen design airplane which was a Boeing stretch 747. The ADP Demo Engine had a 110" fan which was different than the 130" fan required for a stretch Boeing 747. Also, operating conditions (Mach similitude) did not directly correspond to the conditions needed for the stretch 747 engine, particularly for the approach condition. Pratt and Whitney corrected the data to proper operating conditions before sending it to Boeing.

The ADP Demo Engine was not tested in a "hardwalled" configuration. Boeing therefore predicted the fan duct liner attenuation for the ADP Demo Engine and added it back to the scaled and extrapolated noise levels. This process, although crude, produced the best data set available at the time.

The ADP Demo Engine's aft lining definition used for the attenuation predictions is given in Table 5.

Table 5: Definition of the ADP Demo Aft Liner

| | |
|--|------------------|
| Resistance at V=105 cm/s, R105 | 60 cgs Rayls |
| Non-Linearity Factor, NLF | 1.60 |
| Lining Depth, D | 5.08 cm or 2 in. |
| Length to Height, L/H (includes aft fan case lining) | 2.3 |
| Crossover Frequency, fc | 30,000 Hz. |
| BL Momentum Thickness, Θ | 0.3 cm. |

The L/H used for the fan duct included the lining in the interstage area. The attenuations added back to the treated spectra included the effect of the interstage lining. Later in the program, it was decided that the interstage would be handled separately from the aft fan lining. Therefore, the levels used to define the hardwall spectra for the ADP were slightly too high in that they added the attenuations in the interstage area. This difference, although small, was not accounted for.

Figure 31 shows that the far-field, Noy weighted SPLs vary from angle to angle; this is especially true of tones. It was therefore decided to average the 110 and 120 degree spectra to generate a lining design target hardwall spectrum that would not over or under emphasize tones. Figure 32 shows the hardwall design spectrum shapes obtained from the ADP Demo Engine data in this manner.

5.2.2 22" ADP Fan Rig Hardwalled Spectra

There was concern about the validity of the ADP Demo Engine data to predict the 22" ADP Fan Rig hardwall spectra. During a 1995 workshop held at NASA Langley, some preliminary 22" ADP Fan Rig hardwalled data was shown. It was decided during this workshop that the preliminary hardwall data from the 22" ADP Fan Rig would be used to redefine the design hardwalled spectra. Clearly a better definition of the hardwalled design spectra should improve the liner design.

Pratt and Whitney, working with NASA Lewis, produced the hardwall data at the FAR 36 flight conditions. Some interpolation was necessary to produce these data.

Figure 33 shows the approach, cutback, and sideline conditions, respectfully, at the 110, 120, and 130 degree angles. Note that there are some large variations between the spectra particularly at BPF harmonics. Again the process of averaging the 110 and 120 degree angles was used to minimize these fluctuations to produce the hardwall design spectra shown in Figure 34.

5.3 Liner Design Points for the Aft Fan

The aft liner design points were chosen by considering the contribution of the aft fan noise component at each of the FAR 36 conditions (approach, cutback, and sideline). It is known that the cutback condition is aft fan noise dominated. Typically, aft duct liners are designed for cutback condition at Boeing.

The sideline condition, typically dominated by jet noise for lower BPR engines, is dominated by aft fan noise for the ADP because the jet noise levels are very low due to the low jet velocities associated with the ADP engine configuration. Therefore, a lining design for an ADP engine should address the sideline condition.

The approach condition was more of a surprise. Upon examination of the approach condition for the ADP engine one notes that the contribution of aft radiated fan noise is nearly as significant as the inlet radiated fan noise. For these reasons, we chose a combination of the attenuations at the approach, cutback, and the sideline conditions for the design metric. More specifically, we chose:

$$J = \sum_i^{ap, cb, sl} PNLT \text{ Attenuation}_i$$

where J is the cost function which we want to maximize for the best design and is defined as the sum of the PNLT attenuations of the target spectra at the approach, cutback, and sideline conditions.

A better cost function could be developed that considered the masking of aft fan noise by other components, but was not used here. A good definition of the other full-scale engine components was not available for this design.

Typically in-duct SPLs need to be considered during a liner design for each operating condition. In-duct SPLs affect liner impedances by changing the particle velocity through the resistive layers. In this application, however, the impedance of the resistive layers used was only slightly sensitive to SPL. This is best shown by pointing out that the non-linearity factors (NLF) for the materials considered were between 1.2 and 1.4. The non-linearity factor is defined as the ratio of the resistance at 200 cm/s divided by the resistance at 20 cm/s. Values below 1.4 show the material to basically be linear. Perforate liners, on the other hand, have effective NLFs of 10–15.

5.4 Source Noise Modal Energy Assumptions

The modal energy assumption affects both the optimum lining design impedance and the maximum lining attenuation. For this lining design, a modal energy distribution believed to be appropriate for random broad-band noise was used. This assumption is nearly an equal energy modal assumption where the propagating energy of each cut-on mode is identical. The Boeing assumption and an equal energy assumption are the same except near cutoff. The Boeing assumption forces lower energies near cutoff whereas the equal energy assumption would force

extremely high SPLs for modes near cut-off because the energy transport rate down the duct is very small for modes near cut-off. The difference between the Boeing assumption and the equal energy assumption probably does not have a significant effect on the resulting lining design since the modes near cut-off attenuate rapidly down the duct even if the lining design is not optimum for these modes. The energy assumption used by Boeing is:

$$\int_s p^2 dS = \text{constant for each mode}$$

or the integral of the pressure squared over the cross sectional area is constant for each mode.

At the beginning of this program it was anticipated that measurements of the modal energy distributions for the model ADP aft fan noise would be available for use for the lining design. Unfortunately NASA Lewis had problems with the fan duct modal measurement process and were not able to develop this information. As a result, there is no experimental verification of the Boeing modal distribution assumption.

It is believed that the use of a broad-band energy assumption should work well for the ADP. The larger diameter and reduced tip speeds create a situation where the rotor stator interaction generated BPF is always cutoff and at a lower frequency than conventional engines. The rotor stator interaction will cut-on the 2 BPF; however, the 2 BPF still does not dominate the far-field spectrum as can be seen by the Noy weighted design spectra in Figure 34.

The Boeing lining design and attenuation prediction processes used in this exercise use an empirical procedure to radiate noise to the far-field. Although some work was done to create a process to radiate energy based on the work of Rice (Ref. 12), time constraints forced us to use the older, established radiation process. This lining design maximized the PNLT attenuation of the input spectra using the power attenuations at each frequency within an infinite duct. A process that radiates each mode to the far-field and evaluates the attenuation at each angle should perform better and allow the use of hardwalled data at each angle.

5.5 Optimum Liner Impedance for the Aft Fan

The optimum liner impedances were determined using Boeing's Multi-Element Lining Optimization (MELO) program. The MELO program is an infinite duct, modal attenuation code. Given a rectangular, circular, or an annular duct geometry, the program calculates the duct eigenvalues which are directly related to the attenuation per unit duct length of a given mode. Multiplication by the lining length and summing over all the cut-on modes results in the attenuation for a given frequency.

As an infinite duct program, MELO does not consider changes in impedance down the duct. MELO does have the ability to handle a mean flow velocity in the duct with a boundary layer profile. Built around the modal attenuation prediction capability is an optimizer capable of changing the lining impedance to maximize the resulting attenuation. In this manner, an optimum, axially uniform impedance versus frequency can be determined.

The representation of the ADP fan duct lining with MELO is shown in Figure 35. A two dimensional, rectangular duct is assumed with the height of the duct chosen as the average height of the fan duct in the lined region. The lining length input into the MELO program was obtained by measuring the total duct lining length. No credit was taken for lining outside the nozzle exit plane. Different linings were allowed on the two sides of the duct to model the two lining depth constraints for this design. From Figure 30 we see that for the most part a thick

lining depth constraint is across from a thin lining depth constraint. Although the depth constraints swap going down the duct (the thick and thin constraints switch sides) we modelled the geometry by leaving the geometry on each side the same down the duct. This may be a conservative assumption because no credit is taken for modal scattering at the impedance discontinuities.

The optimum uniform impedance versus frequency plot produced with MELO is shown in Figure 36. Only one curve is shown representing the approach, cutback, and sideline conditions. Unlike the shorter inlet, the optimum impedance of the fan duct changes very little with operating condition. Figure 37 shows the predicted optimum impedance at several fan speeds (duct Mach numbers) initially predicted in the program.

In determining the optimum, axially uniform impedance for this ADP lining design, the following assumptions were made:

1. Assumed a two dimensional rectangular duct with different linings on each side
2. Assumed a linear boundary layer profile with momentum thickness of 0.3 cm.
3. Assumed all possible cut-on modes with a modal energies as discussed in Section 3.5.2

The two dimensional rectangular duct was chosen instead of the annular duct because the eigenvalues could be calculated much faster and without having eigenvalue failures. The optimum impedance did not change appreciable by using a rectangular instead of an annular representation of the fan duct as can be seen in Figure 38. Notice that the rectangular and annular duct solutions for optimum impedance are almost identical. This probably because the optimum impedance is controlled mainly by the lowest order modes. Note that for frequencies greater than 3150 Hz that there are no solutions shown for the annular duct. This is due to eigenvalue failures of the MELO program.

The MELO program allows a boundary layer profile to be specified. The effect of the boundary layer on optimum impedance is primarily at the higher frequencies where it increases the reactance and resistance. Figure 39 shows a comparison of the predicted optimum impedance with and without a 0.3 cm thick boundary layer momentum thickness. The boundary layer velocity gradient will tend to bend waves toward the lining for wave propagation in the same direction as the flow, increasing the incidence angle. It is expected that this would increase the optimum reactance (toward zero) but decrease the optimum resistance. The reasons why the boundary layer drove the optimum resistance higher and the optimum reactance to positive values at high frequencies were not investigated.

5.6 Design Methodologies for the Aft Duct

The process used to determine the aft fan duct liner is graphically shown in Figure 40. A description of each block follows.

5.6.1 Optimize Lining Parameters to Match Admittance

The lining's admittance (1/impedance) is matched to ideal admittance calculated with MELO (see Section 5.6) using Boeing's YMATCH program. The YMATCH program uses the lining parameters and constraints, target admittance, and frequency weightings to solve a least squares optimization problem resulting in a lining which minimizes

$$\Sigma[\text{Weight}(f) (\text{Y}(f)_{\text{Target}} - \text{Y}(f)_{\text{Trial}})^2]$$

The lining parameters define the independent and dependent variables in the optimization problem. For the ADP lining study these variables were the depth of the cavities and the resistances of the resistive layers. Additionally, constraints can be set on the problem. One example of a constraint would be a maximum depth constraint so the output liner could fit in the cavity. The target admittance/impedance spectra used for this design was the optimum impedance defined by MELO .

The frequency weightings are multiplied by the square differences between the target admittance and the calculated admittance. In this way, one can highlight important frequency regions where the liner and target admittances should be close. The six sets of frequency weightings used in the 22" ADP fan rig lining design optimization are shown in Table 6.

Table 6: Frequency Weightings Used for YMATCH by Band Number

| # | B27 | B28 | B29 | B30 | B31 | B32 | B33 | B34 | B35 | B36 | B37 | B38 |
|---|-----|-----|-----|-----|-----|-----|-----|-----|-----|-----|-----|-----|
| 1 | 1 | 1 | 3 | 3 | 3 | 3 | 3 | 3 | 3 | 3 | 1 | 1 |
| 2 | 0 | 1 | 1 | 1 | 1 | 1 | 1 | 0 | 0 | 0 | 0 | 0 |
| 3 | 0 | 1 | 2 | 1 | 1 | 1 | 1 | 0 | 0 | 0 | 0 | 0 |
| 4 | 0 | 0 | 0 | 0 | 1 | 1 | 1 | 1 | 1 | 1 | 0 | 0 |
| 5 | 0 | 1 | 2 | 1 | 0 | 0 | 0 | 0 | 0 | 0 | 0 | 0 |
| 6 | 0 | 0 | 0 | 0 | 1 | 1 | 1 | 0 | 0 | 0 | 0 | 0 |

The weightings are shown as a function of one-third octave band number. Band 27 would represent a 500 Hz center frequency and Band 38 represents a 6300 Hz center frequency. Note Weighting #1 has coefficients over 12 one-third octave bands or 4 octaves. Resulting YMATCH designs with this weighting set produced liners with impedance spectra that matched the optimum impedance at bands B30 to B35, but could not match the target outside these frequencies. Examination of the outputs from YMATCH show that single layer linings can match the target impedance over one octave and double layer linings can match a target impedance over two octaves.

YMATCH exhibits some starting point dependence for the output lining. To assure the “best” solution is found, multiple starting points are used and the lining is chosen that “best” matches the admittance target. This is accomplished by a global option that exists within the YMATCH program.

The liners that are output from the YMATCH optimization are next evaluated using a noise metric. Specifically, the lining definitions and hardwall spectra are input into MELO. MELO then calculates the predicted PNLT attenuations that each lining would produce assuming that the lining is on each side of the duct using geometry of Figure 35. These data were used to evaluate which uniform linings perform best.

It should be mentioned that there is a “factor” applied to the calculated attenuations within MELO. This “factor” is an empirical correction of the MELO predicted attenuations to match full-scale measured lining attenuation data. The accepted “factors” used at Boeing are 1.0, 0.8, 0.6 for the approach, cutback, and sideline conditions respectfully. The factors were applied to all the MELO duct attenuation predictions made in this design study.

5.6.2 Optimize PNLT Attenuations (both sides the same)

The next step in the lining design process (the second bubble in Figure 40) was to use MELO to optimize the lining using PNLT attenuation as the cost function. The reason that the YMATCH process was done first is it provided a good starting point for this optimization problem.

Like the YMATCH process, sometimes local maxima instead of global maxima are found in the MELO optimization. Using YMATCH helped minimize, but not completely eliminate, this problem. A global optimization using many starting points was not done in MELO because it would take much too long. Just one optimization takes about 30 minutes. If we used 50 different starting points to make sure we obtained a global optimum, it would take 25 hours.

This process was run with both double and single layer linings, two lining depth constraints, three far-field hardwalled spectra, and three in-duct spectra. Twelve different optimum linings were defined in this process (two lining types times two depth constraints times the three operating conditions and their associated spectra).

5.6.3 Optimize PNLT Attenuations (allow two sides to be different)

In this part of the lining design process the lining was allowed to be different on each side. One side was given a thick total lining depth constraint and the other a thin depth constraint. The lining starting points were the best linings as determined the last step in the process (Optimize PNLT attenuations – both sides the same).

The output from this process was a lining definition for each of the FAR 36 flight conditions (approach, cutback, and sideline) for both single and double layer linings.

5.6.4 Calculate the Cross-Performance

The final step in determining the best lining was to determine the cross-performance. For each of the linings generated from the last step, the attenuations at the other two operating conditions was determined. Then the PNLT attenuations were summed for each lining over the three operating conditions. The best single and double layer linings were chosen as the linings that gave the highest sum PNLT attenuations.

5.7 Predicted Liner Attenuations for the Aft Fan

The final linings and sum PNLT attenuations at approach, cutback, and sideline are shown in Tables 7 and 8.

Table 7: Single Layer/ Single Layer Final Designs

| Side | Rfs (cgs Rayls) | Dfs (full scale) (cm) | Σ Atten (PNLT) |
|------|--------------------|--------------------------|--------------------------|
| 1 | 70.6 | 2.11 | 13.5 |
| 2 | 68.0 | 4.64 | |

Table 8: Double Layer/ Double Layer Final Designs

| Side | Rfs (cgs Rayls) | Dfs (full scale) (cm) | R sep (cgs Rayls) | Dsep (full scale) (cm) | Σ Atten (PNLT) |
|------|--------------------|--------------------------|----------------------|---------------------------|--------------------------|
| 1 | 49.8 | 1.40 | 88.2 | 2.72 | 16.6 |
| 2 | 12.9 | 2.10 | 53.1 | 3.87 | |

NOTE:

Rfs – Resistance of face sheet in cgs Rayls at V=105 cm/s

Dfs – Core depth of upper cavity in cm at full scale (scale factor=5.91)

Rsep – Resistance of the septum in cgs Rayls at V=105 cm/s

Dsep – Core depth of upper cavity in cm at full scale

Σ Atten – Σ PNLT Attenuations at approach, cutback, and sideline

The one-third octave band attenuations versus frequency are shown in Figure 41 for the cutback conditions. Recall the cutback condition has a “factor” of 0.8 multiplied by the attenuations within MELO. There are four lines on the plot representing the optimum (at optimum impedance), the double layer, the single layer, and the baseline single layer lining attenuations. The baseline liner was a DEI built lining that was scaled from the ADP Demo Engine Test. Examination of the attenuation plot shows that the DEI liner is tuned near 1000 Hz and its attenuation falls off rapidly with increasing frequency. This lining looks like it was tuned to lower the 2BPF tones. Recalling Figure 33 we see that the frequencies above 2BPF have NOY values equal to or greater than the 2BPF band. Therefore, the lining should be tuned at higher frequencies to equally attenuate them while attenuating 2BPF.

The single layer design attenuation spectrum resulting from this study is centered around 1600 Hz and has a broader bandwidth than the Baseline design. Notice the baseline liner attenuation spectrum is much more peaked than the optimized single layer design. The broader bandwidth was accomplished by having different depth liners on each side of the duct as well as tuning the lining to a higher frequency. Figure 42 shows the impedances for the liners on each side. Side 1, the thinner, matched the optimum resistance and reactance in the 1600–2000 Hz range and side 2 matches the optimum reactance near 1000 Hz. Generally attenuation falls off rapidly as the resistance falls below the optimum and fairly slowly as the resistance goes above the optimum. The fall off of attenuation as the reactance deviates from the optimum value is more symmetrical with a slope between that for increasing and decreasing resistance. Of note is the small variation of the liner impedances with engine power condition because of the linearity of the face sheet.

The double layer design showed the best overall attenuation and has the broadest bandwidth as expected. MELO predicted at 3.3 dB attenuation improvement summed over the approach, cutback, and sideline conditions relative to the optimized single layer design. The impedance plots, shown in Figure 43, show how the two lining impedances of each side match the optimum impedance. Side 1, the thinner side, nearly matches the optimum reactance in the 1200–4000 Hz range. Side 2 matches the optimum resistance and reactance at 900 Hertz and is pretty close for resistance and reactance from 1000–2500 Hertz. This is consistent with the attenuation plot which showed the double layer liner performing well from 800–4000 Hertz. Again the linearity of the face sheets and septa result in small changes of the impedances with engine power condition.

5.8 Conclusions

The double layer design showed the best overall attenuation and had the broadest bandwidth as expected. A 3.3 dB attenuation improvement summed over the approach, cutback, and sideline conditions relative to the optimized single layer design was predicted. Using different designs on opposite walls within the duct improved the predicted attenuation bandwidth. This is consistent with the attenuation plots which showed the double layer liners performing well from 800–4000 Hz and the single layer liners performing well from 1000 Hz–2500 Hz.

Unlike the shorter inlet, the optimum impedance of the fan duct changes very little with operating condition. It is believed that the reason that there is such a small change is that the optimum impedance is primarily controlled by the lowest order modes due to the large length to height of the duct, L/H.

The effect of the boundary layer on optimum impedance is primarily at the higher frequencies where it reduces the reactance and increases the resistance slightly. One possible explanation of the high frequency behavior has been suggested. The boundary layer velocity gradient tends to bend waves toward the lining increasing the incidence angle and thus increasing the reactance (toward zero). However, this should reduce the optimum resistance which is opposite to the duct propagation code calculation. The reason for this behavior is not understood.

The use of a random broad-band energy assumption is believed appropriate for the ADP. The larger diameter and reduced tip speeds create a situation where the rotor stator interaction BPF is always cutoff and at a lower frequency than conventional engines. The rotor stator interaction will cut-on the 2BPF, however, the 2BPF still does not dominate the far-field spectrum as can be seen by the Noy weighted design spectra.

Examination of the outputs from the impedance design study with YMATCH show that single layer linings can match the target impedance over one octave and double layer linings can match a target impedance over two octaves.

The design process of using an impedance optimization to various frequency weightings followed by an attenuation evaluation to determine a preliminary design and using this preliminary design as a starting point for the attenuation optimization seemed to work well. At Boeing we have had problems with optimizers with liner design to an attenuation cost function. Common optimization problems with local minima and constraints are made more severe by the large number of parameters being optimized. The pre-optimization of the impedance to the target impedance seemed to improve the reliability of the final attenuation cost function optimization.

6. Evaluation of Broadband Liners for a Med-Sized Twin Engine Airplane

The objective of this task was to evaluate the passive duct lining concepts considered earlier (Sec. 3) and the design experience from the model fan duct ADP design (Sec. 5) by applying them to an airplane analysis. Section 3 discussed the evaluation of broad-band lining concepts (linings that have a favorable impedance over a larger frequency range) for a target SPL 1/3 octave spectrum that was flat over a large frequency range(500 Hz to 4 kHz). This design case was chosen because new generation wide-chord fan engines require attenuation over a wide frequency range. A more representative evaluation of the technologies evaluated in the earlier studies could be done by choosing a specific airplane and engine type. Also, the study was expanded to include technologies other than those limited to changing liner impedance, which included increased acoustic lining coverage within an existing nacelle envelope and the “scarf” inlet concept.

This section is organized into three major sub-sections. The first sub-section contains introductory material and includes a description of the details which define the study. The next sub-section covers the results for the trade studies conducted for inlet noise propagation and radiation. The final sub-section describes the trades that were carried out for fan duct noise propagation and radiation.

6.1 Program Overview

6.1.1 Airplane/Engine Definition

The airplane/engine configuration decision controls the engine noise signature and airplane operating conditions which in turn establishes the target noise spectra to be attenuated.

6.1.1.1 Airplane Definition

For this study a mid-sized, twin engine airplane was suggested by NASA LaRC. It was originally suggested that the mid-sized, twin engine airplane defined in a report by Kumasaka (see Ref. 13) would be used as the study airplane. However, the report did not specify all of the parameters needed to accomplish this trade study and additional assumptions about the study airplane were required. This was particularly true in two areas. The first was the desire to consider a wide-chord fan, mid-twin airplane which was not considered in Ref.13. The other was that the definition of the nacelle configuration for the baseline airplane was not specified in Ref.13. Lining coverage area and duct lengths needed to be established to do the study. These areas and lengths varied depending on which of the three engine nacelles currently on the 767 airplane was considered. A nacelle was defined that represented what Boeing was able to manufacture in 1992 and the baseline lining in the nacelle was the best lining that we could have designed in 1992.

The Boeing 767, being a mid-sized twin engine airplane, was used to generate most of the airplane performance data needed for the study. Table 9 shows the operating conditions for the FAR 36 certification flight conditions chosen.

Table 9: FAR 36 Operating Conditions for Trade Study Airplane

| Condition | Altitude (ft.) | Sideline (ft.) | Thrust (lb.) | Mach |
|-----------|----------------|----------------|--------------|------|
| Approach | 394 | 0 | 10,900 | 0.23 |
| Cutback | 1452 | 0 | 30,800 | 0.30 |
| Sideline | 1085 | 1476 | 44,600 | 0.30 |

6.1.1.2 Engine Definition

The thrust requirements for the mid-sized twin engine airplane, as defined in Table 9, require approximately a 90 in. diameter fan. Both wide chord and narrow chord fan engines were considered for this study. Current wide chord fan engines have approximately 20 fan blades while narrow chord fans have approximately 40 blades.

6.1.1.3 Nacelle Definition – Inlet

The nacelle inlet definition determines the location and amount of lining in the inlet. For the mid-sized, twin engine trade studies, the baseline nacelle was chosen to be made from aluminum. The panel splices for such a nacelle would be on the order of 2.7 in. wide, with three axial splices in the inlet.

The inlet baseline nacelle was defined not to have lining next to the fan face. Lining in this region can increase the inlet tone levels enough that hard-walling this region reduces the inlet noise. The effect is caused by the circumferentially non-uniform lining near the fan.

Also, the lining was defined to extend forward to the throat of the nacelle, but not past. This is generally the current requirement for lining in the forward section of the inlet. The length to radius ratio for this nacelle is approximately 0.6.

Figure 44 is a schematic of the nacelle used for the study. Note the inlet splices and the hardwalled area near the lining lip.

6.1.1.4 Nacelle Definition – Aft Duct

The nacelle is much easier to define for the aft duct because the uniform, infinite, rectangular-duct analysis program does not require an exact definition; since it is not capable of analyzing the effect of lining non-uniformities and 3 dimensional geometries like the inlet analysis program. All that is required is a lining length and a duct height to represent the annular fan duct. Figure 45 shows the representation of the fan duct.

6.1.2 Target Spectra

Target hardwall one-third octave SPL spectra were generated for the three FAR 36 certification conditions for both the narrow chord and wide chord engines. The target spectra are generic representations of the narrow and wide chord fan engines and do not represent any particular engine. Boeing technology is well established to predict the attenuations of linings in the inlet and the fan duct. However, in the interstage area, between the fan rotor and the stators, it is difficult to predict acoustic lining attenuations for the inlet or aft fan noise components. Therefore, hardwall target spectra were generated from test data with interstage lining present. No analysis was done to evaluate interstage lining improvements.

6.1.2.1 Inlet Noise

Figure 46 shows the Noy weighted SPLs for the FAR 36 extrapolated conditions for the inlet radiated fan noise source component for both the narrow and wide chord fan engines. These

data were used as the target spectra for the trade study. Note that the narrow and wide chord fans have similar broadband noise, but the narrow chord engine's tones are at higher frequencies than the wide chord engine's. To attenuate both the peak Noy frequencies and provide attenuation at the tone frequencies, which provide a tone correction penalty, requires an extremely broad-band liner for the wide chord engine.

Also, the peak Noy weighted noise occurs at higher frequencies for approach than the higher RPM cutback or sideline conditions. This counter-intuitive observation is primarily due to atmospheric absorption. The atmospheric absorption increases with frequency and the propagation distances for cutback and sideline are considerably longer than the approach distance (see Table 9). Therefore, the cutback and sideline noise levels roll-off at higher frequencies.

6.1.2.2 Aft Fan Noise

Figure 47 shows the Noy weighted SPLs for the aft radiated fan noise source component at the 120 degree emission angle. The data look similar to the inlet noise data discussed above and similar observations can be made.

6.1.3 Types of Nacelle Noise Suppression Technologies

Inlet and aft fan noise suppression technologies studied can roughly be grouped into three categories if changes to the engine hardware are not allowed. These are lining impedance, lining area, and configuration technologies.

In its simplest form, lining impedance noise attenuation technology attempts to build a lining which matches a uniform optimum impedance target over a wide frequency range. This was the approach taken for the present study. A previous analytical inlet lining optimization study conducted at Boeing, using an early version of the ray tracing code used for the present study, showed only a small benefit for varying optimum impedance within an inlet compared to a uniform optimum impedance. Since a ray tracing code does not include modal or scattering effects the possible benefits of scattering were not considered in these optimizations. The lining designs of the present study were primarily aimed at broadband noise, so it was felt that consideration of detailed modal effects were not necessary because of the large number of modes supported by the inlet.

The analysis code used for the fan duct lining study is a very simplified duct wave propagation code which only considers rectangular or circular/annular, axially uniformly treated, infinitely long ducts. Therefore, this code is not capable of analyzing the effect of varying duct geometry, varying impedance or modal scattering. Boeing has found that using the rectangular duct option to model fan ducts does a good job matching engine test data for approach engine power but over predicts engine test data by approximately 20% at cutback engine power and 40% at takeoff engine power. The rectangular duct assumption was used for the present fan duct lining study. The conclusions reached from this study are therefore limited to fan ducts for which the computer modeling assumptions used hold, i.e. broadband noise in relatively long ducts with slowly varying geometry and uniform impedance. While it is understood that this is a fairly limiting set of constraints it was felt that the study was still useful for studying large bandwidth liners; especially since lining attenuation predictions with this code have compared well with engine data in the past. These studies did indicate that there may be a benefit from modal scattering in a fan duct due to the difficulty of attenuating low order modes. This indicates that a fan duct lining configuration which first uses a section of lining to attenuate higher order modes,

is then followed by some method of scattering the low order mode energy into higher order modes (e.g. a reactive lining) and is then followed by an additional lining section to attenuate higher order modes could improve attenuation relative to a uniform lining. It is planned to study this concept when a new 3D code, being developed by Boeing under the AST contract, is available.

Uniform lining impedance technologies use broadband or adaptive liners to better match the liner impedance to the ideal impedance over more frequencies and/or operating conditions. Examples would be linear liners, triple layer liners, parallel element liners, or bias flow liners.

Lining area technologies can improve attenuations by the elimination of hardwall areas in the form of panel splices, areas near the fan or near the anti-ice bulkhead and replacing them with lining. While this technology development was not an explicit element of the AST program, the inlet noise trades show that this technology may be valuable.

Configuration technologies modify the nacelle, not the engine, to change the radiation directivity or propagation of the source noise from the engine. The scarf inlet and sonic inlet are two examples of this type of technology.

This study primarily considers uniform lining impedance changes made through the use of broadband linings. However, some lining area and configuration change results from an internally funded inlet studies are briefly discussed.

6.1.4 Linings Evaluated in the Study

Six different linings were considered in the lining impedance studies for the mid-sized, twin engine airplane. They were single, double, and triple layer perforate and linear liners (see Figure 48).

Single, double, or triple layer liners refer to the number of resistive layers in the lining. The single layer liner has a resistive facesheet with a backing cavity. The double layer liner adds a resistive septum and a backing cavity while the triple layer adds two septa and cavities in series.

The linear or perforate liner classifications refer to the type of resistive layer. Linear liners are often made of wire and are sometimes called wire liners in these studies. They resist flow through them predominantly by viscosity and tend to have resistances that vary only weakly with particle velocity. Perforate resistive layers, on the other hand, use non-linear jetting as the primary loss mechanism and are dependent on particle velocity.

6.2 Inlet Trade Studies

The inlet trade study was only performed at the approach condition. This condition requires the widest liner bandwidth because the target spectra are generally broader. Therefore, the study examined the condition where liner technology should make the largest difference. However, the trade of how different liners work at off-design conditions is clearly absent and deserves attention. Some “quick look” data suggests that some of the advanced liner concepts may work better at the off-design points and thus their value may be underestimated with respect to a single point design.

The inlet component trades are based on an inlet fan noise source component Effective Perceived Noise Level (EPNL) metric. The use of component EPNLs can be problematic because of other components masking certain frequencies in the complete noise signature. This is particularly a problem when calculating tone corrections that are applied to the Perceived

Noise Levels (PNL). It may be desirable to define other noise components so the value of a change could be evaluated in the overall delta EPNL of the airplane. In practice, however, this is difficult because the answer is dependent on the other source levels which are also changing in the context of the total AST program.

6.2.1 Technologies Evaluated

The primary focus and original reason for doing this study was to look at how much noise improvement would result from applying uniform liner impedance control technologies. Uniform impedance technology improvements refer to the use of advanced linings to better match the optimum impedance over a larger frequency range. As mentioned above, a previous study showed that varying impedance over the inlet lining did not provide appreciable benefit over a uniform optimum impedance.

Some trade studies were also performed to evaluate lining area changes for the inlet. In particular, lining area changes associated with the ability to minimize segment splices in linings to 0.5 inches were studied. Smaller splices also allowed lining to be added near the fan where lining had been removed to reduce BPF tone noise generated by scattering of cut-off modes. Finally, the effect of lining extended from the throat up to the anti-ice bulkhead of the inlet was considered.

Trades were also performed to determine the value of a scarf inlet. A triple layer lining was chosen and the value of a scarf with different lining coverage areas was determined.

6.2.2 Liner Depth Constraints

A two inch depth constraint was used for the inlet of the study airplane. This constraint may be a little conservative in that there may often be more room in the barrel part of the inlet. However, near the fan-face two inches is a reasonable limit because of blade containment issues. Also, most of the lower degree of freedom liners optimized to a thickness that was considerably thinner than the 2 inch constraint. The triple layer linear liners optimized to the 2 in. depth constraint and may have benefitted from additional depth.

6.2.3 Source Assumptions

The analysis code used for the inlet trade study was a Boeing ray tracing code called RDIFF. The source region used in RDIFF for this study was a source covering the outer half of the annulus formed between the fan containment ring and the centerbody at the station containing the fan. This is the red region shown in Figure 44. Past experience has shown that this source location area results in radiation predictions which match the measured data well.

RDIFF assumes that all the rays that go from the receiver to the source are uncorrelated or equivalently any two different points on the source region are uncorrelated. As a result of this source distribution, RDIFF predicts broad-band attenuations well, but does not do as well predicting tone attenuations. Tone attenuations would be dominated by a few propagating modes whereas the source distribution defined has many modes and is more like a broad-band source. Past experience shows that RDIFF typically under-predicts the tone attenuations.

6.2.4 Optimum Liner Impedances

The optimum or “target” uniform lining impedance used in this study was $Z = 2.0 - i 0.5$ when normalized by qc . This target was based on experience from running the RDIFF program in previous studies.

6.2.5 Evaluation Process

The evaluation process used for this trade study is shown in Figure 49. There are basically four steps to the process which are described below.

6.2.5.1 Optimize Lining Parameters to Match Admittance

The lining's normalized impedance is “matched” to the normalized optimum impedance of $2.0 - i * 0.5$. This target impedance was chosen because it represented the current thinking at Boeing on the best inlet impedance. The YMATCH program uses the lining parameters and constraints, target impedance, and frequency weightings to solve a least squares admittance (1/impedance) optimization problem resulting in the best lining.

$$\text{Min } \Sigma[\text{Weight}(f) (Y(f)_{\text{Target}} - Y(f)_{\text{Trial}})^2]$$

The lining parameters define the independent and dependent variables in the optimization problem. For this study the independent variables were the total lining depth, depth of all but one of the cavities and parameters controlling the resistances of the resistive layers. The dependent parameter was the depth of the remaining cavity (if any) depending on the total depth constraint used. For the inlet trade study a constraint was set such that the maximum depth of the lining would be 2 inches.

The frequency weightings are multiplied by the square of the differences between the target admittance and the calculated admittance. In this way, one can highlight important frequency regions where the liner and target admittances should be close. The four sets of frequency weightings used for the inlet trade study are shown in Table 10.

Table 10: YMATCH Frequency Weightings for the Inlet

| # | B27 | B28 | B29 | B30 | B31 | B32 | B33 | B34 | B35 | B36 | B37 | B38 |
|---|-----|-----|-----|-----|-----|-----|-----|-----|-----|-----|-----|-----|
| 1 | 0 | 0 | 0 | 0 | 1 | 1 | 2 | 3 | 1 | 2 | 1 | 1 |
| 2 | 0 | 0 | 0 | 0 | 1 | 1 | 1 | 1 | 2 | 1 | 0 | 0 |
| 3 | 0 | 0 | 0 | 0 | 0 | 0 | 1 | 2 | 1 | 0 | 0 | 0 |
| 4 | 0 | 0 | 0 | 0 | 0 | 0 | 0 | 0 | 0 | 1 | 1 | 1 |

The weightings are shown as a function of one-third octave band number. Band 27 would represent a 500 Hz center frequency and Band 38 represents a 6300 Hz center frequency. Note Weighting #1 has coefficients over 12 one-third octave bands or 4 octaves. YMATCH results with this weighting set produced results that matched the one-third octave bands B30 to B35, but could not match the target outside these frequencies. Examination of the outputs from YMATCH show that single layer linings can match the target impedance over one octave and double layer linings can match a target impedance over two octaves.

YMATCH exhibits some starting point dependence for the output lining. To assure the “best” solution is found, multiple starting points are used and the lining is chosen that “best” matches the admittance target. This is accomplished by a global option that exists within the YMATCH program.

6.2.5.2 Run RDIFF Code to Determine Lining Attenuations

The next step in the design process was to predict the lining attenuations using the RDIFF program. RDIFF is a 3-D, ray tracing code developed at Boeing that allows the actual 3-D

nacelle geometry and lining definition to be used as inputs. The program works well when the ray acoustic assumptions are valid (i.e. duct diameter is much greater than the acoustic wavelength, broadband noise). These assumptions are generally met for the modern HBPR engines where the inlets are very large and the important Noy weighted frequencies are from broadband noise around 2–4 kHz.

The attenuations as a function of frequency and emission angle can then be calculated by determining the level change with and without the defined lining in the inlet nacelle.

6.2.5.3 Add Attenuations to the Hardwall Data

The predicted attenuations from RDIFF are added to the static, 150° polar hardwall data discussed in the section on the target spectra (Section 6.1.2.5). RDIFF determines attenuations in a reference frame fixed with the fan. Therefore, lining attenuations need to be applied at frequencies in this frame and not the Doppler shifted frequencies that would be measured at the FAR 36 flight conditions.

6.2.5.4 Extrapolate Data to FAR 36 Condition

The final step in the process to determine the FAR 36 noise levels is to extrapolate the static, 150° polar data to the flight. In this step, the correct atmospheric attenuations and Doppler shifts are applied to the data.

6.2.6 Trade Study Results

Two separate trade studies were carried out for the inlet. The first was a study to determine the benefit of broad-band linings for the mid-size, twin engine airplane. This was a lining design impedance study. The second study looked at the effect of changing the lining coverage areas and the effect of a scarf inlet on inlet noise. These are considered area and configuration technology changes.

6.2.6.1 Impedance Trade Study

Table 11 tabulates the results of the inlet lining impedance study for narrow and wide chord fan engines. The table gives the inlet fan component EPNL attenuations (calculated as the difference of the hardwalled inlet fan EPNL minus the treated inlet fan EPNL) and the percent improvement relative to the double layer perforate design. The double layer perforate design was chosen as the baseline because it was the Boeing standard in 1992.

Table 11: Results of the Impedance Study for the Inlet Component at the Approach Condition

| Lining | Narrow Chord | | Wide Chord | |
|-------------------|------------------|------------|------------------|------------|
| | Atten (EPNdB) | improv (%) | Atten (EPNdB) | improv (%) |
| 1 layer perforate | 3.48 | -12.7 | 2.89 | -11.1 |
| 1 layer linear | 3.86 | -3.3 | 3.15 | -3.1 |
| 2 layer perforate | 3.99 | Base | 3.25 | Base |
| 2 layer linear | 4.09 | 2.5 | 3.37 | 3.7 |
| 3 layer perforate | 4.07 | 2.0 | 3.35 | 3.1 |
| 3 layer linear | 4.21 | 5.5 | 3.48 | 7.1 |
| Optimum | 4.38 | 9.7 | 3.67 | 12.9 |

Figure 50 shows the results of Table 11 graphically. The independent axis has the number of degrees of freedom of the liner. A single layer lining had two parameters that could change (depth and resistance of the facesheet) and thus has two degrees of freedom. Likewise, the double and triple layer liners had 4 and 6 degrees of freedom respectfully. The attenuation from an imaginary liner with “optimum” impedance at all frequencies is also shown on the plots at zero degrees of freedom. The dependent variable of the plots is the inlet component EPNL attenuation.

The plots show the EPNL attenuation for the narrow (upper plot) and wide (lower plot) chord fan engines. Notice that the linear or “wire” designs outperform the perforate designs. Also, the curves increase with the number of degrees of freedom, but are tending to flatten out as the attenuations approach the optimum lining value.

Figure 51 shows the predicted impedance of the different linings at the approach condition. Notice that all the linings do well at matching the target resistance of $R/q_c=2.0$. However, the linings tend to match the target reactance of $X/q_c=-0.5$ better as the lining complexity increases (single to double to triple layer). This benefit was expected to improve the lining attenuations for the narrow and wide chord fan target spectra. At the approach power condition the linear liner attenuation benefit relative to a perforate liner was due primarily to a flatter reactance curve with frequency. This resulted in the linear liner having reactances closer to the optimum value of $-i(.5)q_c$ over a wider frequency range than the perforate. This flatter reactance results from the lower mass reactance associated with linear liner materials (woven wire for example). The lower mass reactance allows the linear liner to be deeper than the perforate. This increases the low frequency reactance while keeping the high frequency reactance lower than for the perforate liner.

Clearly large inlet component EPNL benefits were not achieved by lining improvements at the approach condition design point. Even the optimum impedance lining, which has the target impedance at every frequency, only gives about a 10% improvement in attenuation. The reason why this happens can best be explained with ray acoustics (see Figure 52). Rays leaving the source (the fan) hit hardwalled areas such as splices in the inlet or hardwalled areas near the lip and are reflected to the observer. Even though other rays hit “good” lining and thus are attenuated, the rays that strike the hardwalled areas make a “noise floor.” This is the reason that even an optimum impedance liner cannot achieve appreciable gains in attenuation at the design point.

It needs to be pointed out that the impedance of the higher bandwidth liners tends to be less dependent on engine power condition (see Figure 53). The triple layer perforate is much less affected by the change in engine power conditions than the single or double layer perforate. Also, note that the resistance and reactance are changed from their values at the approach condition (Figure 51) when compared to those for cutback condition in Figure 53. As the engine power condition increases, the in-duct sound level also increase causing an increase in the resistance. Additionally, the perforates are much more sensitive to in-duct sound level changes than the linear liners.

The independence of lining impedance to SPLs is extremely advantageous for two reasons. First, SPLs change as the noise travels down the duct. Although this study did not take this into account when performing the attenuation calculations it is believed that the linings that are the least affected should perform better because they will remain closer to the optimum impedance target over a larger area. Second, the performance of broadband liner concepts will be greatly

improved because they should be able to match the optimum impedances over a greater range of the engine operating conditions (assuming the optimum impedance spectrum does not change significantly with engine operating condition). No quantification was done of the off-design engine condition performance improvements in this study due to time constraints. However it is believed that inlet impedance technologies should consider the control of impedance over a range of operating conditions as opposed to a single condition.

6.2.6.2 Lining Area and Configuration Trade Study

Two lining area technologies and one configuration technology were evaluated in the lining area and configuration trade study. The first lining area technology was designated AMAX after a Boeing in-house program to reduce splice widths. For this study the AMAX technology was assumed to reduce all inlet splices to 0.5" from the original 2.7" splice width. Also, as defined in this study, AMAX would further allow lining to be put near the fan where it is currently being hardwalled to reduce tone noise caused by an interaction with the splices. Figure 54 shows a diagram of the conventional and area technology nacelles.

The other lining technology considered for this study was the extension of the acoustic treatment to the thermal anti-ice bulkhead. This technology was termed "bulkhead" (BH) lining for obvious reasons. Figure 54 also shows a picture of this type of nacelle.

The configuration technology considered for this study was the scarf inlet. The Boeing company is currently developing this concept to allow the technology to be put on an airplane product. A drawing of the scarf inlet compared to a conventional inlet is included as Figure 55. The scarf inlet changes the inlet nacelle to preferentially radiate upward and not to the important 50–60 degree angles below the airplane. The same AMAX and BH lining additions considered for the conventional inlet were evaluated for the scarf inlet.

The results of the study are shown in Table 12. The first column indicates that the nacelle is a conventional or scarf inlet and shows the percentage length increase if any. The next column shows what type of lining was put into the nacelle. Most the configurations were evaluated with a triple layer perforate because the study was to look at the effectiveness of area and configuration technologies and not at linings. The next three columns show whether the AMAX and BH lining technologies were on the nacelle, and the total lining area. Finally, the lining attenuations and percent improvement over a conventional nacelle with a double layer perforate are shown for both a narrow and wide chord fan target spectrum. Notice that relatively large attenuation improvements can be made with lining area and/or configuration technologies.

Table 12: Results of the Lining Area and Configuration Study for the Inlet Component

| Nacelle | Lining | Lining Tech. | | Area (ft ²) | Narrow Chord | | Wide Chord | |
|----------|---------|--------------|----|----------------------------|------------------|---------------|------------------|---------------|
| | | Amax | BH | | Atten (EPNdB) | Improv (%) | Atten (EPNdB) | Improv (%) |
| Conv | HW | – | – | 0 | N/A | | N/A | |
| Conv | 2L perf | N | N | 66.0 | 3.25 | Base | 2.69 | Base |
| Conv | 3L perf | N | N | 66.0 | 3.30 | 1.5 | 2.71 | 0.7 |
| Conv+10% | 3L perf | N | N | 74.1 | 3.93 | 21 | 3.25 | 21 |
| Conv+20% | 3L perf | N | N | 83.5 | 4.31 | 33 | 3.55 | 32 |
| Conv+40% | 3L perf | N | N | 101.1 | 4.79 | 47 | 3.90 | 45 |
| Conv | 3L perf | Y | N | 83.5 | 4.56 | 40 | 3.92 | 46 |
| Conv | 3L perf | Y | Y | 94.9 | 5.82 | 79 | 4.96 | 84 |
| Scarf | HW | – | – | 0.0 | 1.94 | -40 | 2.53 | -30 |
| Scarf | 3L perf | N | N | 65.5 | 4.51 | 39 | 4.51 | 68 |
| Scarf | 3L perf | Y | N | 82.9 | 5.72 | 76 | 5.72 | 112 |
| Scarf | 3L perf | Y | Y | 94.3 | 7.13 | 119 | 7.13 | 165 |

The attenuation predictions shown in Table 12 are plotted in graphical form versus lining area in Figure 56.

These data show liner impedance improvements result in relatively small attenuation improvements and that larger attenuation improvements need to focus on lining area and configuration technologies.

6.2.7 Conclusions

The major conclusion from the above study is that improvements in inlet liner impedance characteristics alone will not result in 25% increased noise reduction relative to 1992 technology. The liner assumed for 1992 technology was double layer perforate liner using the Boeing buried septum technology. Optimum liners, non-physically realizable liners with optimum impedance at each frequency, were predicted to result in improvements of approximately 10% for inlets. A previous analytical inlet lining optimization study conducted at Boeing showed only a small benefit for varying optimum impedance within an inlet compared to a uniform optimum impedance. Hence, the above conclusion is assumed to apply to inlets with varying impedance as well. Liners with increased degrees-of-freedom, such as triple layer perforates were estimated to offer only 2% – 3% improvement for inlets. Liners with linear resistance elements such as linear double and linear triple layer liners were estimated to offer 6% – 7% improvement. A ray tracing code does not include modal or scattering effects the possible benefits of modal scattering were not considered in these optimizations. However, these effects are not believed to be important for broadband noise attenuation in an inlet because of the large number of modes propagating.

The benefit of linear resistive liner elements is probably underestimated by these results. At the approach power condition, the linear liner attenuation benefit relative to a perforate liner was

due primarily to a flatter reactance curve with frequency. This resulted in the linear liner having reactances closer to the optimum value of $-i(.5)Q_c$ over a wider frequency range than the perforate. This flatter reactance results from the lower mass reactance associated with linear liner materials (woven wire for example). The lower mass reactance allows the linear liner to be deeper than the perforate. This increases the low frequency reactance while keeping the high frequency reactance lower than for the perforate liner. A Boeing internal study (scarf inlet design) which considered the FAR 36 cutback condition as well as the landing condition showed that the linear liner designed for landing also behaved much better at the cutback condition than was the case for the perforates. The increase in impedance due to increased grazing flow Mach number and internal SPL for the cutback condition relative to landing is significantly larger for perforates compared to current approximately linear liners. Although the cutback condition target impedance has a larger resistance than for landing the resulting increase for current perforates is much larger than desired. Current “linear” liner resistive elements such as woven wire are not truly linear and the resulting resistance increase is close to what is desired for the inlet lining.

Additional nacelle advances, such as liner structural design improvements to allow reduction in panel area used for fasteners or understanding of the effects of liners on boundary layer growth in the inlet throat region, may allow additional lining in inlet nacelles. This work is expected to gain an additional 40% – 80% in attenuation improvement relative to 1992 technology. In addition, the scarf inlet concept being developed uses the inlet shape to direct noise upward above the airplane while reducing energy propagating to the ground. This concept is expected to give an additional 40%–80% improvement.

The results from the study of the application of advanced liners to a medium twin airplane showed approximately 1/4 of the improvements relative to 1992 perforate double layer liner technology found in the NASA/FAA study conducted in 1993–94. The primary reasons for this discrepancy are the source noise characteristic assumed and the evaluation metric used. For the NASA/FAA study, the assumed source spectrum was a one–third octave spectrum with constant SPL from 500 Hz to 4000 Hz. The evaluation metric was overall power level (OAPWL) . For the medium twin study, the evaluation metric was fan component EPNL and the source spectrum had maximum Noy weighting in the frequency range of 2 to 5 kHz. The maximum attainable attenuation in this frequency range is significantly lower than in the lower frequencies because of the beaming character of higher frequency modes. Also, attenuation bandwidth was not as important for the airplane study as it was for the 500 Hz to 4000 Hz power level attenuation study. This was even the case for the wide chord fan which had a relatively low frequency BPF at approach (630 Hz band) with a resulting 2.2 dB tone correction. Attenuation of noise in the BPF frequency region in this case had only a small contribution to PNLT attenuation for the twin study since the tone correction did not change very much. Only the fan noise component was considered for this study. In reality the masking effect of other noise sources such as airframe noise would probably cause the tone correction to be reduced as the inlet radiated fan noise is reduced in the BPF region. However, this effect was not accounted for in the airplane study.

6.3 Aft Duct Trade Studies

The following section covers the aft fan noise trade study. The aft fan study was performed assuming both the approach and cutback condition as the design condition. Also, the off–design performance was evaluated for each resulting lining design. This allowed some conclusions to be made about the value of broadband lining concepts at off–design conditions.

The liner attenuations were calculated using Boeing's Multi-Element Lining Optimization (MELO) program. The MELO program is a very simplified infinite duct wave propagation, modal attenuation code. Given a rectangular, circular, or an annular duct geometry and an impedance wall specification, the program calculates the duct eigenvalues which are directly related to the attenuation of a given mode per length. Multiplication by the lining length and summing over all the cut-on modes results in the attenuation for a given frequency. MELO does have the ability to handle 1-D flow in the duct and a boundary layer profile. As an infinite duct program, MELO does not consider changes in impedance down the duct. Therefore, this code is not capable of analyzing the effect of varying duct geometry, varying impedance and modal scattering. The studies described in Section 3 showed that the triple layer liner attenuation bandwidth is equivalent to what one would expect from varying impedance liners with broadband noise and a large number of modes.

Boeing has found that using the rectangular duct option to model fan ducts does a good job matching engine test data for approach engine power but over-predicts engine test data by approximately 20% at cutback engine power and 40% at takeoff engine power. The rectangular duct assumption was used for the present fan duct lining study. The conclusions reached from this study are therefore limited to fan ducts for which the computer modeling assumptions used hold, i.e. broadband noise in relatively long ducts with slowly varying geometry and impedance. While it is understood that this is a fairly limiting set of constraints, it was felt that the study was still useful for studying large bandwidth liners, especially since lining attenuation predictions with this code have compared well with engine data in the past. These studies did indicate that there may be a benefit from modal scattering in a fan duct due to the difficulty of attenuating low order modes. This indicates that a fan duct lining configuration which first uses lining to attenuate higher order modes, is then followed by some method of scattering the low order mode energy into higher order modes and is then followed by additional lining could improve attenuation relative to a uniform lining. It is planned to study this concept when a new 3D code being developed a Boeing under AST contract is available.

The aft fan component trades are based on the tone corrected perceived noise level (PNLT) at the 120 deg radiation angle. Past experience has shown that PNLT attenuation at maximum PNLT radiation angle is representative of the aft fan component EPNL attenuation. The MELO attenuation prediction program used in these studies predicts power level attenuations which past experience has shown apply reasonably well to the maximum PNLT radiation angle. These attenuations are applied to the target spectrum to determine the PNLT attenuations.

6.3.1 Technologies Evaluated

The primary objective was to determine how much noise improvement could be obtained by applying axially uniform impedance improvement technologies. No studies were done to evaluate varying impedance, modal scattering, lining area or configuration differences affecting the aft fan component because of the inherent limitations of the analysis code used. These studies are planned after a new 3D code presently being developed is complete (approximately 1999).

6.3.2 Liner Depth Constraints

The lining depth constraints for the aft duct are much more severe than the inlet depth constraints. For this study depth constraints of 1.0, 1.5, and 2.0 inches were considered. The

actual aft duct lining depth constraints would be somewhere near these numbers and would depend on where the lining was located.

6.3.3 Source Modal Energy Assumptions

The modal energy assumptions affect both the optimum lining design impedances and the maximum lining attenuations. For this lining design, a modal energy distribution believed to be appropriate to random broad-band noise was used within our design program. This assumption approximates an equal energy modal assumption which states that the propagating energy of each cut-on mode is identical. The Boeing assumption and an equal energy assumption are the same except near cutoff where the assumption forces lower energies near cutoff where the equal energy assumption would force extremely high SPLs because the energy transport rate down the duct is very small. The difference between the Boeing assumption and the equal energy assumption probably does not have a significant effect on the resulting lining design since the modes near cut-off attenuate rapidly down the duct even if the lining design is not optimum for these modes. The energy assumption used by Boeing is:

$$\int_S p^2 dS = \text{constant for each mode}$$

or the integral of the pressure squared over the cross sectional area is constant for each mode.

The use of a broadband energy assumption works well for fan ducts where the spectrum is broadband dominated. This is somewhat the case for the target spectra for the approach and cutback conditions which can be seen in Figure 47.

6.3.4 Optimum Liner Impedances

The optimum liner impedances were determined using Boeing's Multi-Element Lining Optimization (MELO) program. Built around the modal prediction capability is an optimizer capable of changing the lining impedance to maximize the resulting attenuation. In this manner, an optimum impedance versus frequency can be determined.

The representation of the fan duct lining with MELO is shown in Figure 45. A two dimensional, rectangular duct was modeled with the height of the duct chosen as the average height of the fan duct in the lined region for a mid-sized, twin engine airplane. The lining length used for the MELO program was obtained by estimating the average lining length.

The optimum impedance versus frequency plot produced with MELO for both approach and cutback is shown in Figure 57. Notice the optimum impedance of the fan duct changes very little for these two operating conditions.

In determining the optimum impedance for the mid-sized, twin engine fan duct, the following assumptions were made:

- 1 A two dimensional rectangular duct with the same lining on each side
- 2 A linear boundary layer profile with momentum thickness of 0.3 cm.
- 3 Cut-on modes with a modal assumptions as discussed in the Source Assumptions section.

6.3.5 Evaluation Process

The process used to determine the aft fan duct liner design is graphically shown in Figure 58. A description of each block follows.

6.3.5.1 Optimize Lining Parameters to Match Admittance

The lining's admittance (1/impedance) is matched to ideal admittance (1/ideal impedance) as calculated with the MELO program using Boeing's YMATCH program. This is basically the same procedure as described in Section 6.2.5.1 except the ideal impedance is different and different weightings are used in the least squares optimization problem.

Like the inlet problem, the lining parameters define the independent and dependent variables in the optimization problem. Three different depth constraints were used for the aft duct problem.

The frequency weightings used for the narrow and wide chord fan spectra at the approach and cutback conditions are shown in Tables 13, 14, 15, and 16. Different weightings were chosen for each target spectra because the target spectra were different.

Table 13: Frequency Weightings Used for the Narrow Chord Fan at Approach

| # | B27 | B28 | B29 | B30 | B31 | B32 | B33 | B34 | B35 | B36 | B37 | B38 |
|---|-----|-----|-----|-----|-----|-----|-----|-----|-----|-----|-----|-----|
| 1 | 0 | 0 | 0 | 0 | 1 | 1 | 1 | 3 | 2 | 2 | 1 | 1 |
| 2 | 0 | 0 | 0 | 0 | 0 | 1 | 1 | 1 | 1 | 1 | 1 | 0 |
| 3 | 0 | 0 | 0 | 0 | 0 | 0 | 1 | 2 | 1 | 0 | 0 | 0 |
| 4 | 0 | 0 | 0 | 1 | 2 | 1 | 0 | 0 | 0 | 0 | 0 | 0 |

Table 14: Frequency Weightings Used for the Narrow Chord Fan at Cutback

| # | B27 | B28 | B29 | B30 | B31 | B32 | B33 | B34 | B35 | B36 | B37 | B38 |
|---|-----|-----|-----|-----|-----|-----|-----|-----|-----|-----|-----|-----|
| 1 | 0 | 0 | 0 | 0 | 0 | 1 | 4 | 1 | 1 | 2 | 1 | 1 |
| 2 | 0 | 0 | 0 | 0 | 0 | 1 | 2 | 1 | 1 | 1 | 1 | 0 |
| 3 | 0 | 0 | 0 | 0 | 0 | 0 | 0 | 0 | 1 | 2 | 1 | 0 |
| 4 | 0 | 0 | 0 | 0 | 0 | 1 | 2 | 1 | 0 | 0 | 0 | 0 |

Table 15: Frequency Weightings Used for the Wide Chord Fan at Approach

| # | B27 | B28 | B29 | B30 | B31 | B32 | B33 | B34 | B35 | B36 | B37 | B38 |
|---|-----|-----|-----|-----|-----|-----|-----|-----|-----|-----|-----|-----|
| 1 | 0 | 2 | 0 | 0 | 1 | 1 | 1 | 2 | 2 | 1 | 0 | 0 |
| 2 | 0 | 0 | 0 | 0 | 1 | 1 | 1 | 1 | 1 | 1 | 0 | 0 |
| 3 | 0 | 0 | 0 | 0 | 0 | 0 | 1 | 1 | 1 | 0 | 0 | 0 |
| 4 | 0 | 2 | 1 | 1 | 0 | 0 | 1 | 1 | 1 | 0 | 0 | 0 |

Table 16: Frequency Weightings Used for the Wide Chord Fan at Cutback

| # | B27 | B28 | B29 | B30 | B31 | B32 | B33 | B34 | B35 | B36 | B37 | B38 |
|---|-----|-----|-----|-----|-----|-----|-----|-----|-----|-----|-----|-----|
| 1 | 0 | 0 | 0 | 3 | 1 | 1 | 1 | 1 | 1 | 1 | 0 | 0 |
| 2 | 0 | 0 | 0 | 1 | 1 | 1 | 1 | 1 | 1 | 0 | 0 | 0 |
| 3 | 0 | 0 | 0 | 0 | 0 | 0 | 1 | 1 | 1 | 0 | 0 | 0 |
| 4 | 0 | 0 | 1 | 3 | 1 | 0 | 0 | 0 | 0 | 0 | 0 | 0 |

The weightings are shown as a function of one-third octave band number. Band 27 would represent a 500 Hz center frequency and Band 38 represents a 6300 Hz center frequency. Note Weighting #1 for the narrow chord fan target spectra at approach has coefficients over 8 one-third octave bands or about 3 octaves. Examination of the outputs from YMATCH show that single layer linings can match the target impedance over one octave and double layer linings can match a target impedance over two octaves. When YMATCH was used to match a single or double layer lining over 3 octave bands it produced results that matched the center bands, but not the edges. This process produced four designs for each type of liner (perforate and linear single, double and triple layer), each depth constraint (1 in., 1.5 in. and 2 in.), each type of fan (narrow chord and wide chord) and each design point power condition (approach and cutback). The impedance spectra of these four designs were examined and one chosen (subjective evaluation) for the starting point of a duct attenuation optimization calculation.

6.3.5.2 Optimize PNLT Attenuations Using the YMATCH Starting Points

MELO was next used in the optimization mode to find lining designs for each type of liner (perforate and linear single, double and triple layer), each depth constraint (1 in., 1.5 in. and 2 in.), each type of fan (narrow chord and wide chord) and each design point power condition (approach and cutback). The YMATCH defined liner definitions were used as starting points. Specifically, the lining definitions and hardwall spectra are input into MELO. MELO then uses the optimizer to find a design which minimizes the attenuated spectrum PNLT by varying the specified geometry parameters, with defined constraints. These results were used to determine a set of attenuations to evaluate which liners performed best.

Since this process was run with perforate and linear single, double and triple layer linings, three lining depth constraints and two design points for both the narrow chord and wide chord fan engines, 72 optimizations were run.

It should be mentioned that there is a “factor” applied to the calculated attenuations within MELO. This “factor” is an empirical correction for the MELO predicted attenuations to match full-scale, ground test measured lining attenuation data. The accepted “factors” used at Boeing are 1.0, 0.8, and 0.6 for the approach, cutback, and sideline conditions respectfully. The factors were applied to all the MELO duct attenuation predictions made in this design.

6.3.5.3 Choose Best Lining Based on PNLT Attenuations

The best lining for each set of target spectra and constraints was chosen from the set generated with MELO. This part of the process was nothing more than choosing the linings that gave the highest attenuations.

6.3.5.4 Calculate the Off-Design Performance

The final step in determining the best lining was to determine the cross-performance. For each of the linings generated from the last step, the attenuation at the other operating condition was determined.

6.3.6 Trade Study Results

Liner impedance design trade studies were completed for the fan duct to evaluate the benefit of broadband linings for the approach and cutback operating conditions for both narrow and wide chord fan target spectra. Additionally, some work was done to evaluate point design linings for approach and cutback at the off-design points.

6.3.6.1 Approach Design Point Impedance Study

Six different linings were evaluated for the approach impedance study. These were the single, double, and triple layer perforate and linear linings as discussed in the section on Linings Evaluated in this Study. The purpose of the study was to evaluate how much improvement broadband linings could offer for a point design.

Table 17 gives the results of the study. Note that although triple layer linings offer more component attenuation improvement compared to the inlet, the improvements are still relatively small. Note also that a optimum uniform lining (one that matches the ideal impedance at every frequency) cannot reach the 25% attenuation improvement AST program goal.

Table 17: Results of the Impedance Study for the Aft Component at Approach

| Lining | Narrow Chord | | Wide Chord | |
|-------------------|-------------------|------------|-------------------|------------|
| | Atten (PNLTdB) | improv (%) | Atten (PNLTdB) | improv (%) |
| 1 layer perforate | 6.6 | -20.5 | 5.3 | -25.4 |
| 1 layer linear | 7.9 | -4.8 | 6.7 | -5.6 |
| 2 layer perforate | 8.3 | Base | 7.1 | Base |
| 2 layer linear | 8.8 | 6.0 | 7.6 | 7.0 |
| 3 layer perforate | 8.8 | 6.0 | 7.5 | 5.6 |
| 3 layer linear | 8.9 | 7.2 | 7.7 | 8.5 |
| Optimum | 10.3 | 11.3 | 8.4 | 18.3 |

Figure 59 shows a graphical representation of the approach design point attenuation results. As expected, the linear liners outperformed the perforates and the higher number of degrees freedom liners outperformed the lower.

6.3.6.2 Cutback Design Point Impedance Study

Table 18 and Figure 60 show the cutback power design point results. Generally, the results are similar to the approach design condition with the exception that the “optimum” liner shows larger attenuation improvements than is seen for approach.

Table 18: Results of the Impedance Study for the Aft Component at Cutback

| Lining | Narrow Chord | | Wide Chord | |
|-------------------|-------------------|------------|-------------------|------------|
| | Atten (PNLTdB) | Improv (%) | Atten (PNLTdB) | Improv (%) |
| 1 layer perforate | 6.5 | -18.8 | 3.9 | -29.1 |
| 1 layer linear | 7.0 | -12.5 | 4.2 | -23.6 |
| 2 layer perforate | 8.0 | N/A | 5.5 | N/A |
| 2 layer linear | 8.1 | 1.3 | 5.8 | 5.5 |
| 3 layer perforate | 8.1 | 1.3 | 6.0 | 9.1 |
| 3 layer linear | 8.3 | 3.8 | 5.9 | 7.3 |
| Optimum | 10.2 | 27.5 | 9.1 | 65.5 |

6.3.6.3 Off-Design Impedance Study

The off-design performance of the point linings defined for approach and cutback were evaluated at the other operating condition. Figure 61 shows the sum of the approach and cutback attenuations for each lining. Note that the cutback designs tended to have slightly higher summed attenuations than the approach designs. This suggests that if a point design was going to be used for both conditions, that a cutback design should be chosen.

6.3.7 Conclusions

As for the inlet, the major conclusion from the above study is that improvements in nacelle liner average impedance characteristics alone will not result in 25% increased nacelle noise reduction relative to 1992 technology. The liner assumed for 1992 technology was a double layer perforate liner using the Boeing buried septum technology. Optimum uniform liners, non-physically realizable liners with optimum impedance at each frequency, were predicted to result in improvements of approximately 15% for the fan duct at the airplane landing condition. Liners with increased degrees-of-freedom, such as triple layer perforates, were estimated to offer 6% – 10% improvement for the fan duct. Liners with linear resistance elements, such as linear double and linear triple layer liners, were estimated to offer 7% – 10% benefit. Since previous studies have shown that the triple layer liner gives attenuation values similar to liners with slowly varying impedance for broadband noise and a large number of modes, the above conclusion are expected to apply to ducts with slowly varying impedance as well.

These studies did indicate that there may be a benefit from modal scattering in a fan duct due to the difficulty of attenuating low order modes. This indicates that a fan duct lining configuration which first uses a broadband lining to attenuate higher order modes, is then followed by some method of scattering the low order mode energy into higher order modes (such as a reactive liner segment) and is then followed by additional broadband lining could improve attenuation relative to a uniform lining. It is planned to study this concept and the effects of varying non-circular/annular geometry when a new 3D code being developed a Boeing under AST contract is available.

Consideration of the FAR 36 cutback condition showed that if both landing and cutback are given equal weight, the design optimized for cutback (design point) was superior to that designed for landing, for the narrow chord fan engine. If the approach condition is chosen as the

design point, the benefit of using a linear liner was significant (approximately 16% relative to the sum of landing and cutback attenuation for a double layer perforate liner).

For the wide chord fan the landing plus cutback attenuation was not appreciably different for the landing or cutback optimized liners. The benefit of triple layer or linear liners for this metric was similar to that seen for the design point PNLT attenuations (approximately 10%).

Additional nacelle advancements such as liner structural design improvements to allow reduction in panel area used for fasteners and strength reinforcement, are presently being studied at Boeing but the noise reduction from this technology for the fan duct was not explicitly evaluated as part of this study. Preliminary estimates show a potential for increasing the lining area by approximately 30%.

7.0 References

1. Parrott, T. L.; Watson, W. R.; and Jones, M. G.: NASA TP-2679, 1987.
2. Utsuno H. et al., Transfer function method for measuring characteristic impedance and propagation constant of porous materials”, J. Acoust. Soc. Am. 86(2), August 1989
3. Yaniv S. ”Impedance tube measurement of propagation constant and characteristic impedance of porous acoustical material”, J. Acoust. Soc. Am. 54(5) 1973
4. Delaney M. & Bazley E., Appl. Acoust. 3, 105 (1970)
5. Voronina N. N., ”Influence of the structure of fibrous sound-absorbing materials on their acoustical properties”, Sov. Phys. Acoust, 29(5), Sept.–Oct. 1983
6. Beranek,L., ”Noise and Vibration Control”, p 248, 1971 Edition
7. Dean P., ”On the ”In-Situ” Control of Acoustic Liner Attenuation”, ASME Paper No. 76-GT-61, Gas Turbine Conference, New Orleans, La., 3–21–76
8. Hersh A. S. & Rogers T., ”Fluid Mechanical Model Of The Acoustic Impedance Of Small Orifices”, AIAA 75-495, March, 1975
9. Rogers T. & Hersh A. S., ”The Effect Of Grazing Flow On The Steady State Resistance Of Square- Edged Orifices” AIAA 75-493, March, 1975
10. Ingard U. & Ising H., ”Acoustic Nonlinearity of an Orifice”, JASA, Vol.42, No. 1, 6–17, July 1967
11. NASA Contractor Report 198298, ”Definition of 1992 Technology Aircraft Noise Levels and the Methodology for Assessing Airplane Noise Impact of Component Noise Reduction Concepts,” H. A. Kumasaka, M. M. Martinez, and D. S. Weir, June 1996.
12. Rice E. J. & Saule A. V., ”Far-Field Radiation Of Aft Turbofan Noise”, NASA TM 81506, 1980
13. Kumasaka H. A. & Martinez M. M., ”Definition of 1992 Technology Aircraft Noise Levels and the Methodology for Assessing Airplane Noise Impact of Component Noise Reduction Concepts”, NASA CR 198298, June 1996

Bielak, G., Diamond, J., ”Analytical Study Of Turbofan Engine Nacelle Acoustic Liners For Broadband Attenuation With Emphasis On Parallel Element Liners” Submitted to NASA Langley May 1994

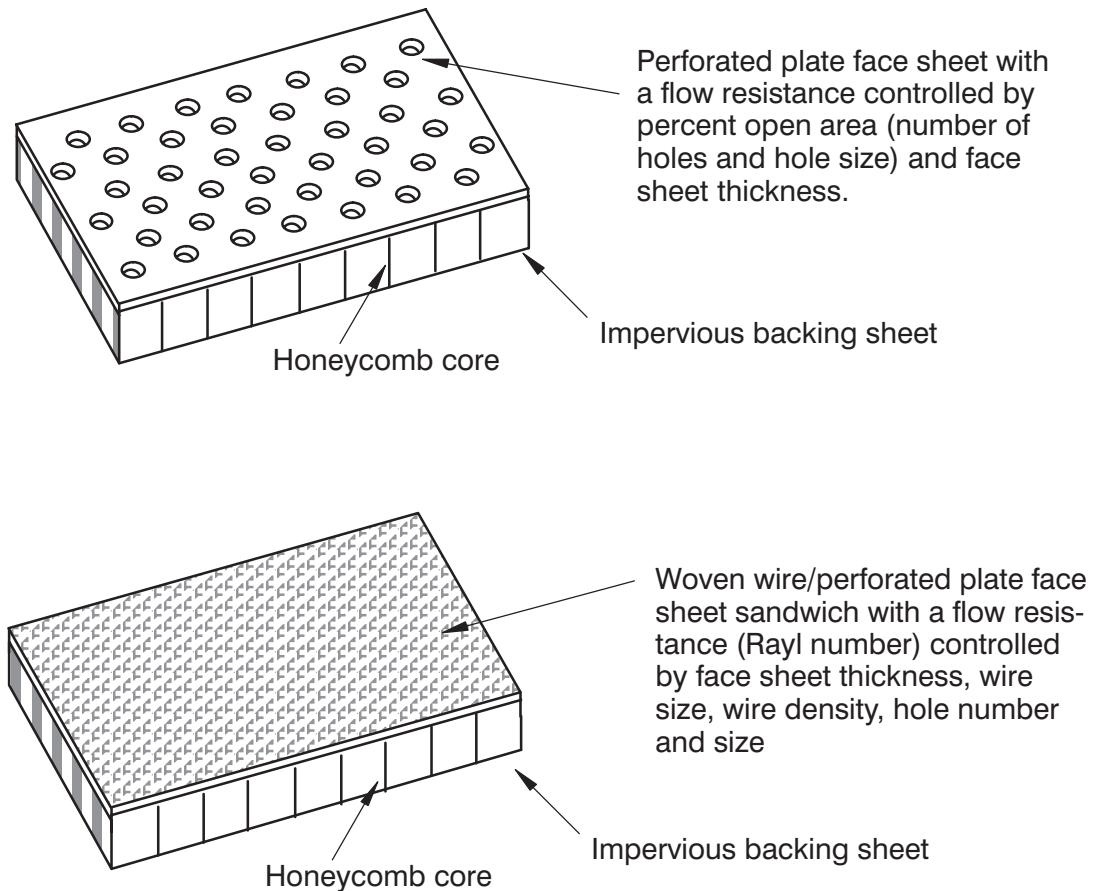
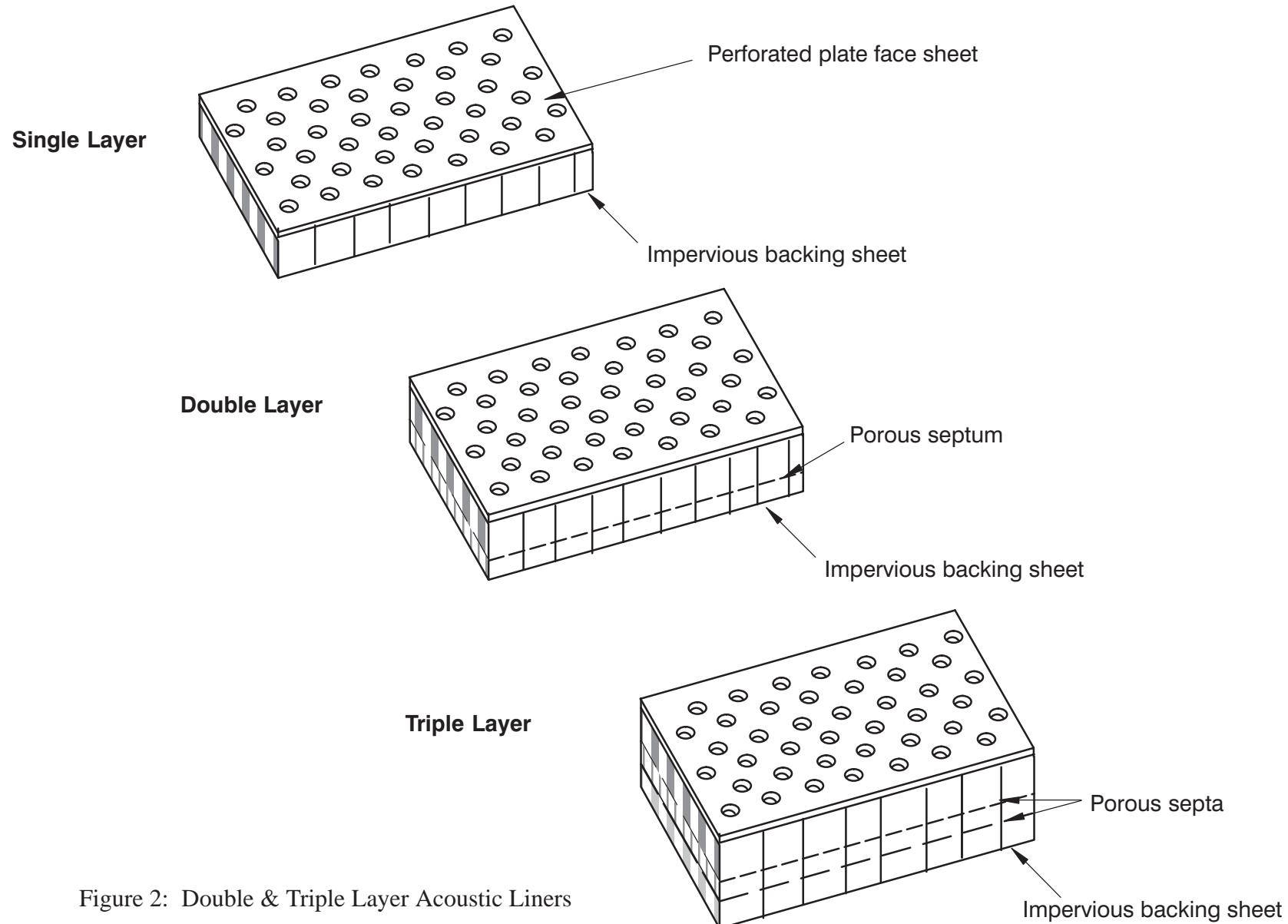


Figure 1: Single Layer Acoustic Liners

NOT TO SCALE



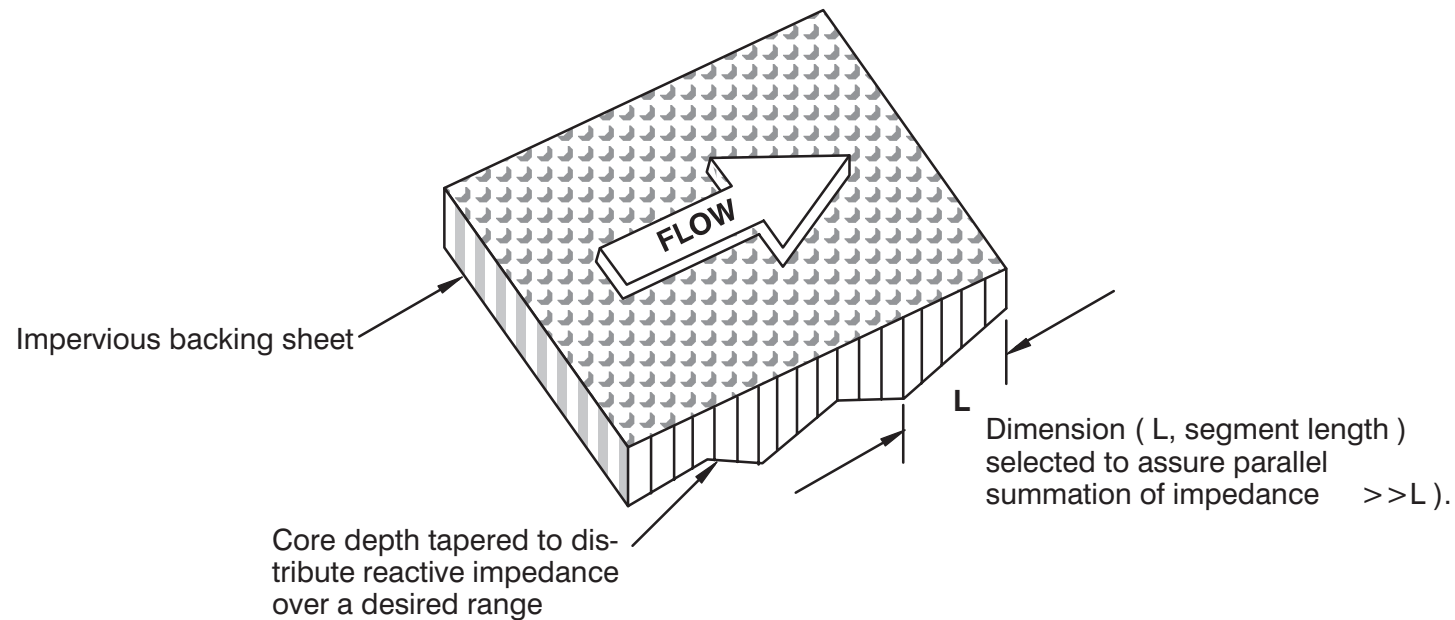


Figure 3: Parallel Element Acoustic Liner

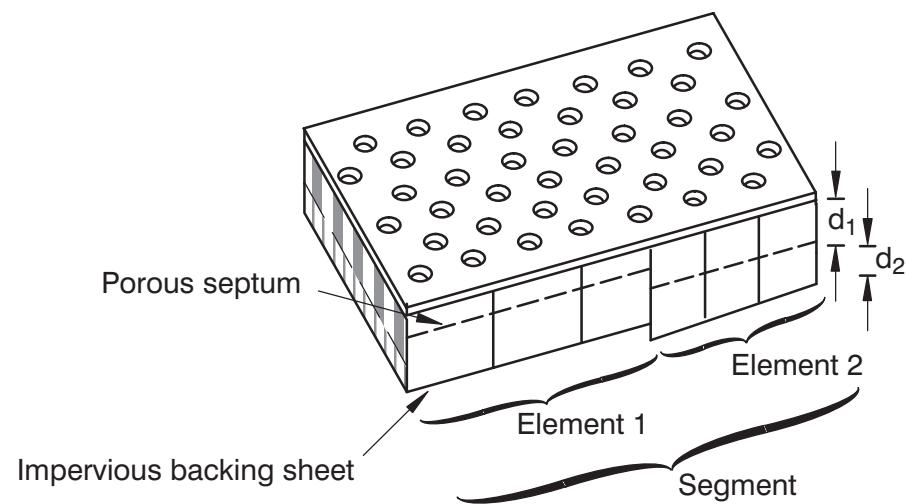


Figure 4: Double Layer Parallel Element Acoustic Liner

NOT TO SCALE

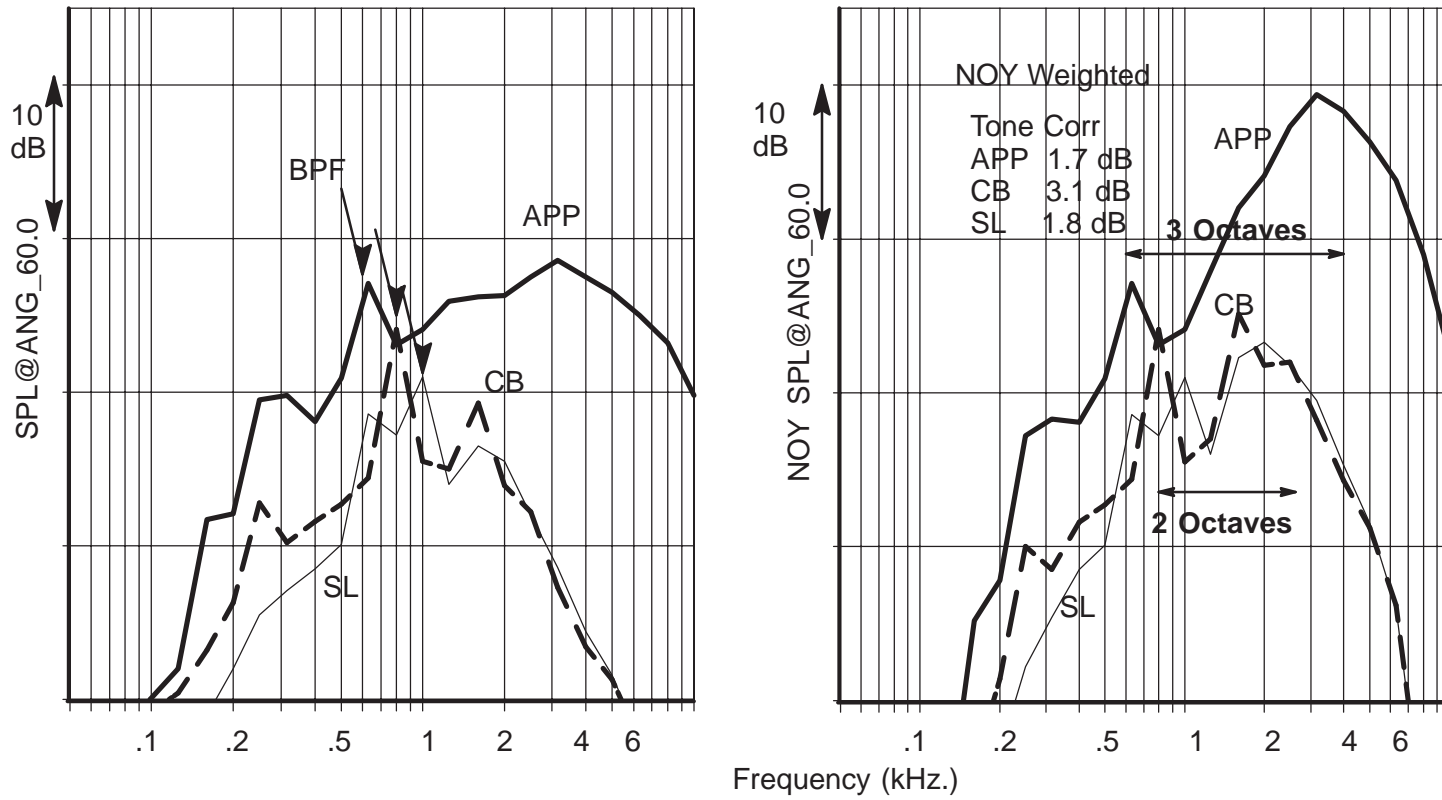


Figure 5: Typical Wide Chord Fan Spectrum Shapes At Peak PNLT Inlet Angle

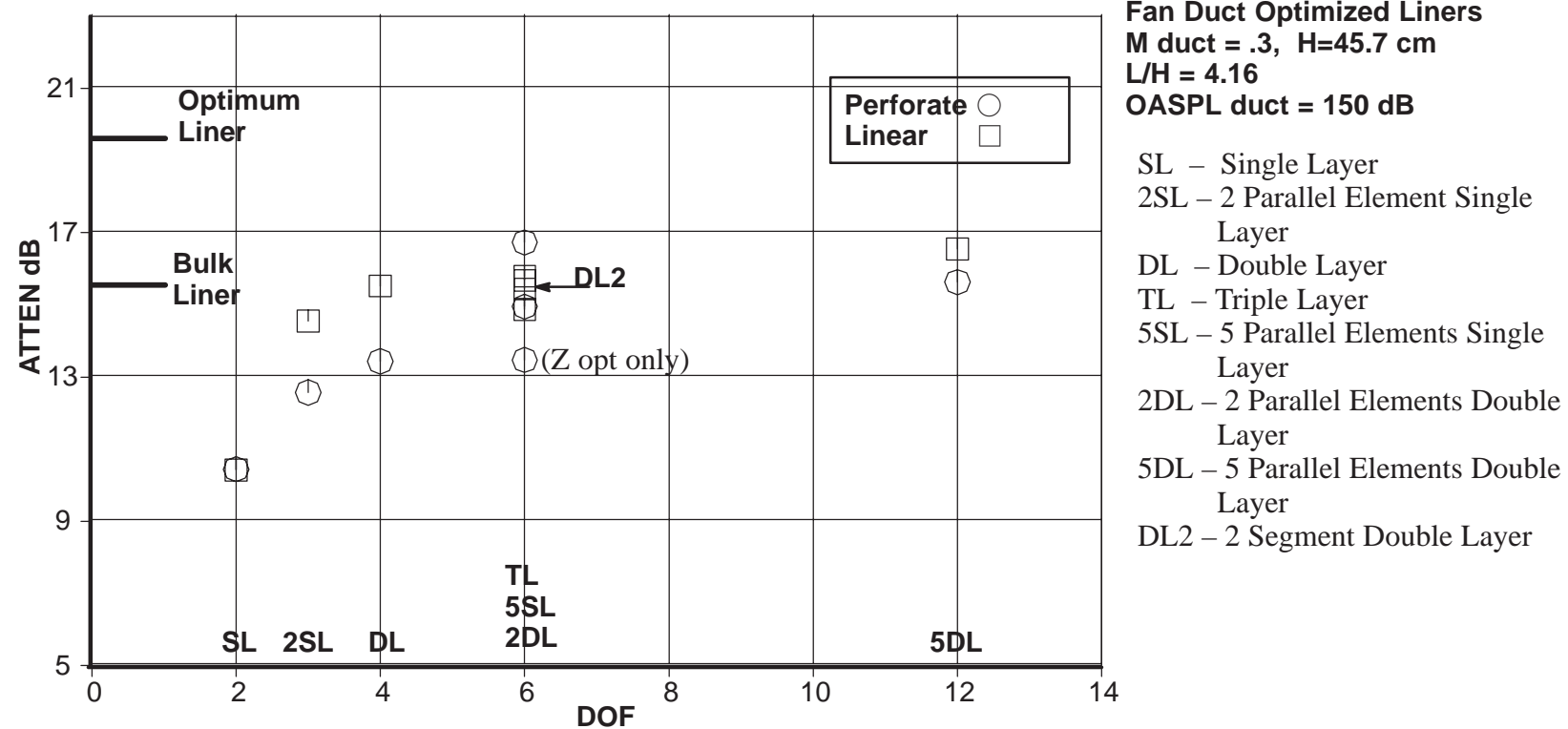


Figure 6: Fan Duct OAPWL Attenuations

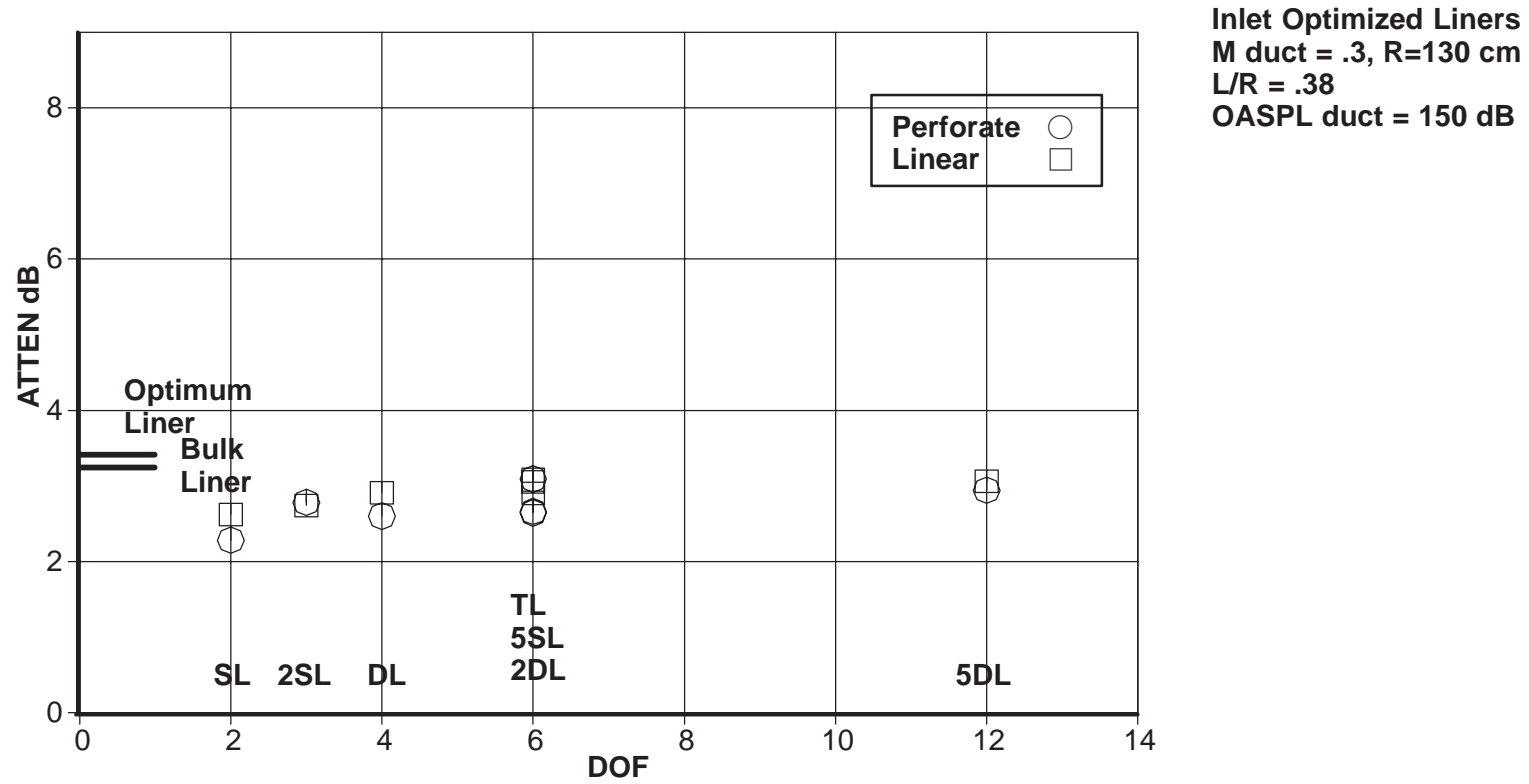


Figure 7: Inlet OAPWL Attenuations

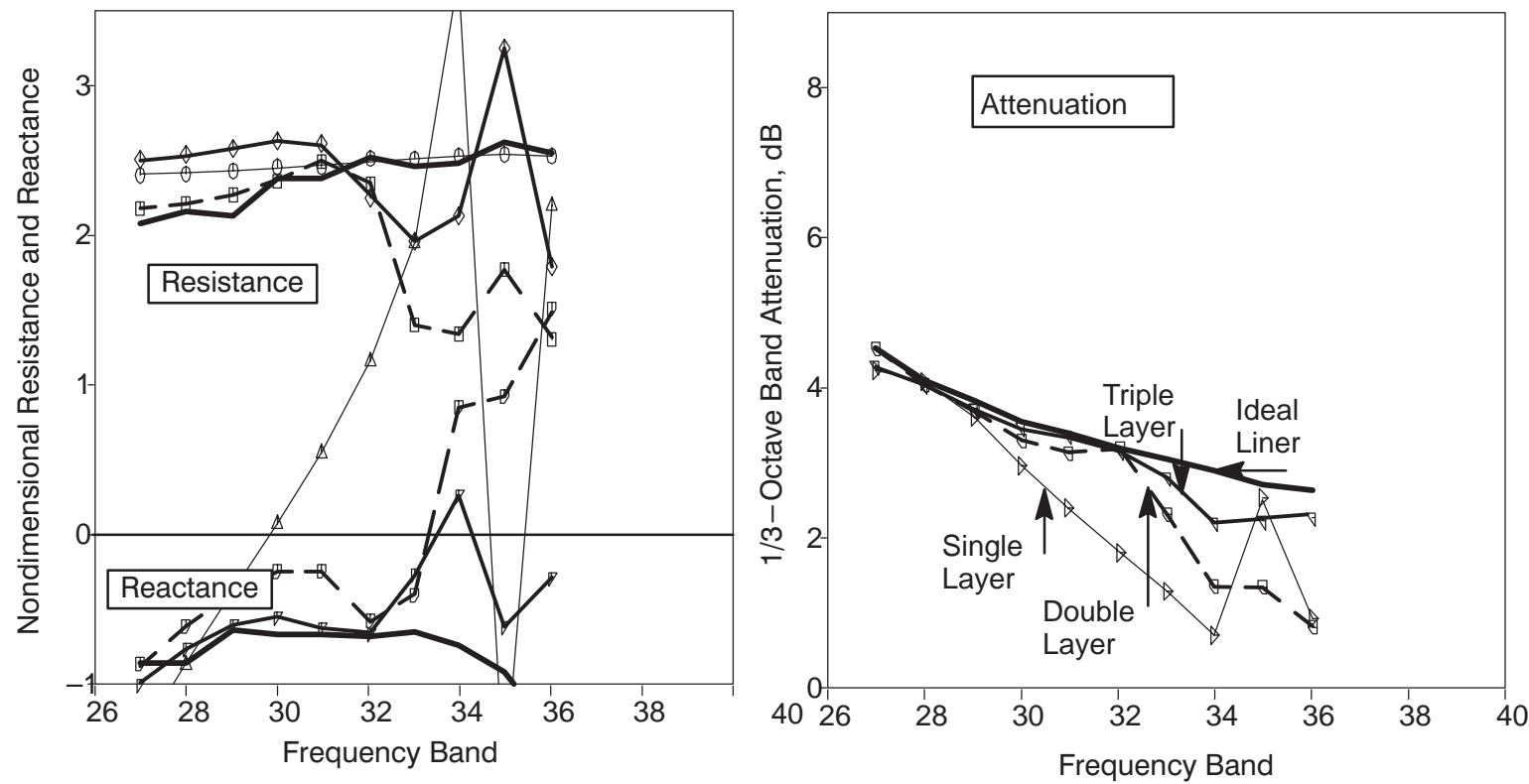


Figure 8: Inlet Impedance and Attenuation Spectra

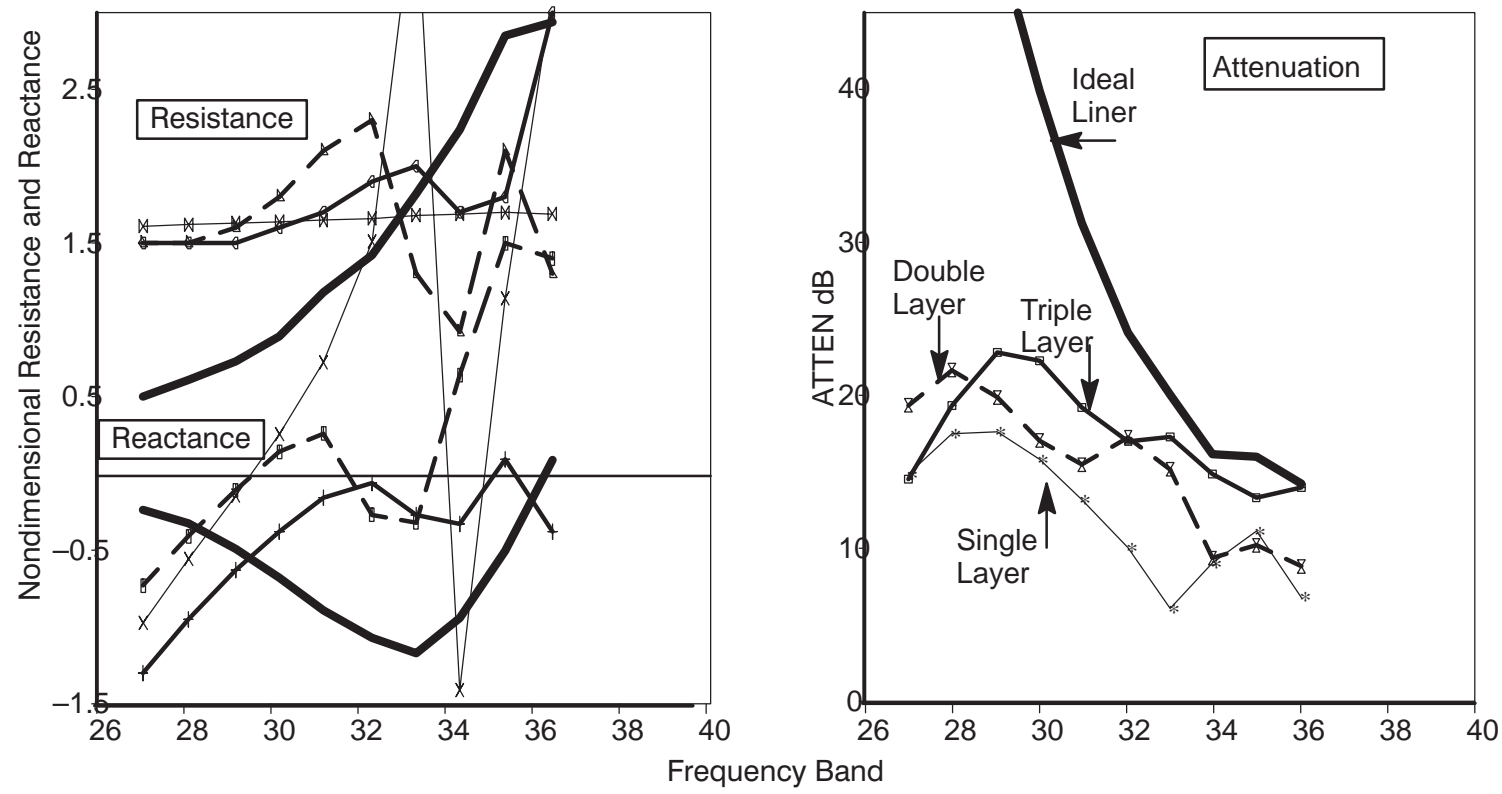


Figure 9: Fan Duct Impedance and Attenuation Spectra

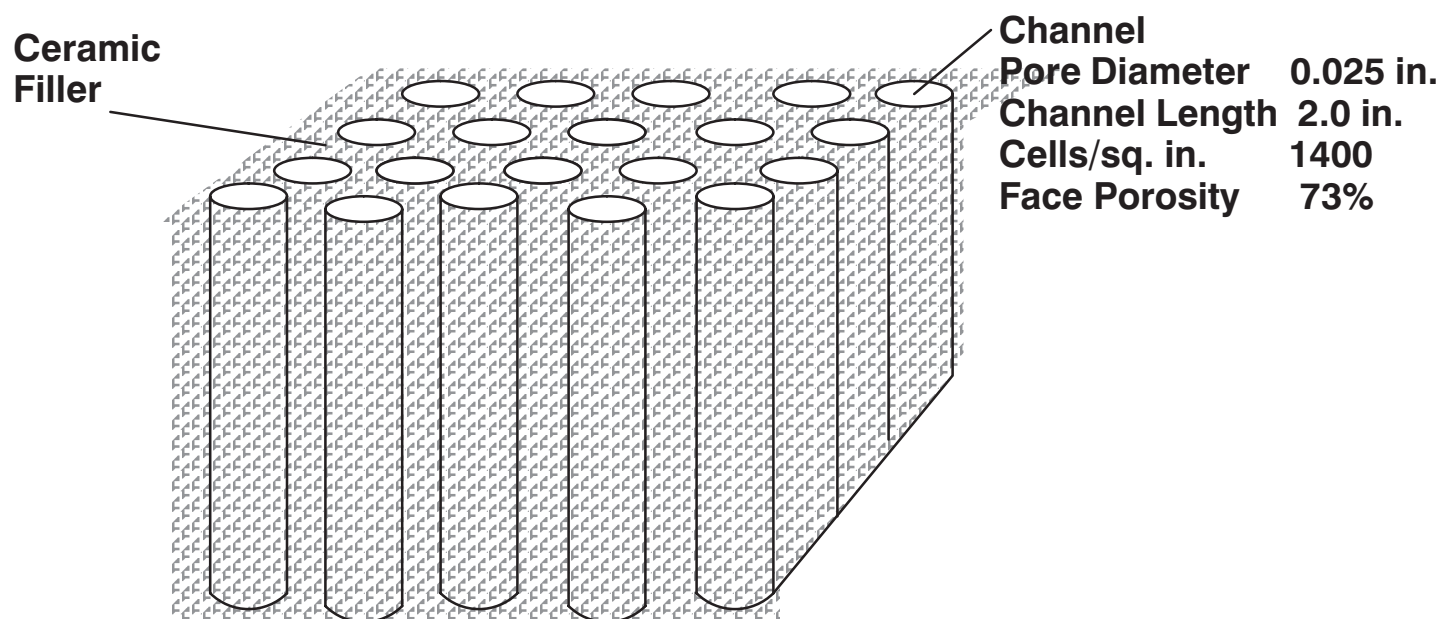


Figure 10: Schematic of NASA Langley Standard Grazing Flow Impedance Sample

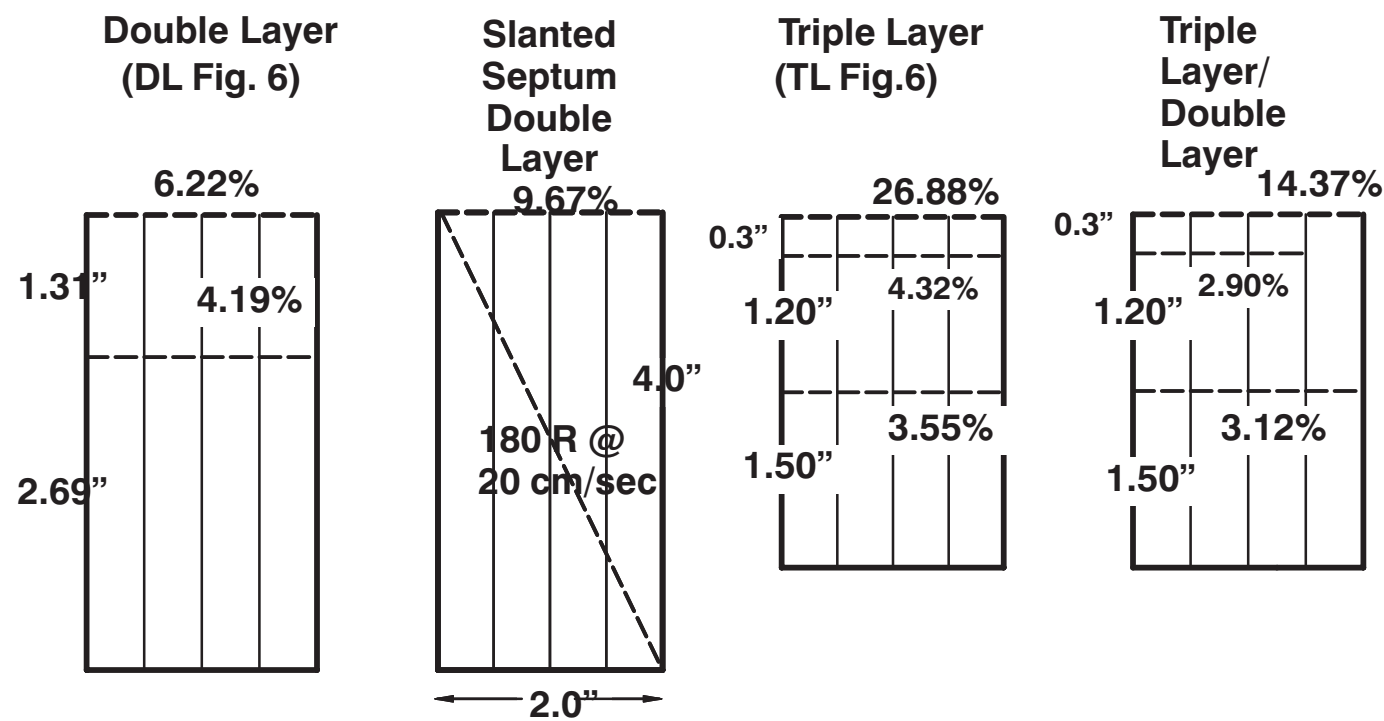


Figure 11: Passive Liner Test Designs

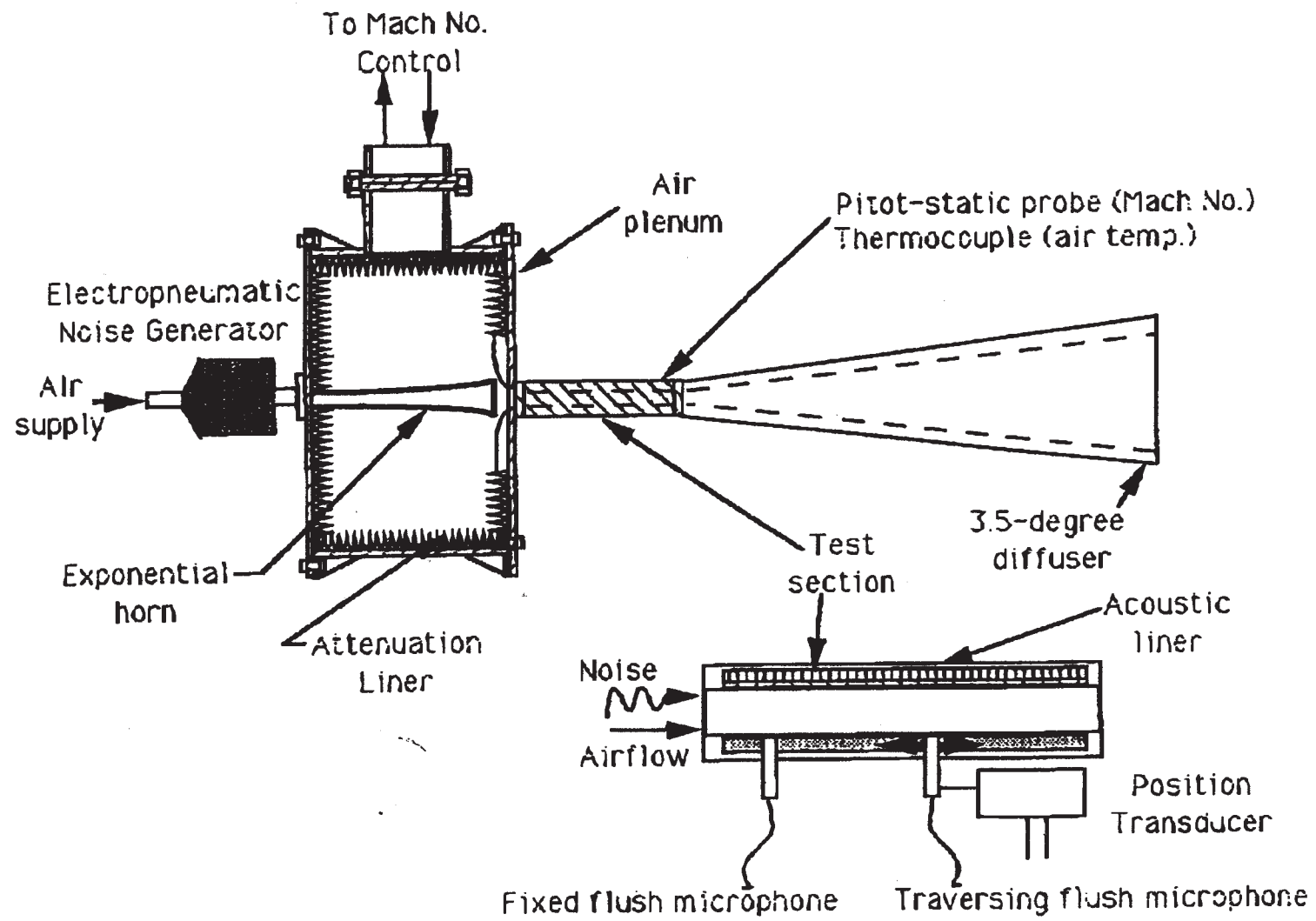
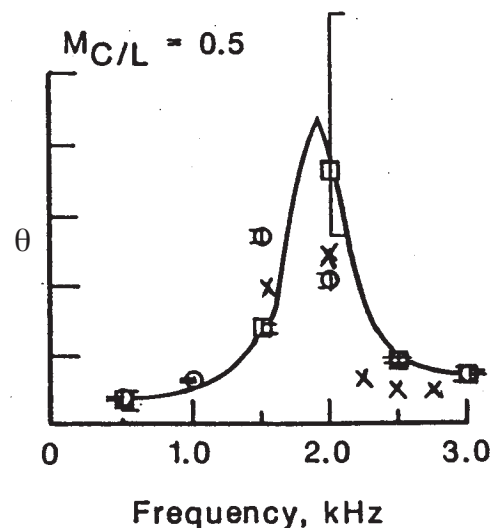
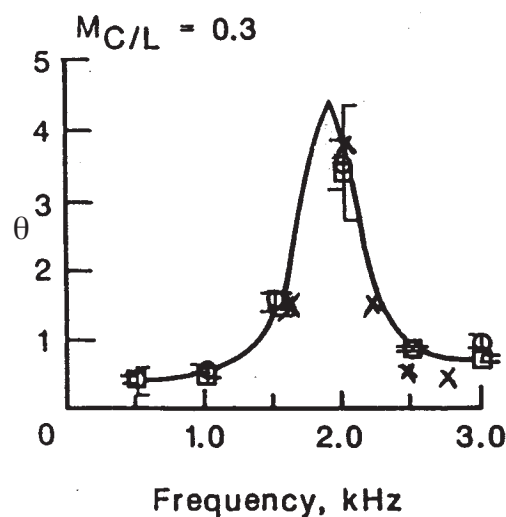
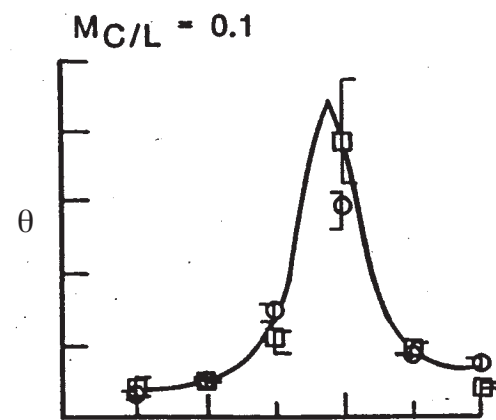
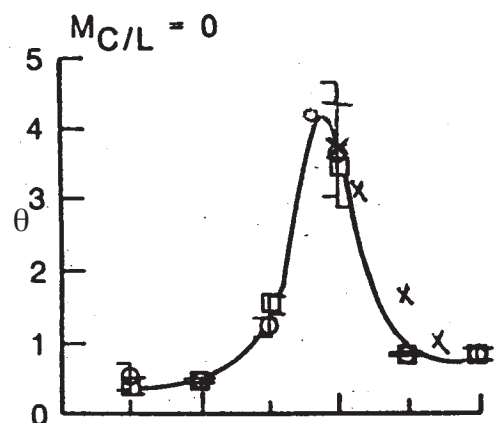


Figure 12: Schematic Of Wichita Grazing Flow Impedance Measurement System

NASA Langley Data TP2679

X – Boeing Grazing Flow
Impedance Data

- Downstream propagation with error bounds
- Upstream propagation with error bounds
- Normal incidence
No Grazing Flow



(a) Normalized acoustic resistance, $\theta = R/Qc$

Measured grazing-incidence impedance as inferred from two-dimensional shear-flow model.

Figure 13: Comparison Of NASA And Boeing Wichita Grazing Flow Resistance Test Data

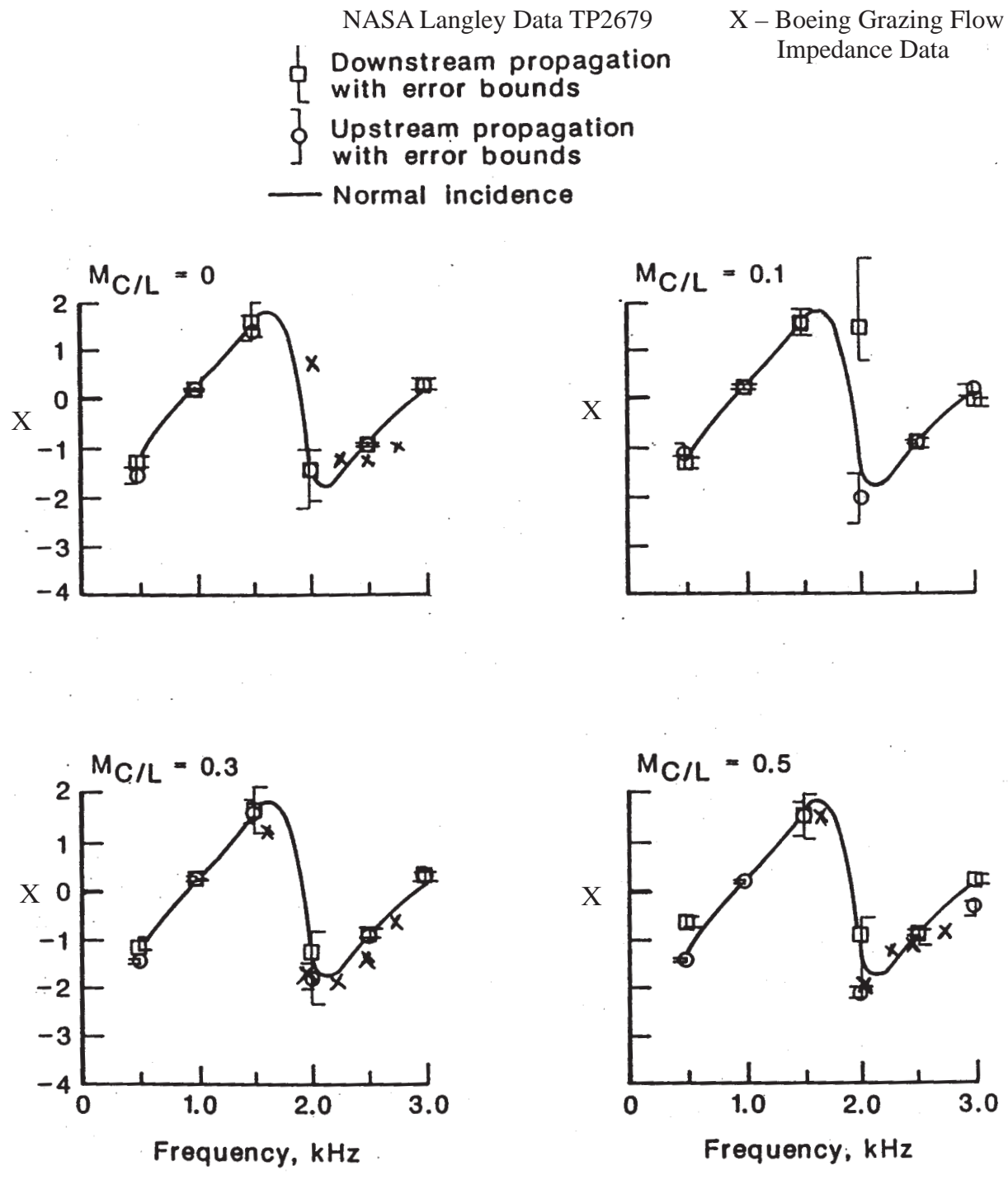


Figure 14: Comparison Of NASA And Boeing Wichita Grazing Flow Reactance Test Data

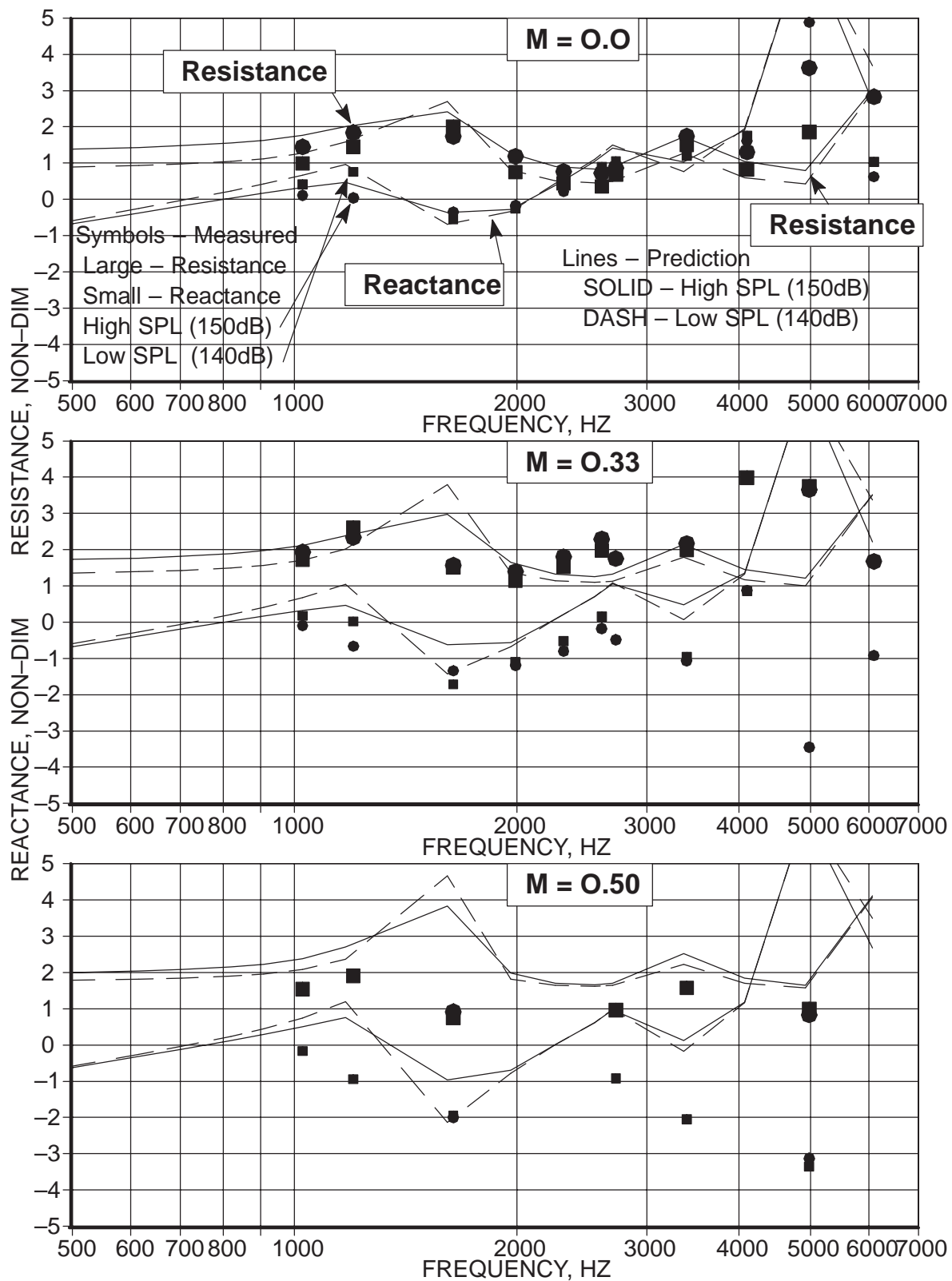


Figure 15: Measured And Predicted Impedance Of The Double Layer Liner Shown In Figure 11.

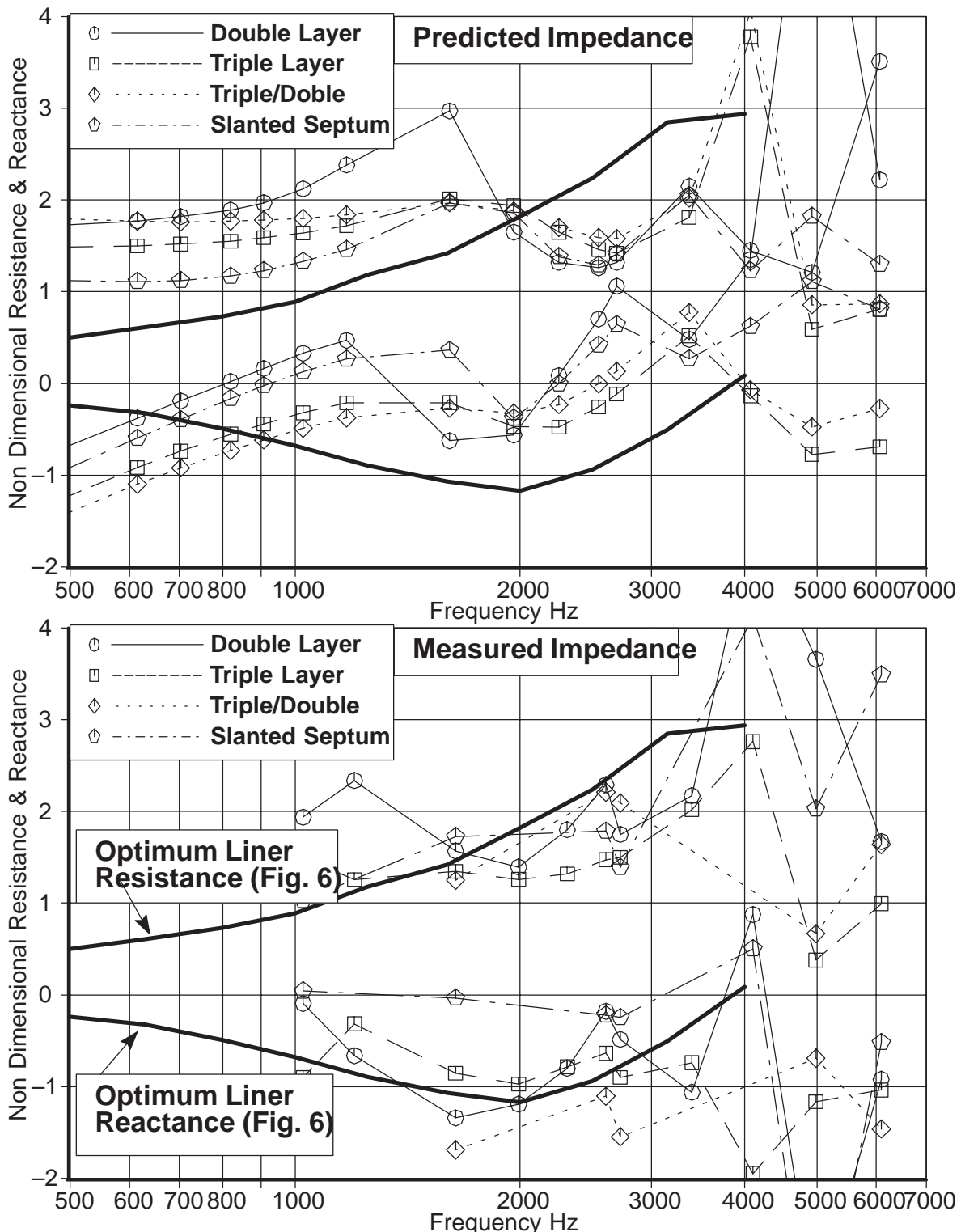


Figure 16: Measured And Predicted Impedances Of Liners Shown In Figure 11 Compared To Target Impedance ($M = 0.33$, Mom Thickness = .08 cm, OASPL = 150 dB)

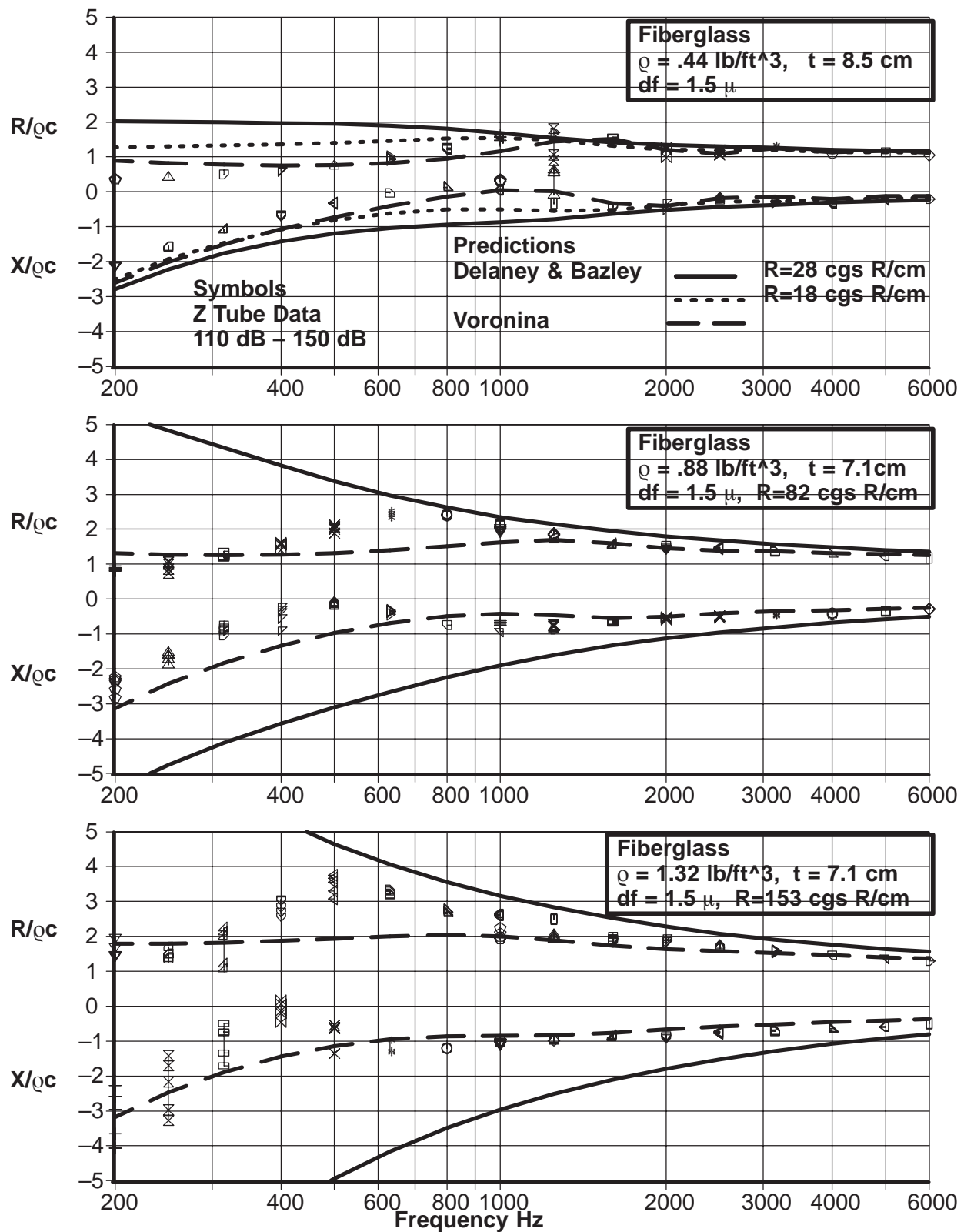


Figure 17: Measured vs. Predicted Surface Impedance – Fiberglass Bulk Absorber

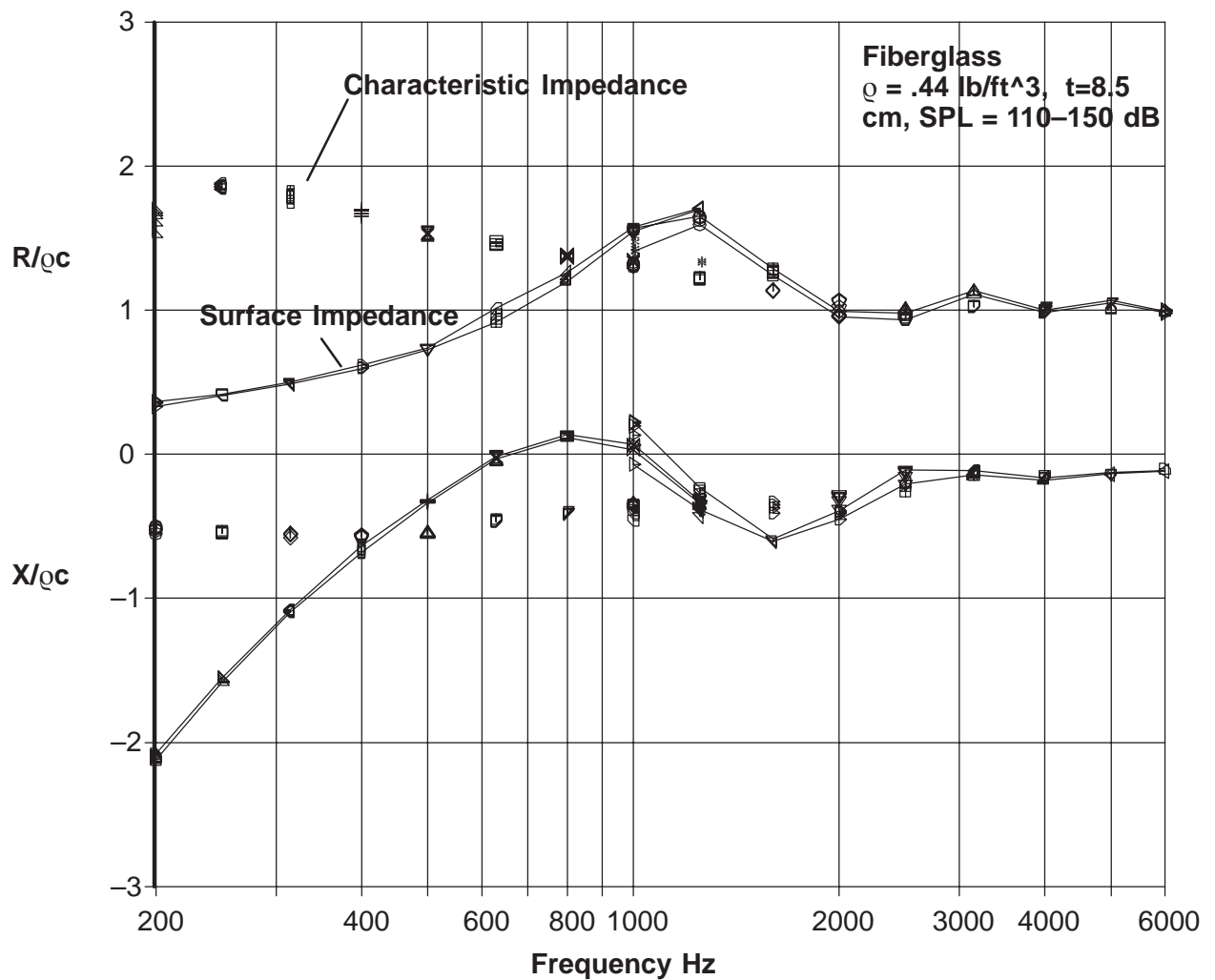


Figure 18: Measured Surface and Characteristic Impedance

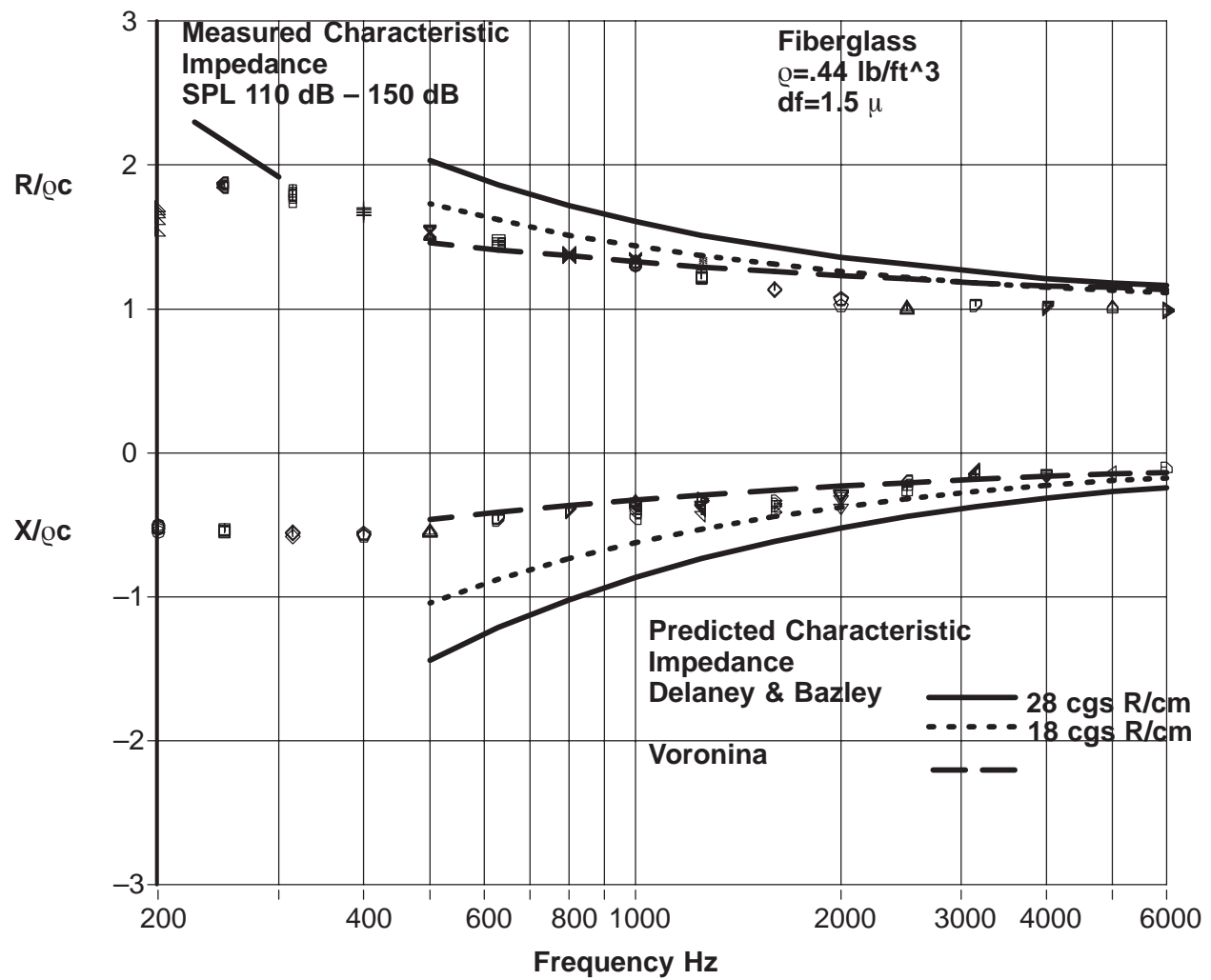


Figure 19: Measured vs. Predicted Characteristic Impedance

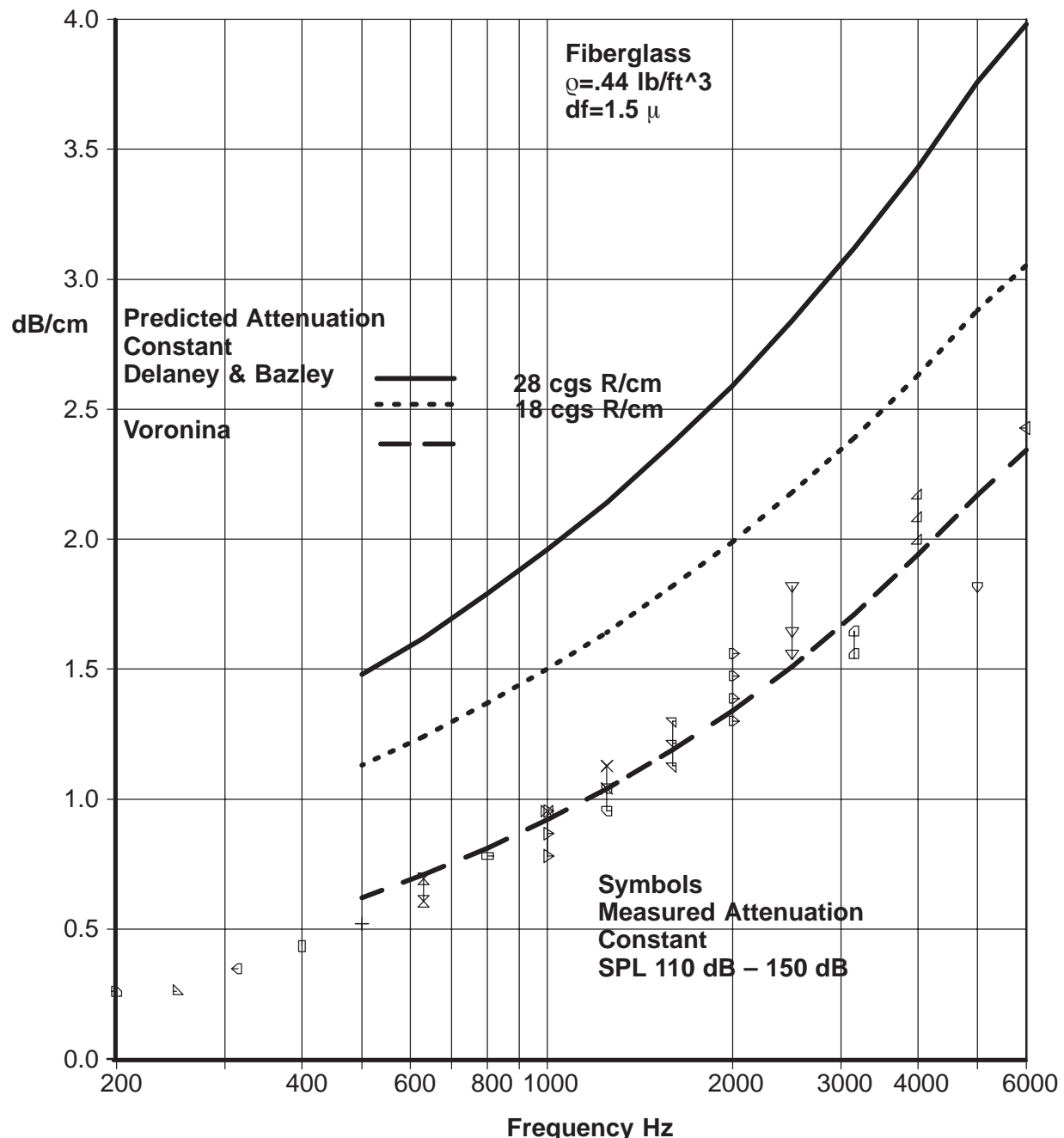


Figure 20: Measured vs. Predicted Attenuation Constant

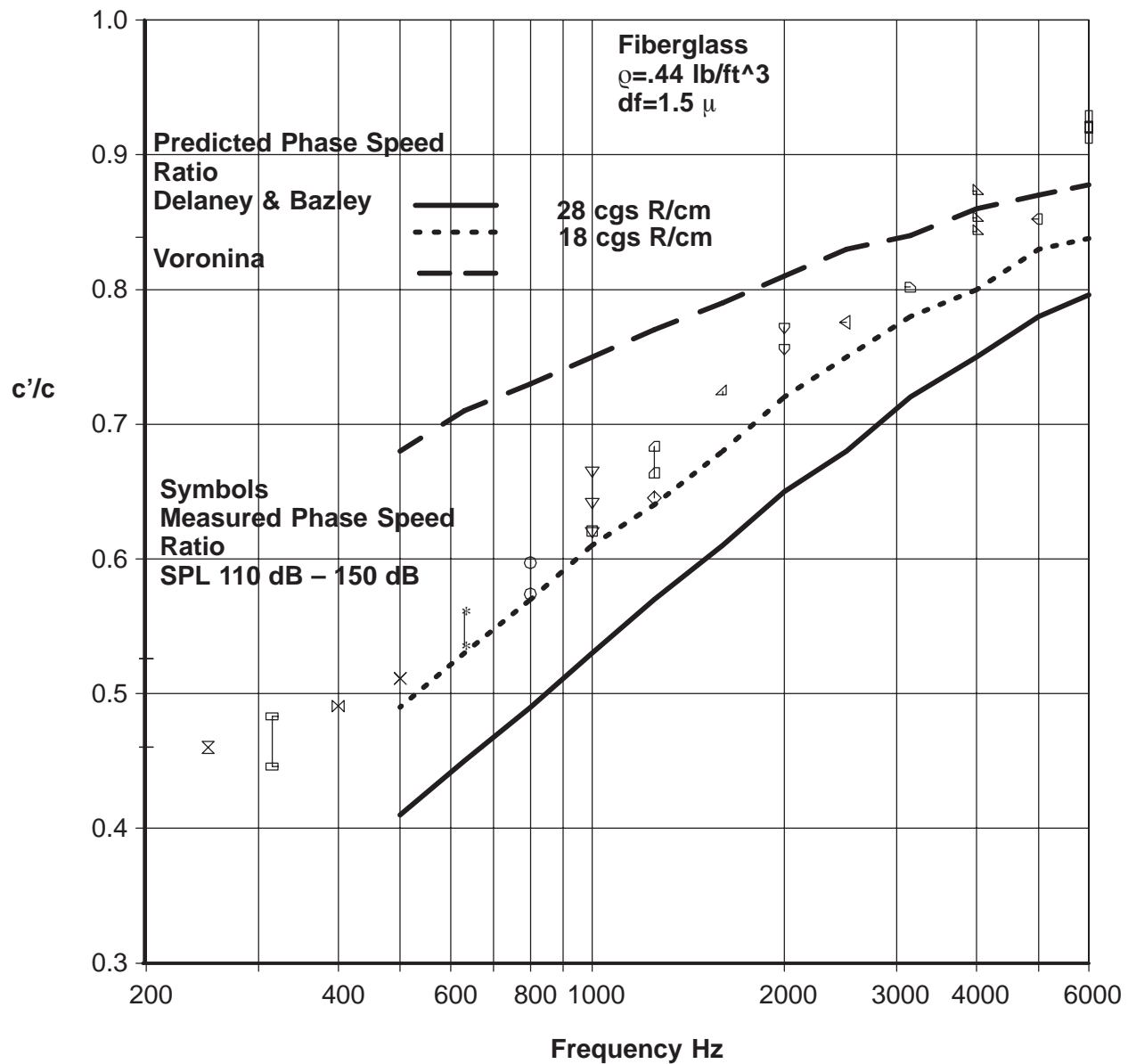


Figure 21: Measured vs. Predicted Phase Speed Ratio

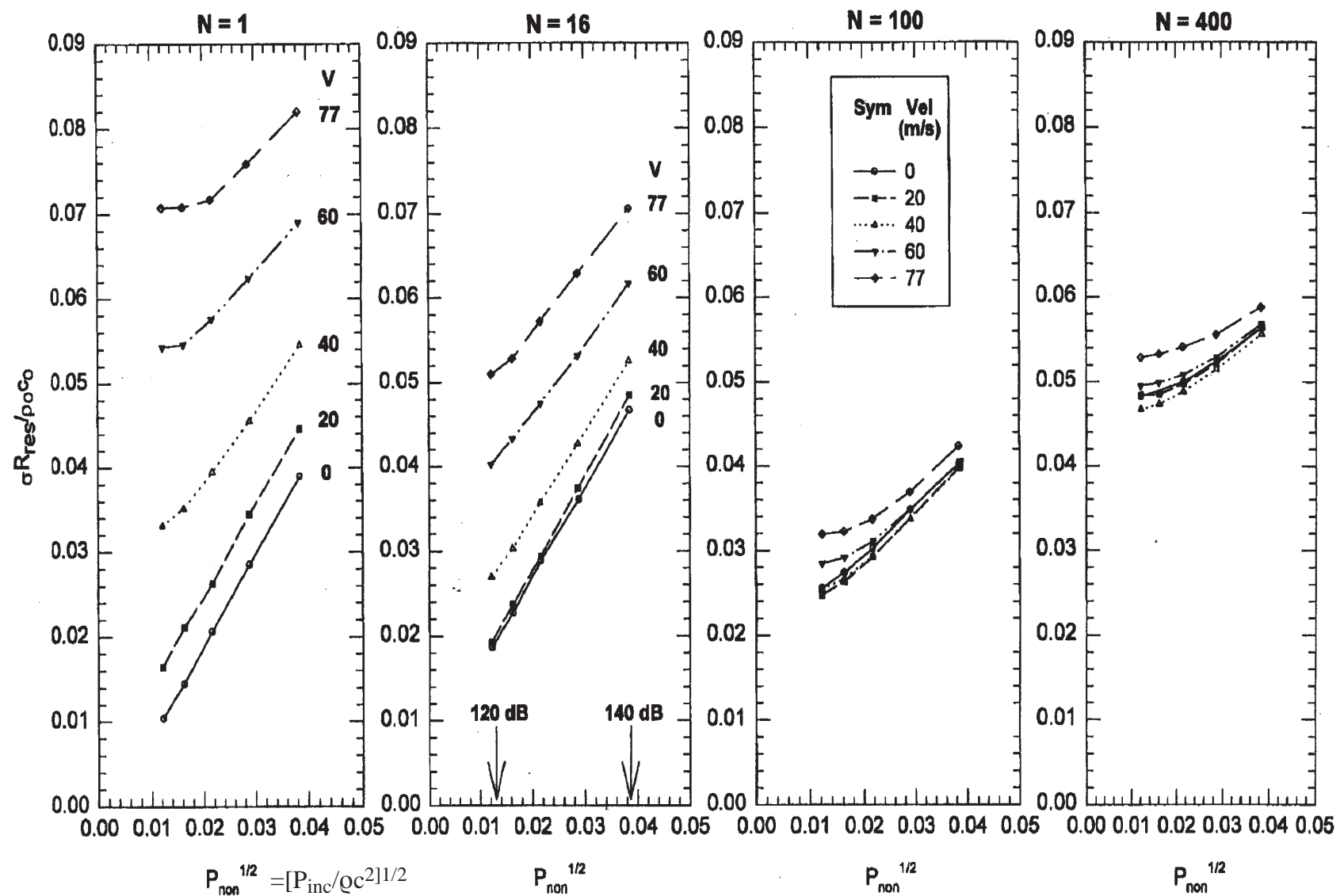


Figure 22: Effect Of Orifice Number, Grazing Flow Speed and SPL on Resonator Tuned Resistance

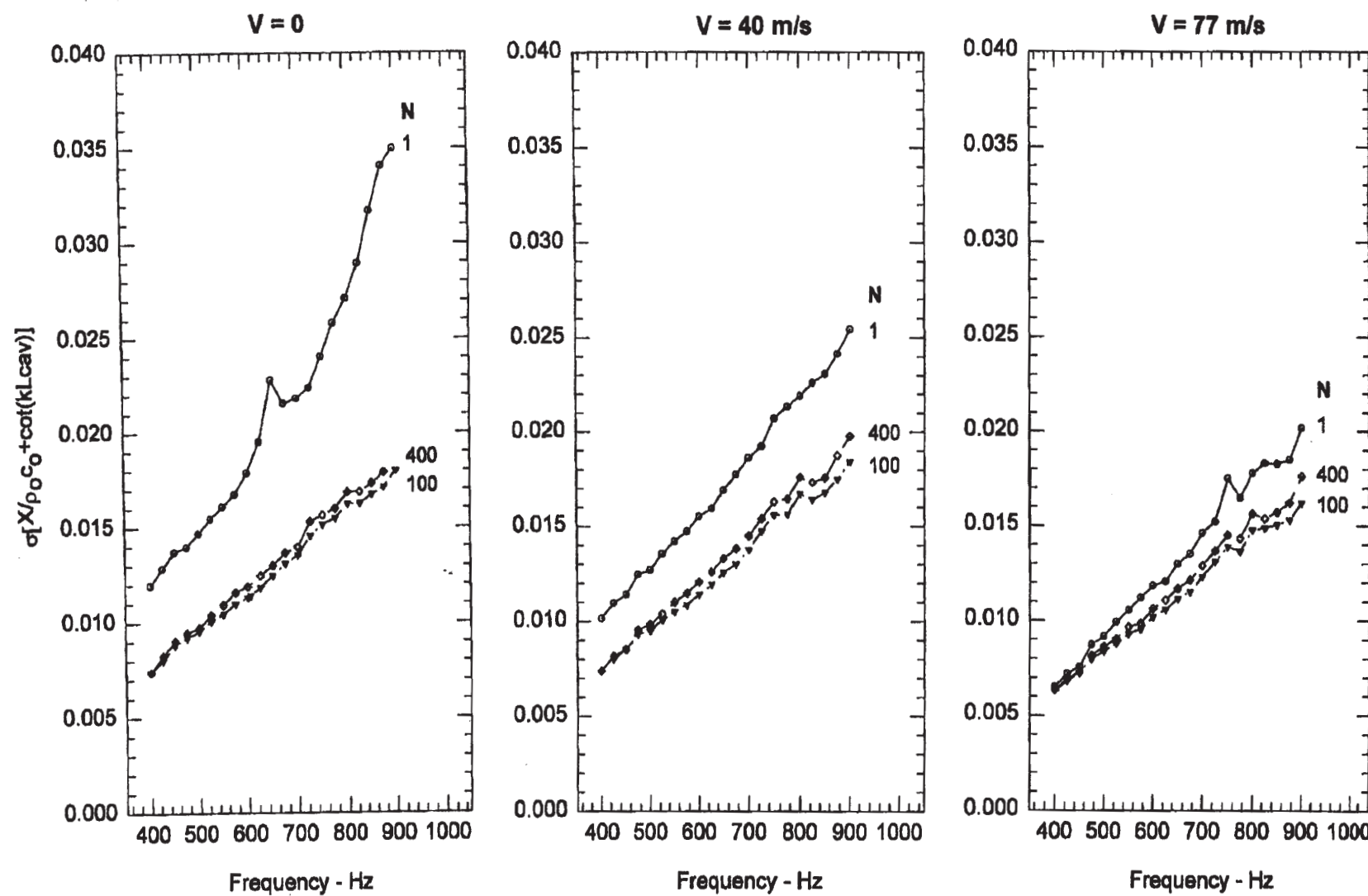


Figure 23: Effect Of Orifice Number and Grazing Flow Speed on Resonator Face-Sheet Mass Reactance: SPL = 135 dB

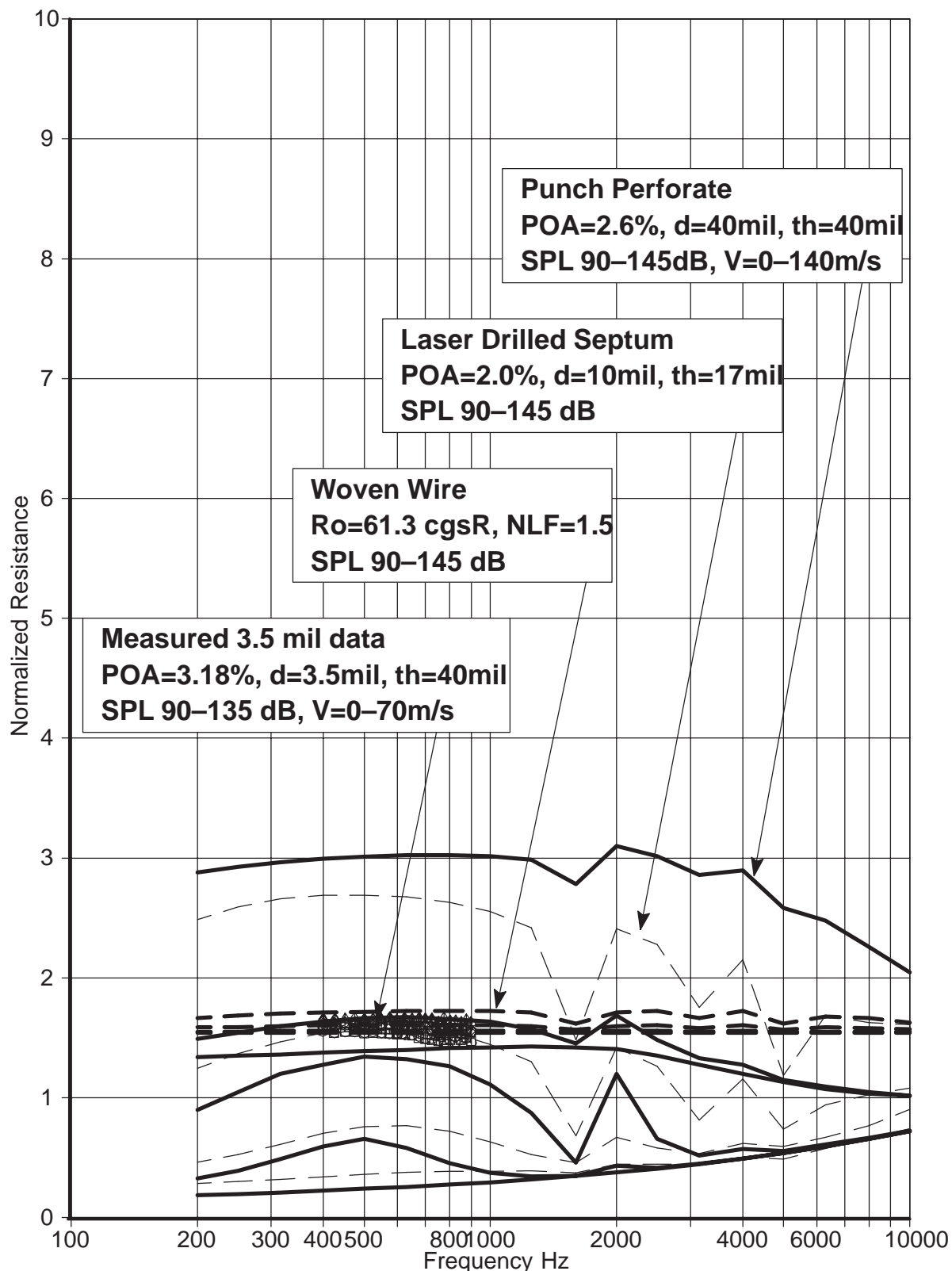


Figure 24: Comparison Of Effect Of Grazing Flow And SPL Changes
On Acoustic Resistance Of Currently Used Perforates With Micro-Perforate

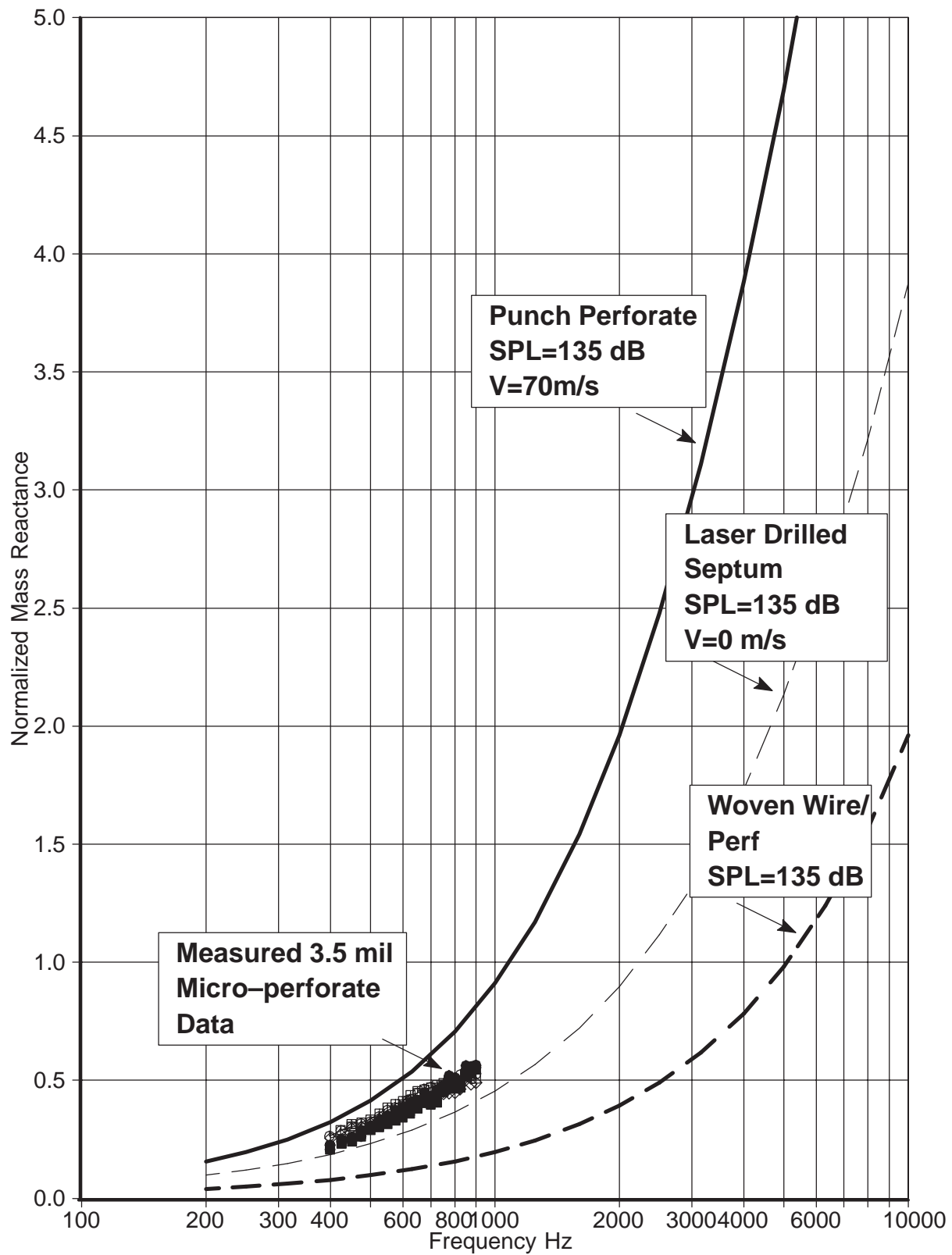


Figure 25: Comparison Of Acoustic Mass Reactance For Currently Used Perforates With Micro-Perforate

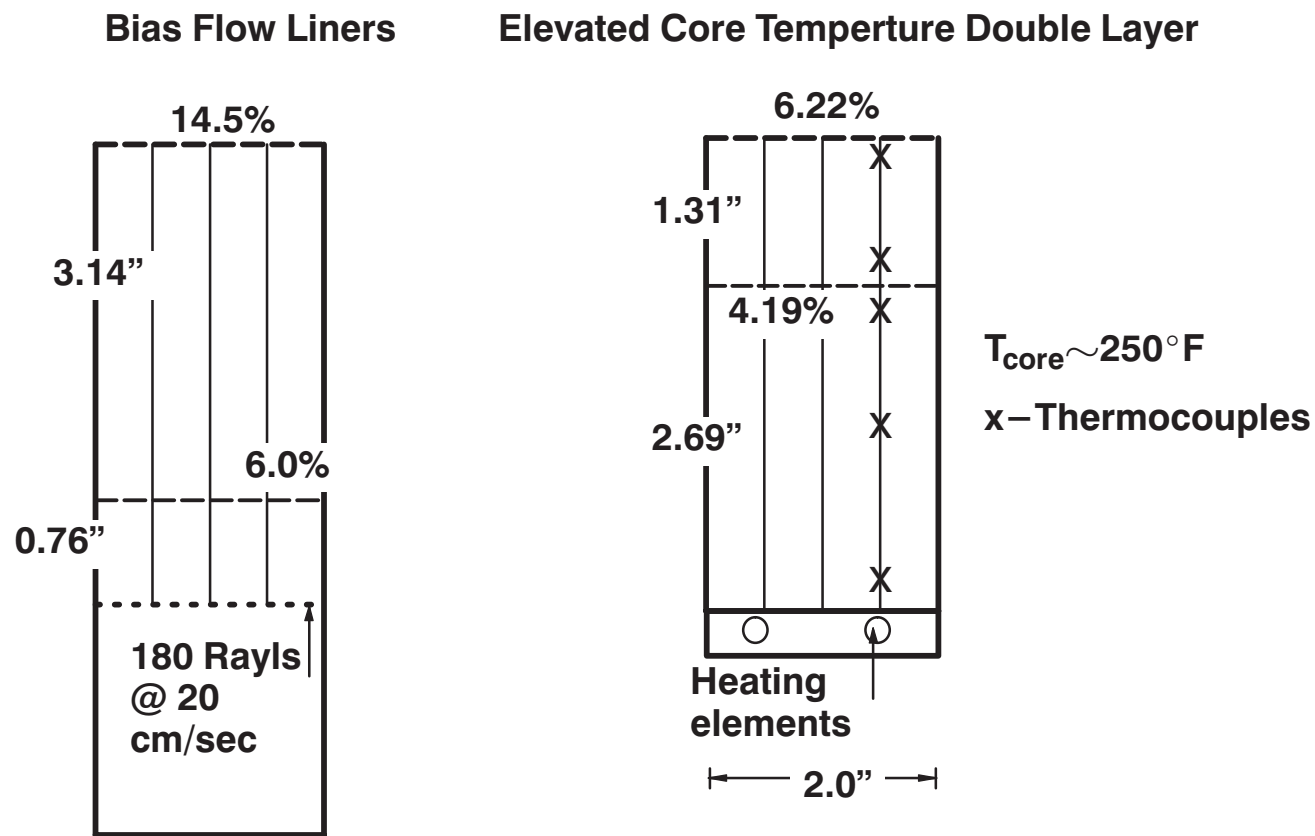


Figure 26: Adaptive Liner Test Designs

Predictions include the
effect of the cavity behind the
180 Rayl septum

Approach Condition

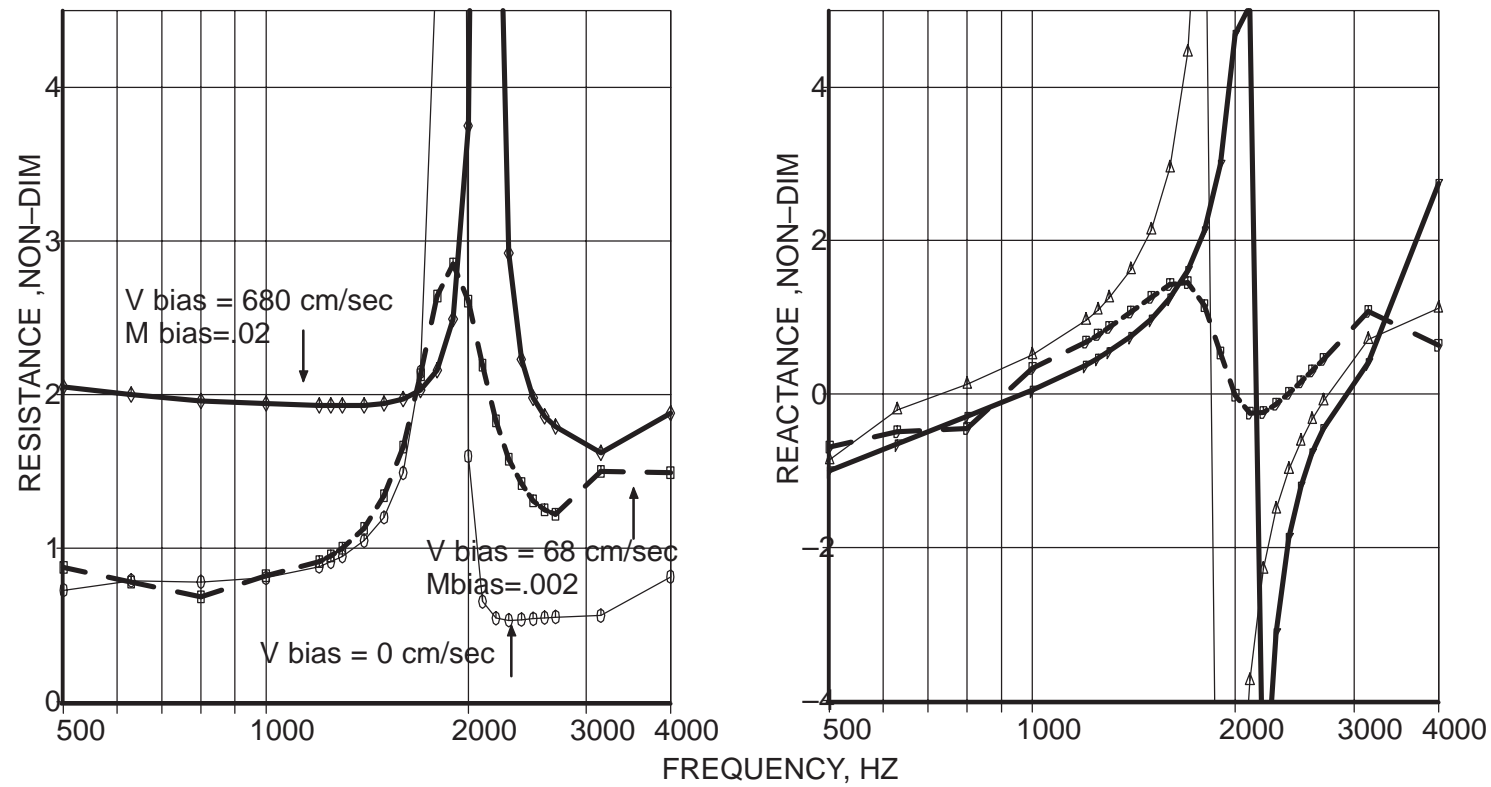


Figure 27: Predicted Bias Flow Impedance Changes For Test Liner

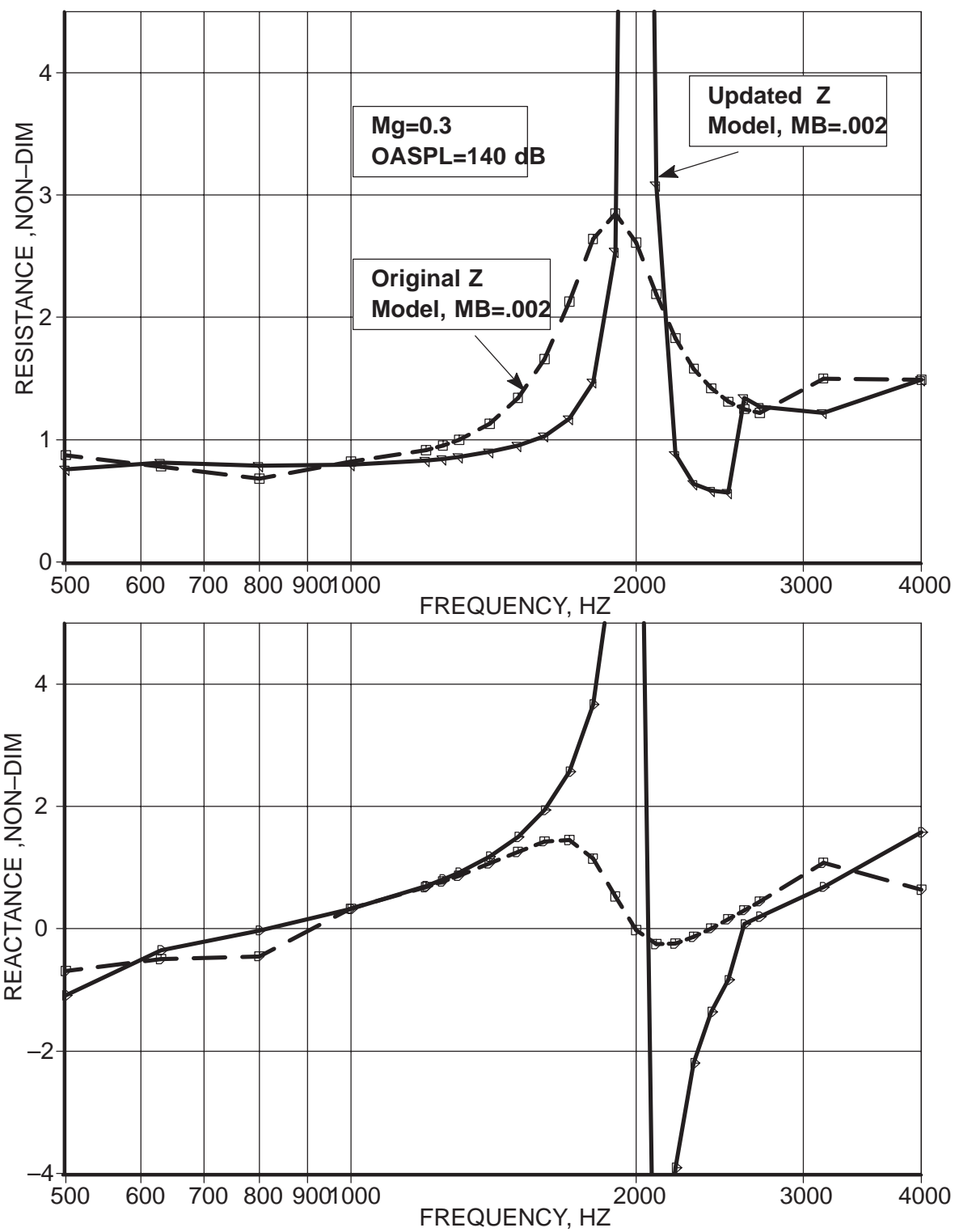


Figure 28: Comparison Of Predicted Impedance Spectra For The Bias Flow Test Liner With The Original And Updated Bias Flow Impedance Models.

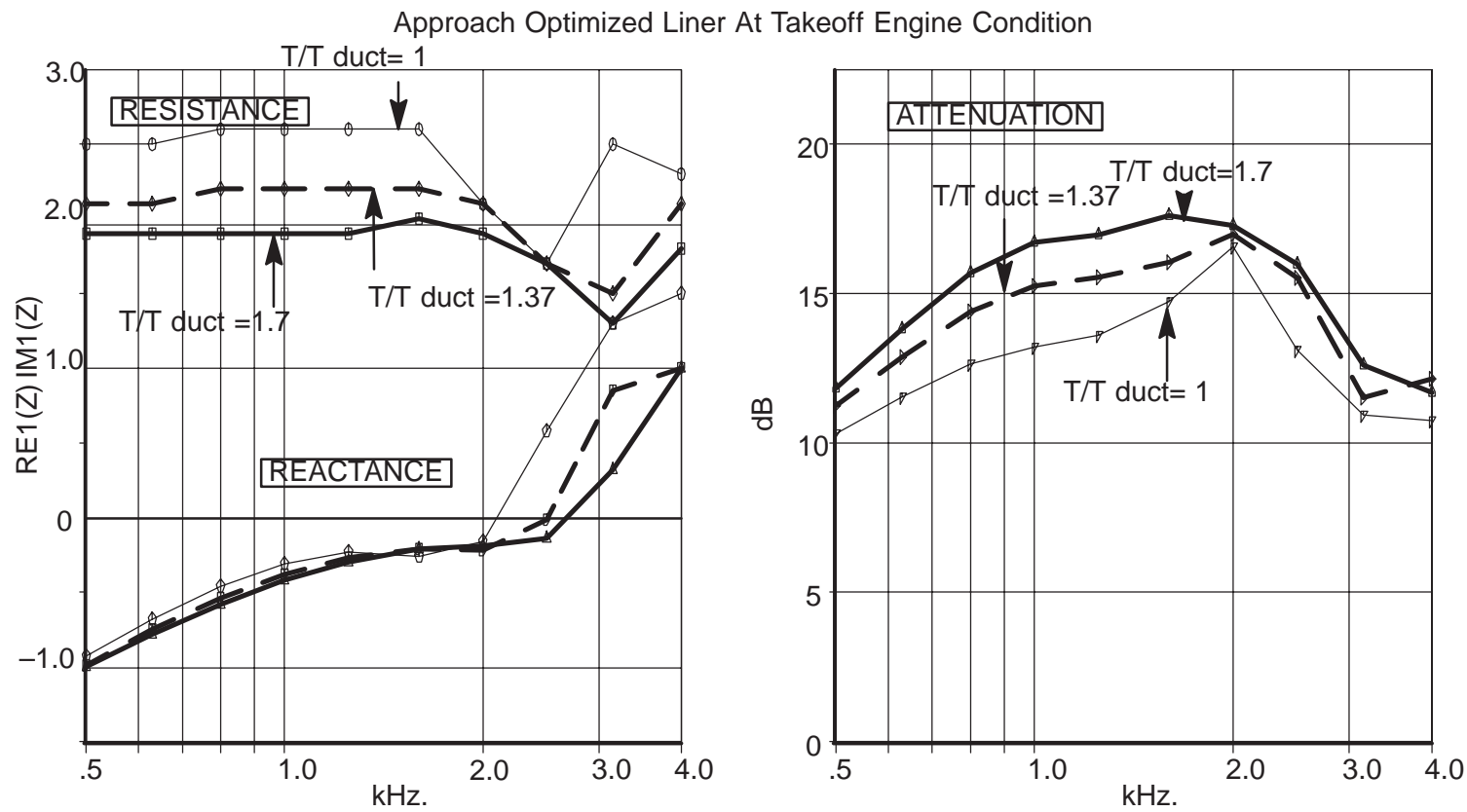


Figure 29: High Temperature Liner Predicted Impedance and Attenuation

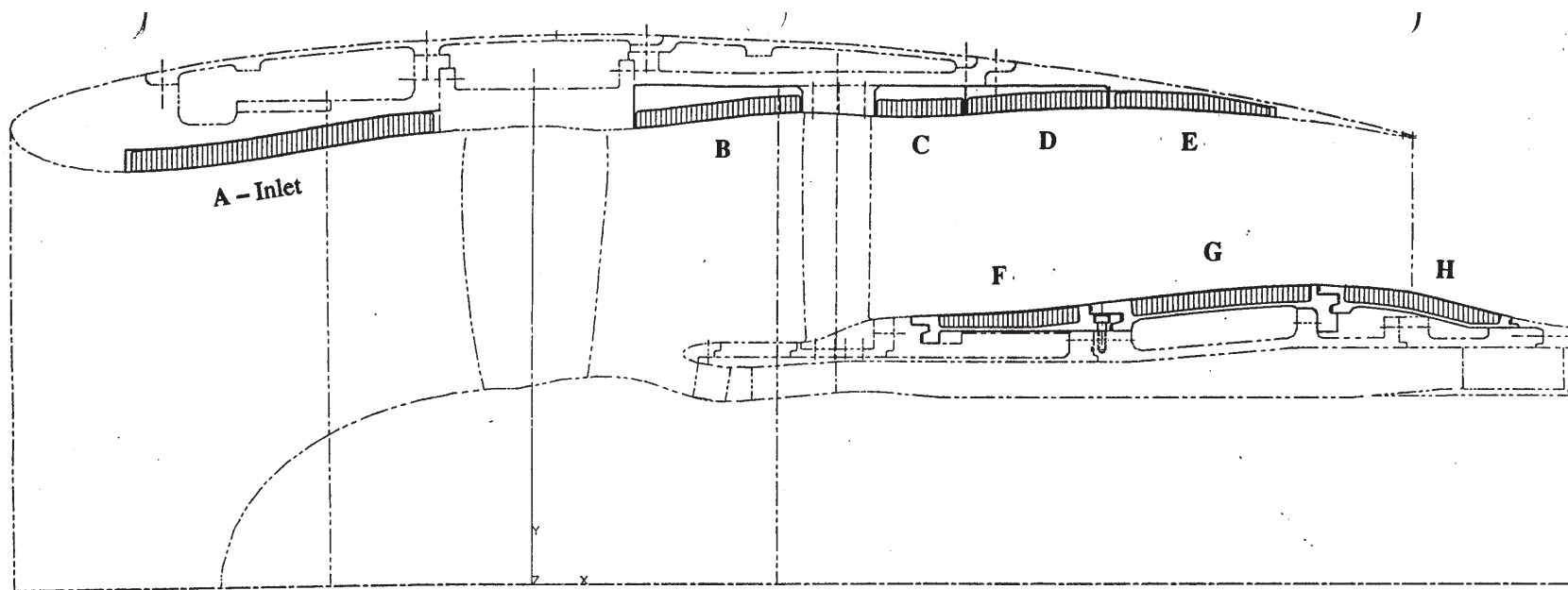


Figure 30: Cartoon of Lining Segments
Supplied by Pratt and Whitney

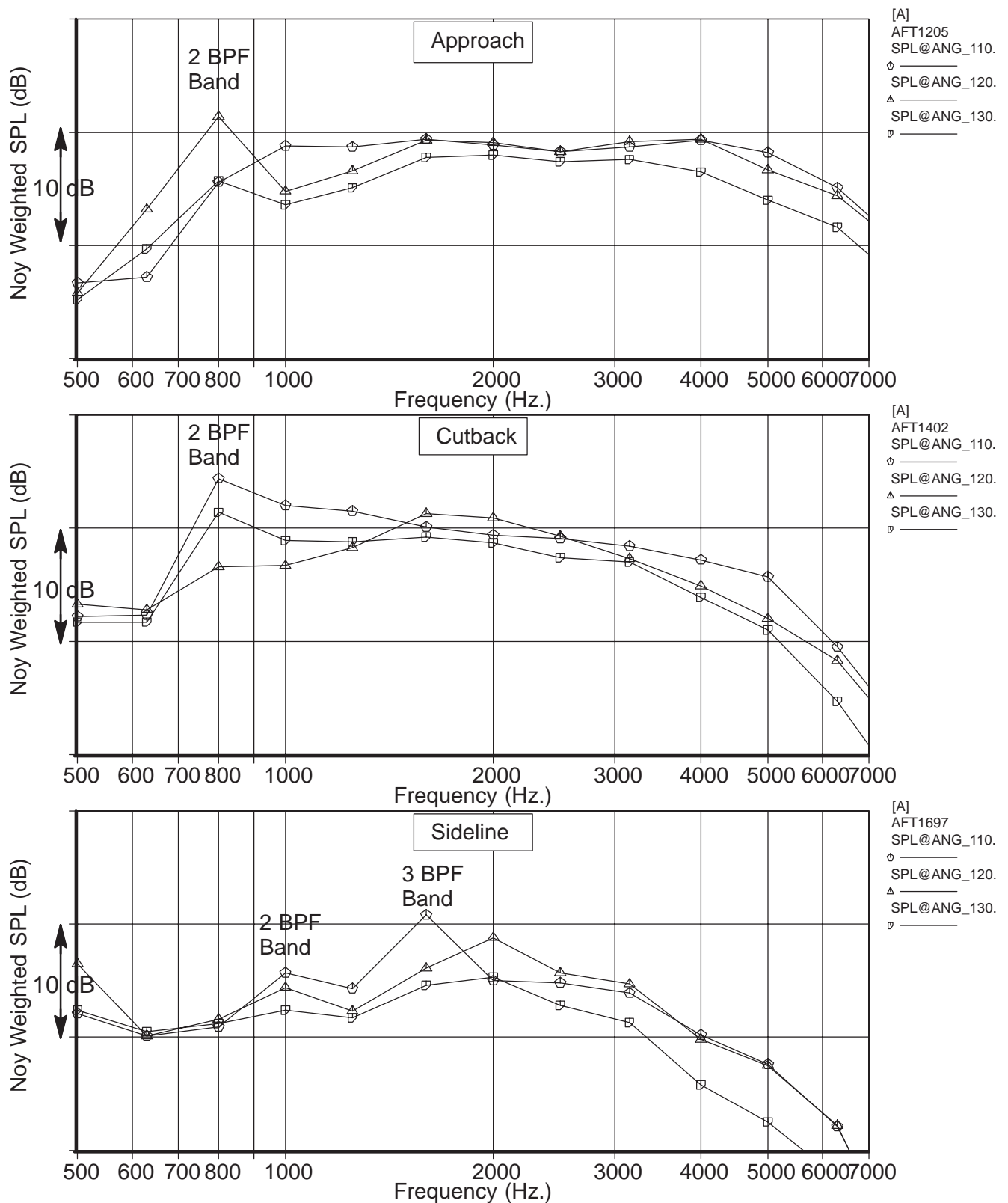


Figure 31: Comparison of the Design ADP Hardwalled Data Prediction SPL vs Frequency for 110, 120, and 130 Degrees (Approach, cutback, and sideline conditions)

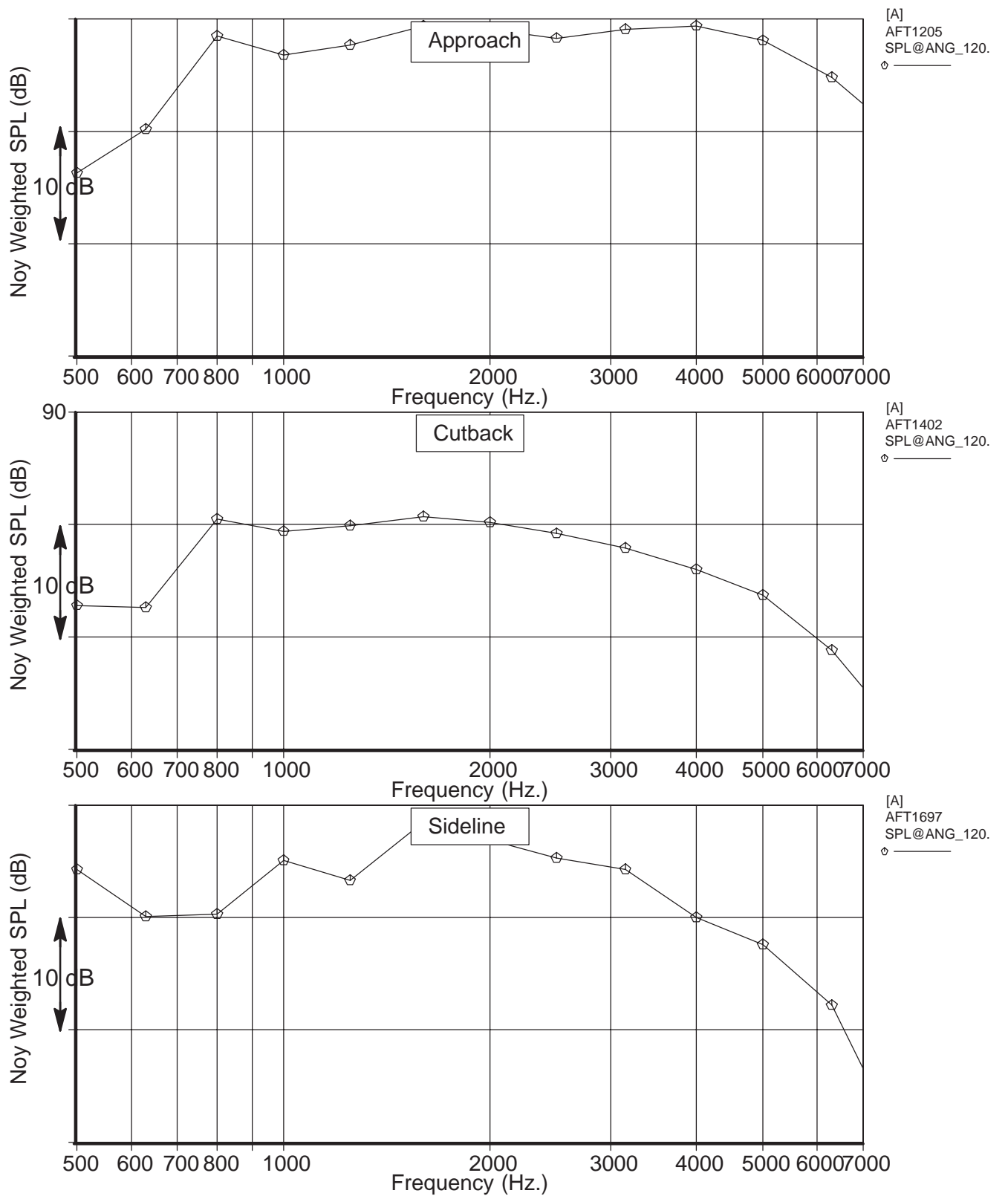


Figure 32: Hardwall Target Spectra Based On ADP Demo Data
 SPL vs Frequency for the average of 110 and 120 Degrees
 (Approach, cutback, and sideline conditions)

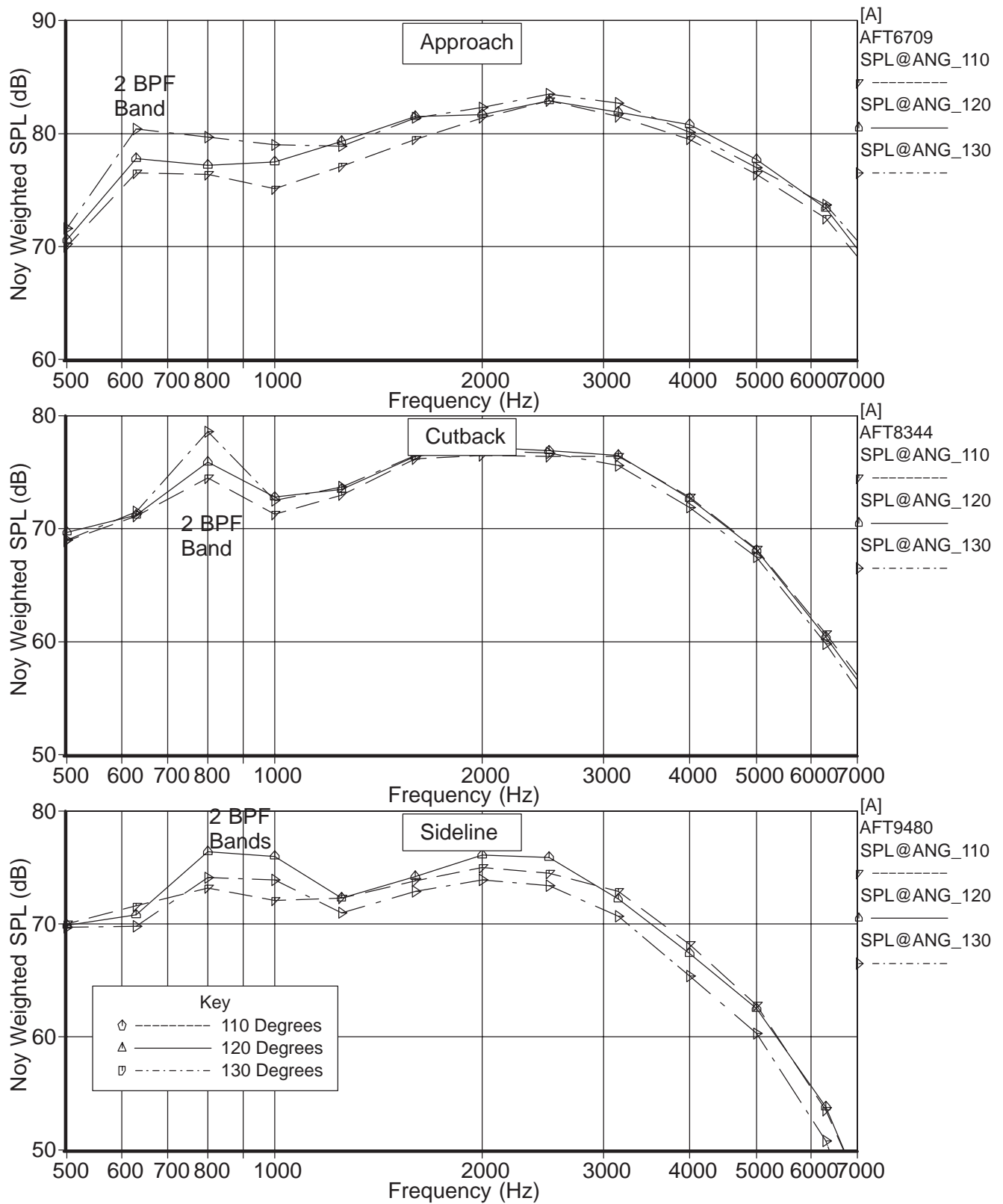


Figure 33: Comparison of Hardwalled 22" ADP Data
SPL vs Frequency for 110, 120, and 130 Degrees
(Approach, cutback, and sideline conditions)

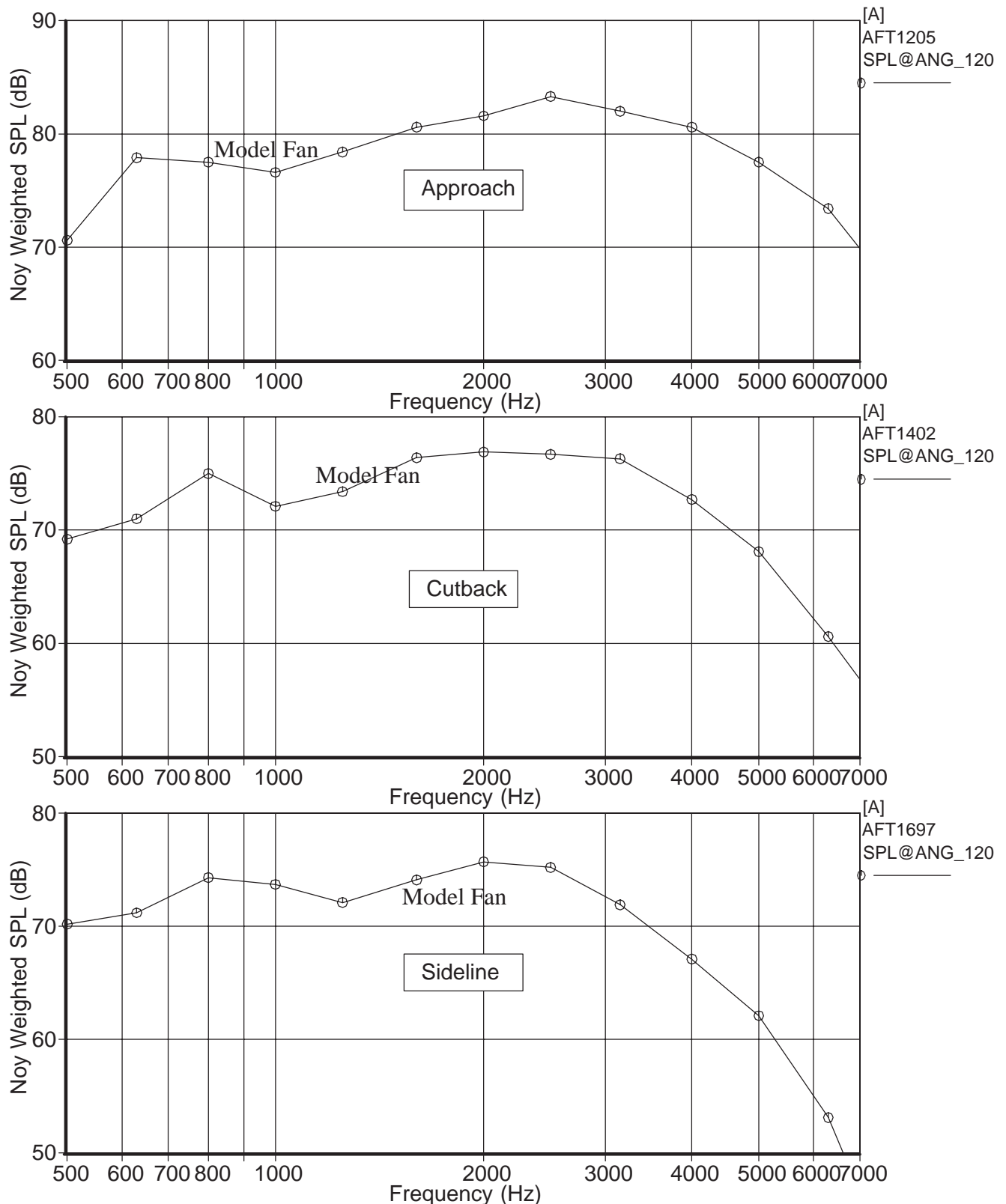


Figure 34: Hardwall Target Spectra Based On ADP Model Fan Data
 SPL vs Frequency for the average of 110 and 120 Degrees
 (Approach, cutback, and sideline conditions)

Fan Duct Model For Attenuation Calculations

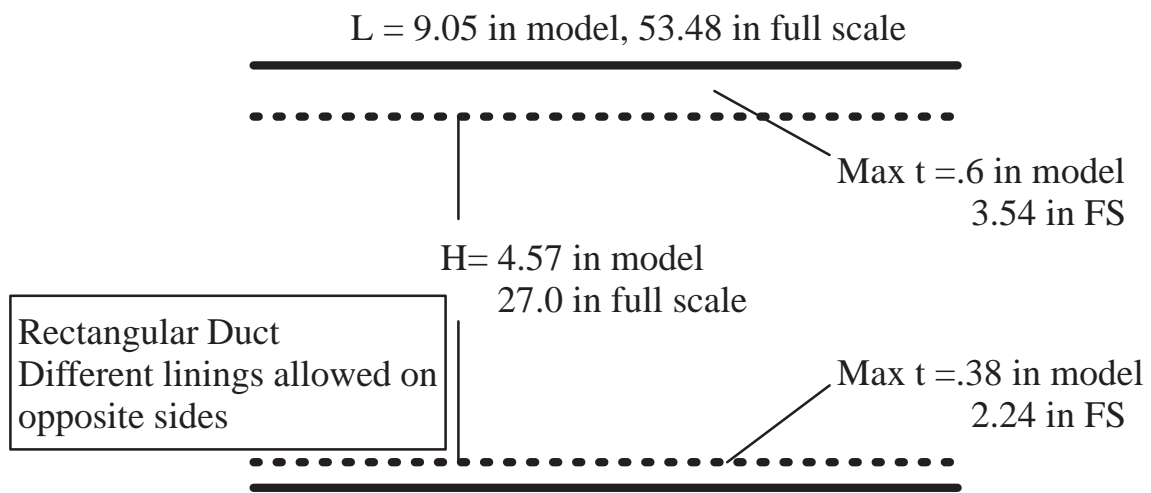


Figure 35: Representation of the Fan Duct with the MELO Program

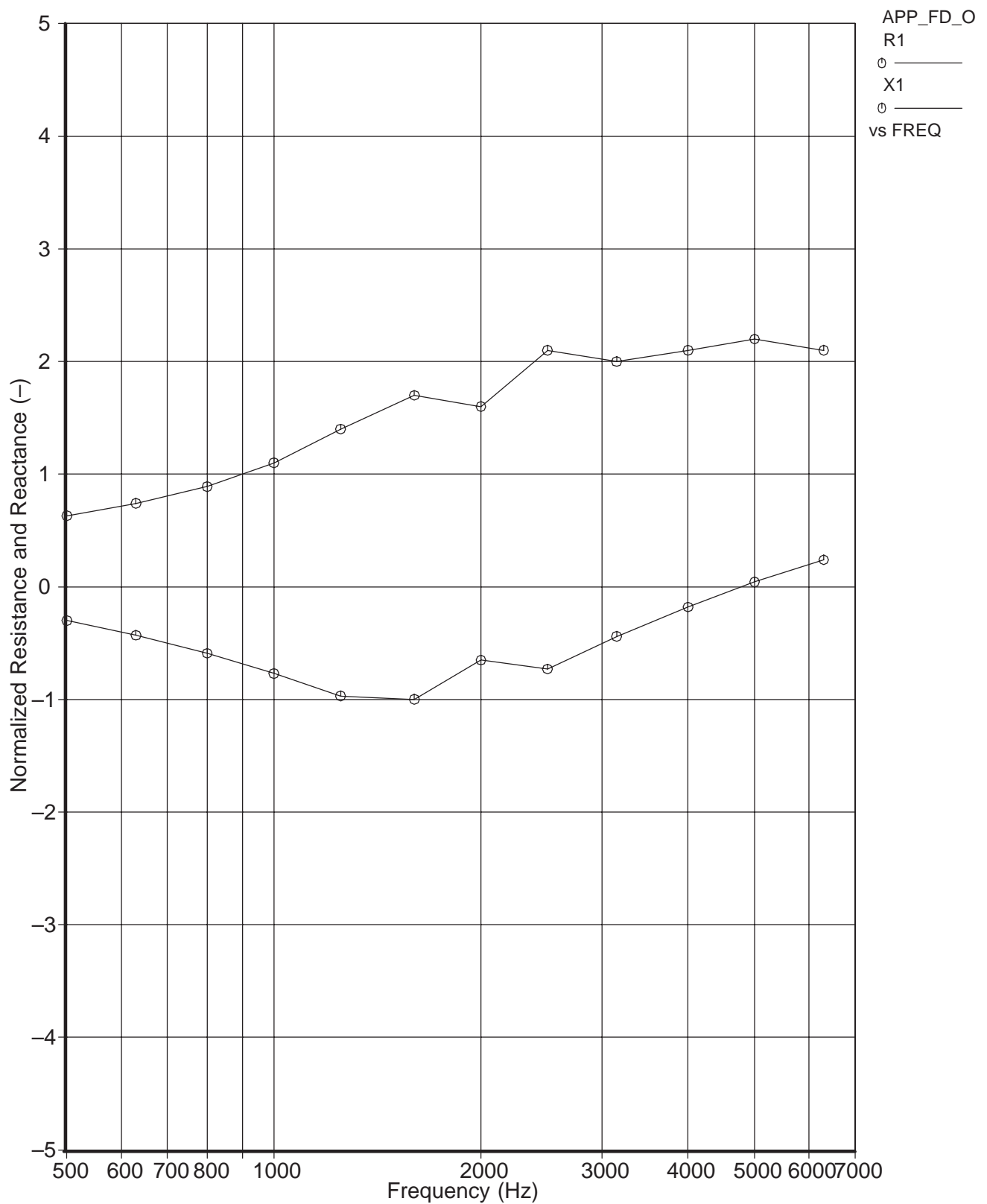


Figure 36: Optimum Lining Impedance for the ADP Fan Duct
Predicted using Boeing's MELO Program
(Boundary Layer Thickness = 0.3 cm)

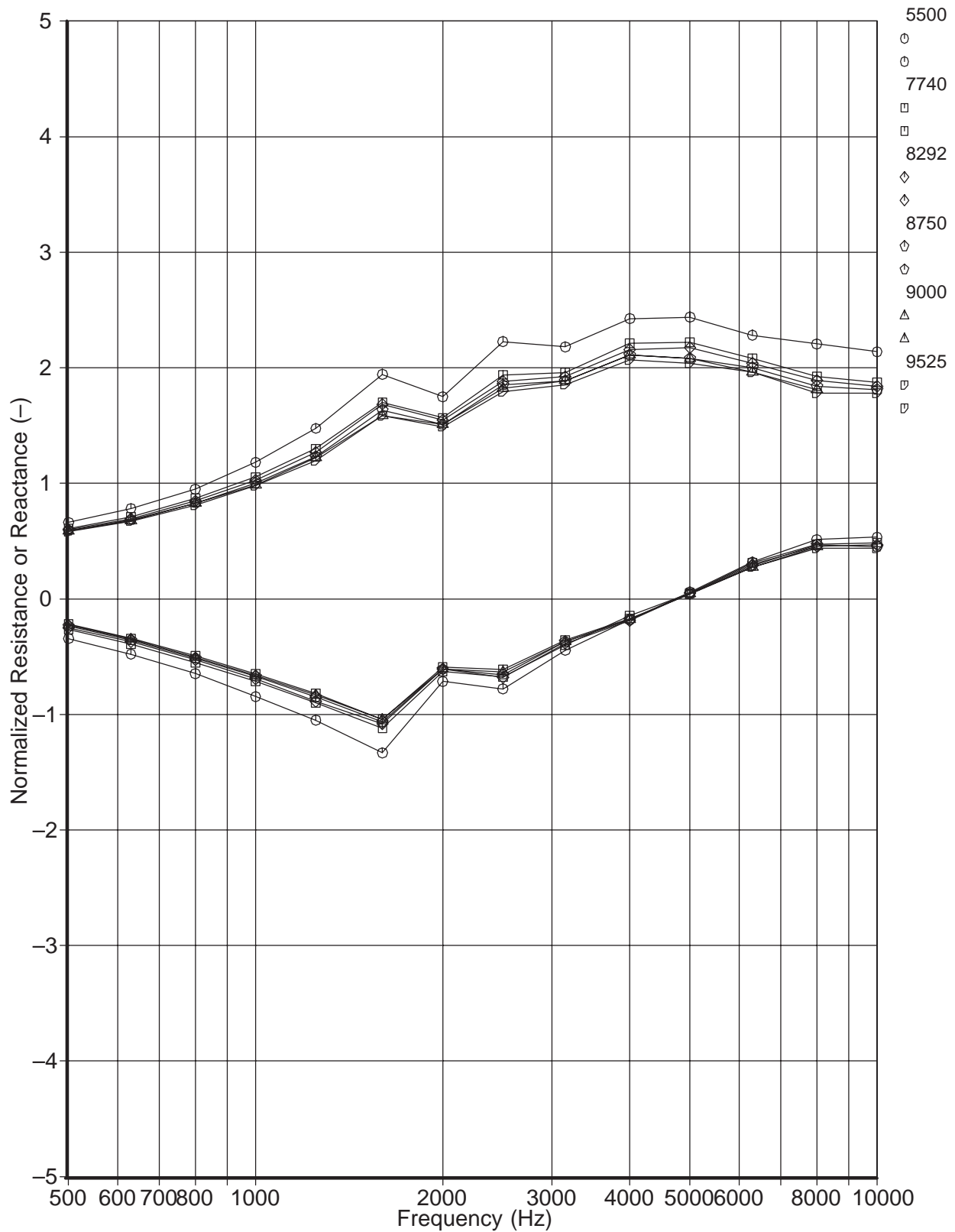


Figure 37: Preliminary Ideal Impedance Calculations for the ADP Fan Duct
Based on Boeing Program MELO

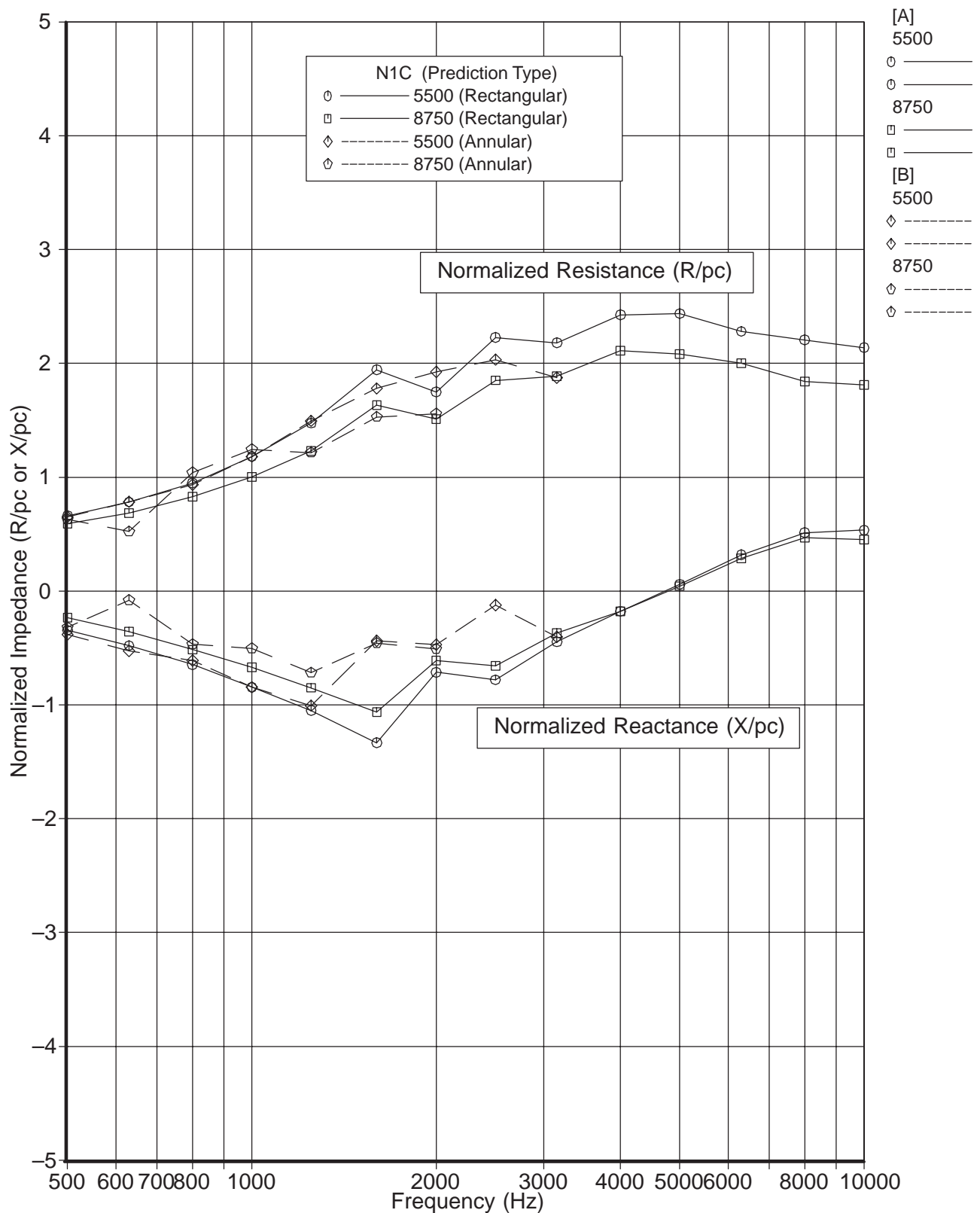


Figure 38: Ideal Impedance Calculations for the ADP Fan Duct
Comparison of Annular and Rectangular Solutions from MELO

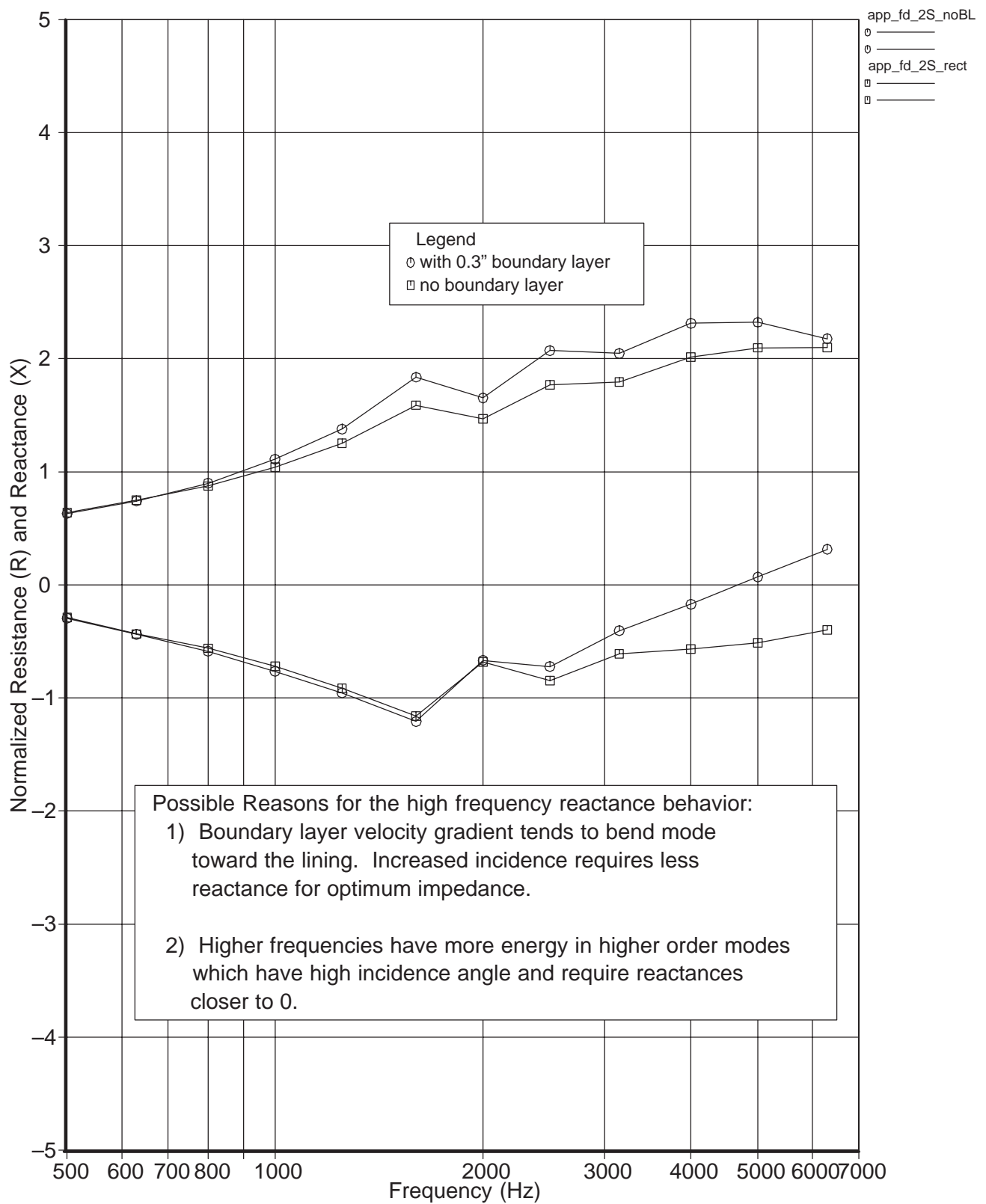


Figure 39: Comparison of Boundary Layer Effect on Optimum Impedances
(2 sided w/BL and 2 sided w/out BL)

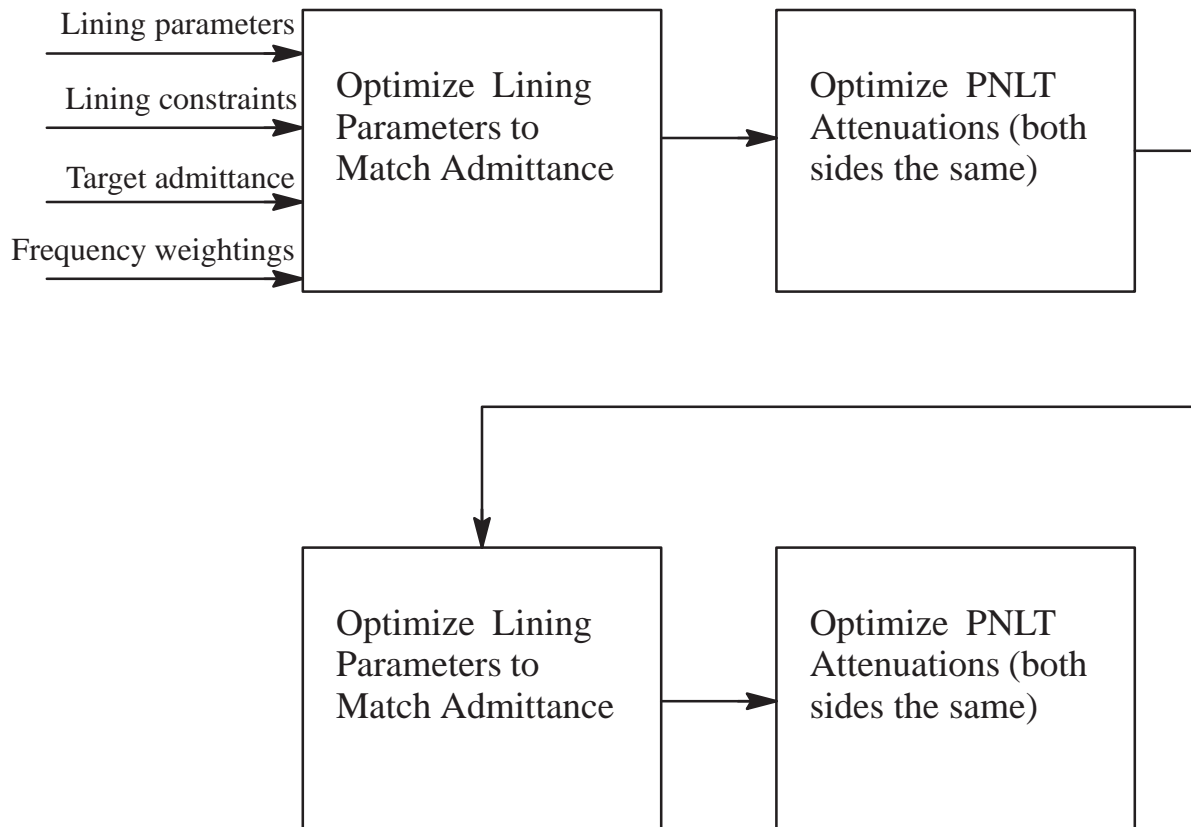


Figure 40: Block Diagram of the Design Process

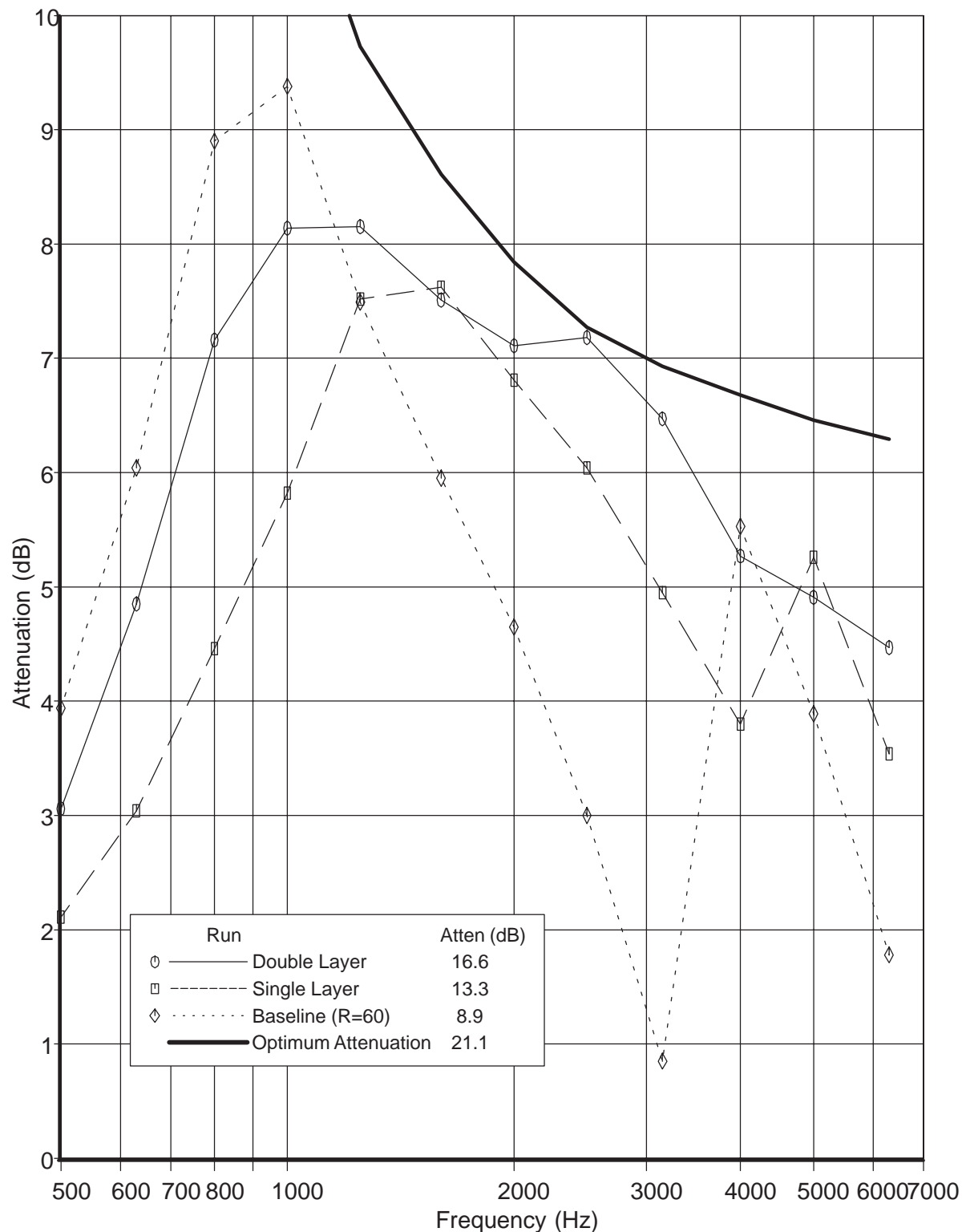


Figure 41: MELO Predicted Lining Attenuations vs the Optimum Attenuations
Two-Sided Single and Double Layer Linings at Scaled Frequencies
(at the cutback condition)

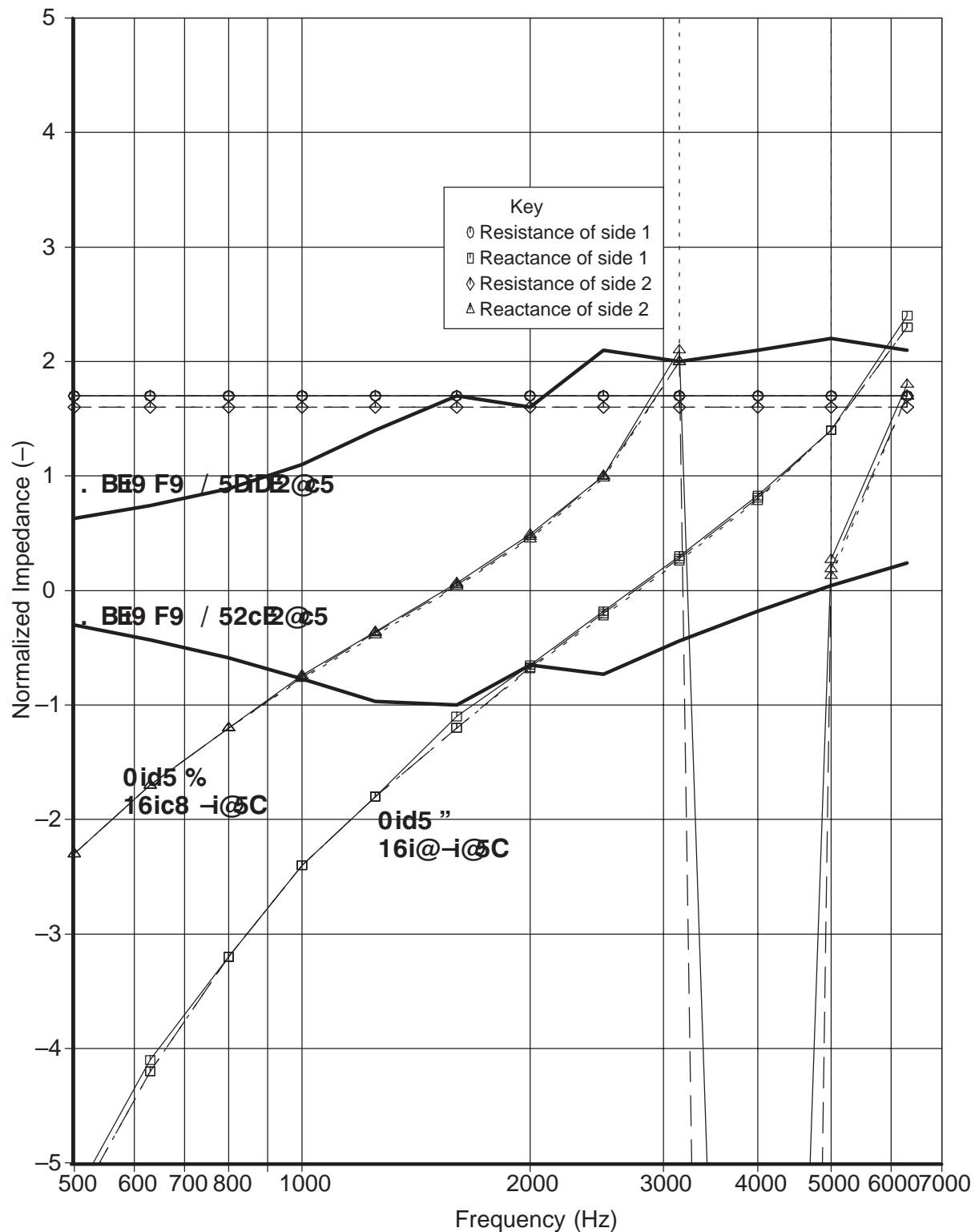


Figure 42: Predicted Lining Impedance vs the Optimum Impedance
Two-Sided Single Layer Lining at Scaled Frequencies
(approach, cutback, and sideline)

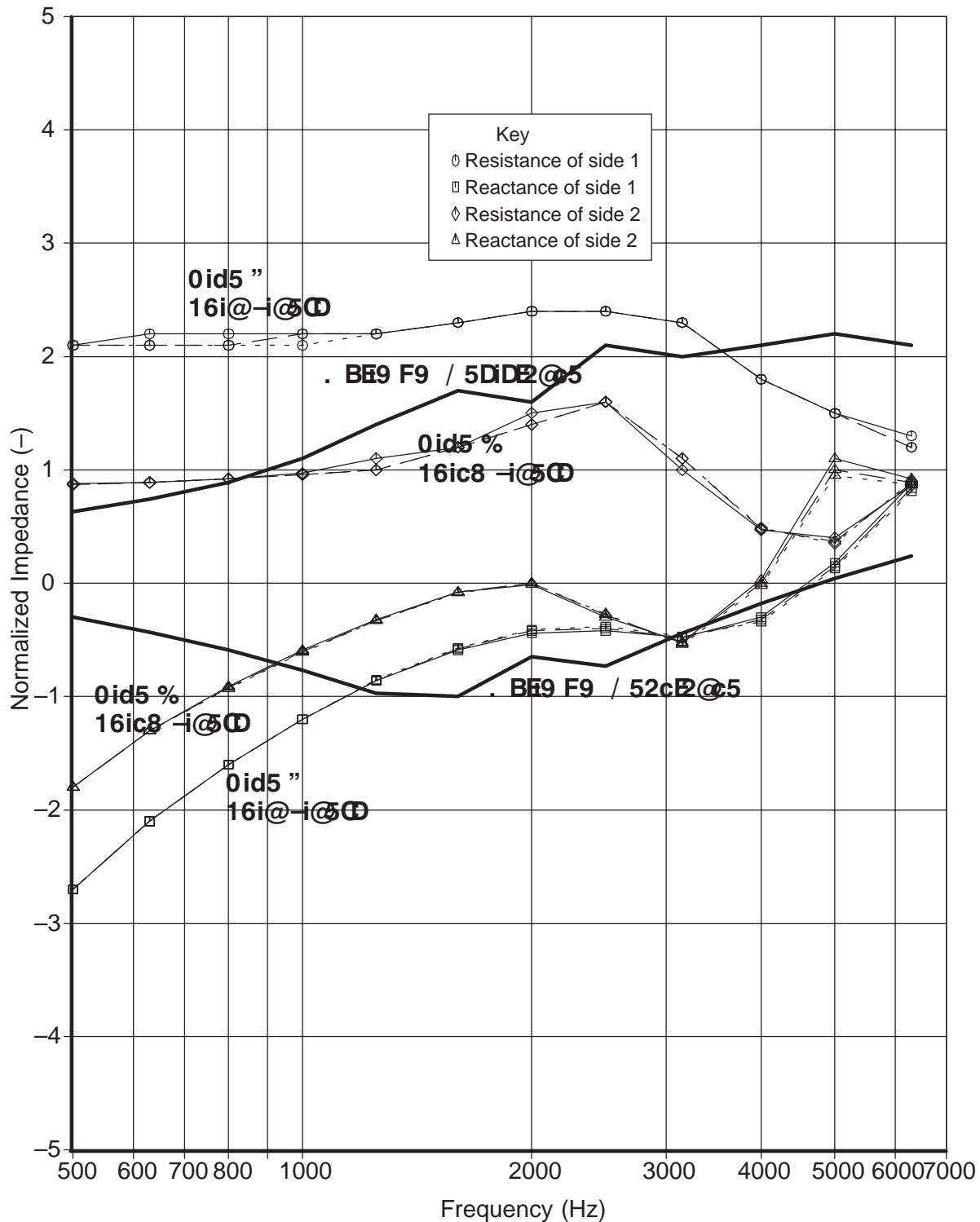
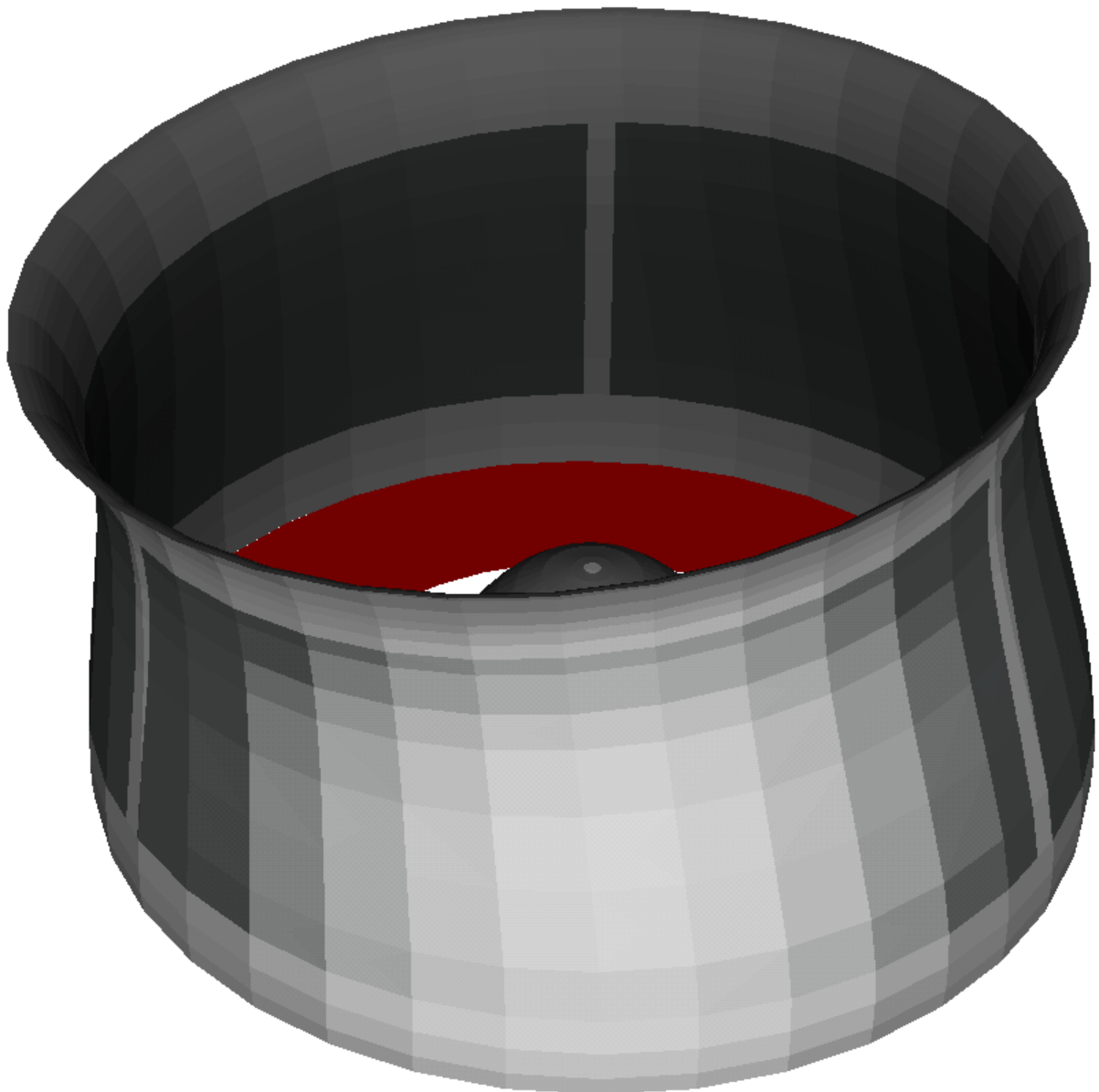


Figure 43: Predicted Lining Impedance vs the Optimum Impedance
 Two-Sided Double Layer Lining at Scaled Frequencies
 (approach, cutback, sideline)

Figure 44: Conventional Inlet Used for the Inlet Trades



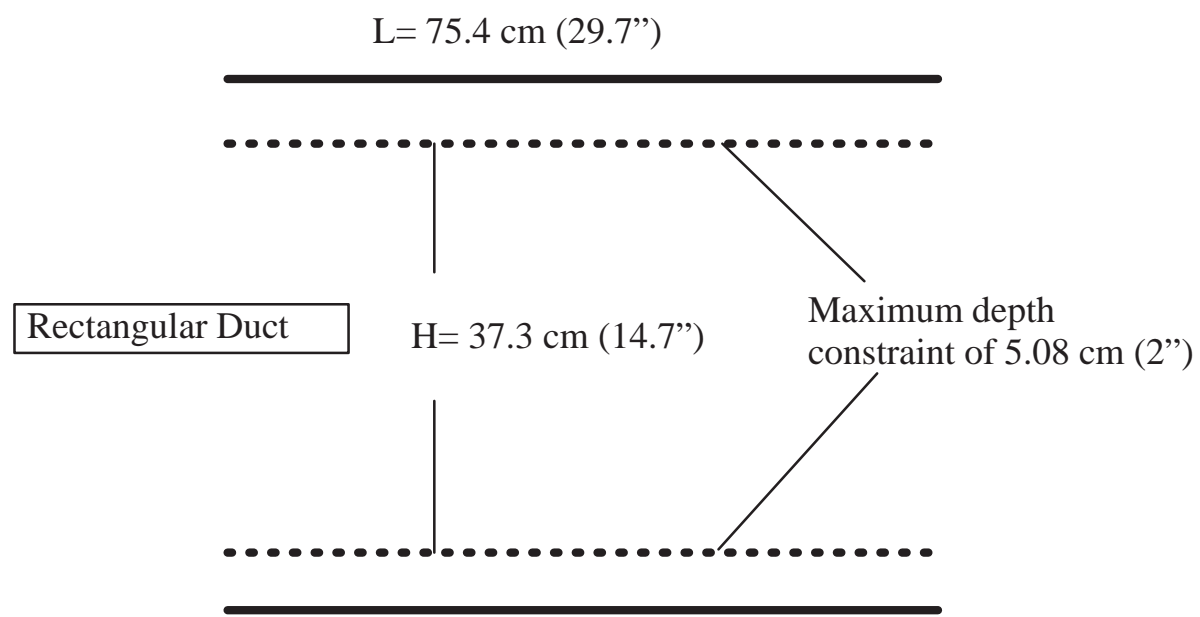


Figure 45: MELO Representation of the Fan Duct Nacelle

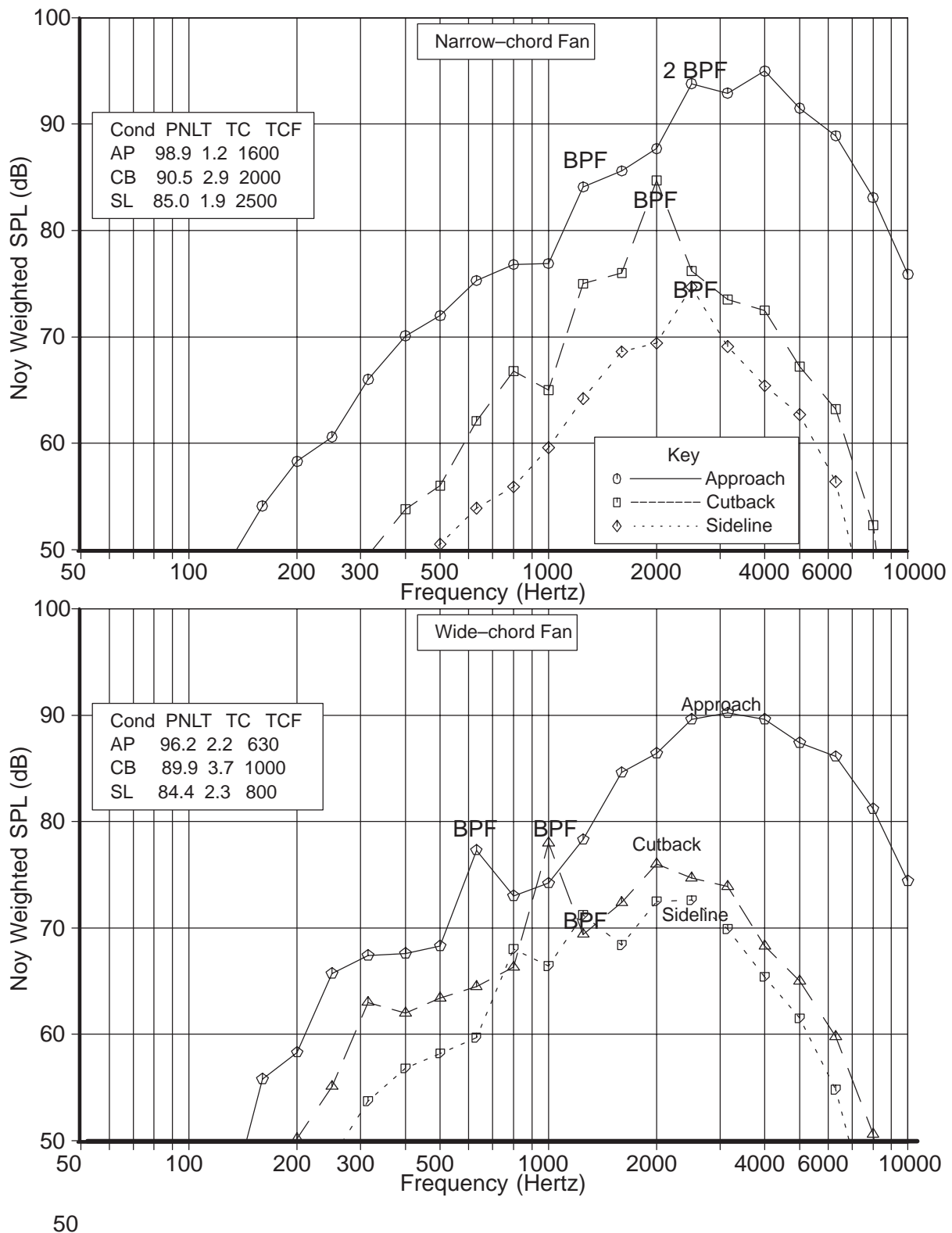


Figure 46: Inlet Spectra for the Approach, Cutback and Sideline Conditions
(for the narrow and wide chord fan engines at 60 degrees)

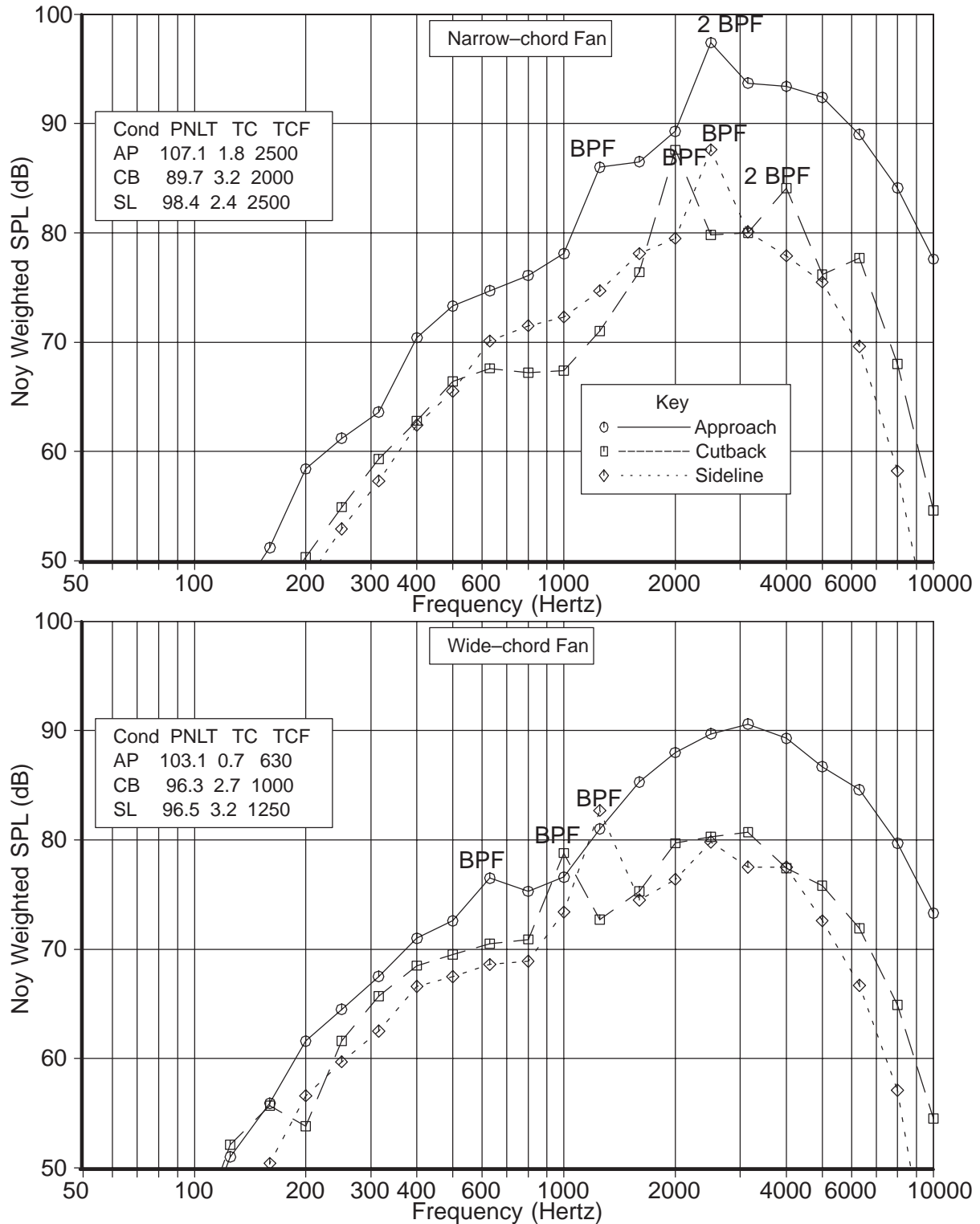
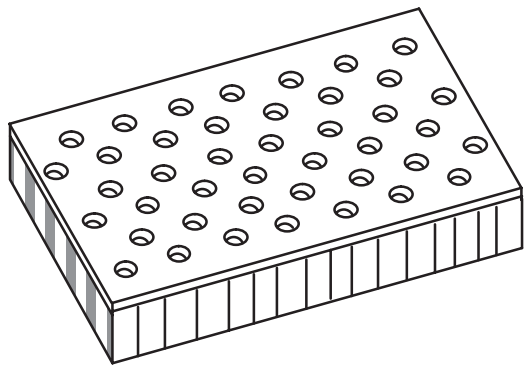
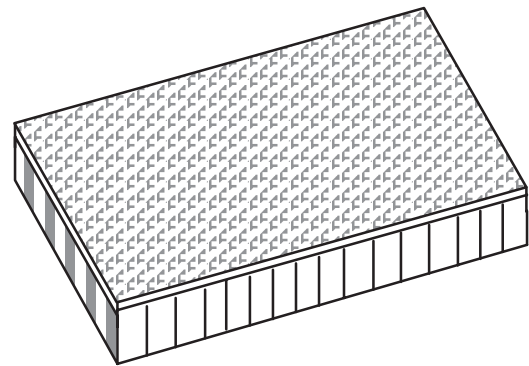


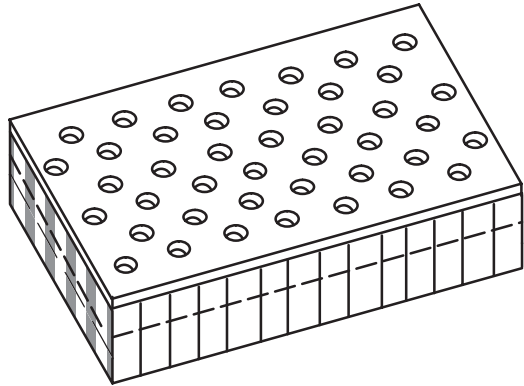
Figure 47: Aft Duct Spectra for the Approach, Cutback and Sideline Conditions (for the narrow and wide chord fan engines at 60 degrees)



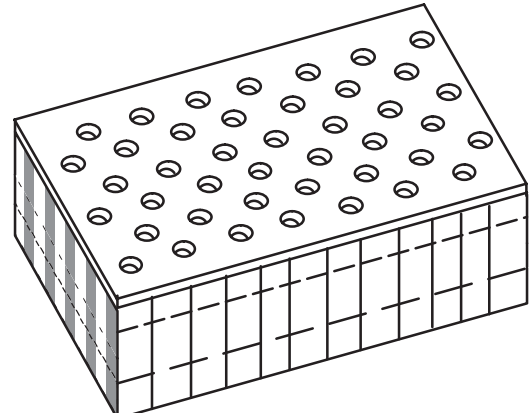
Perforate Single Layer



Linear Single Layer



**Perforate Double Layer
(one septum)**



**Perforate Triple Layer
(two septa)**

Figure 48: Examples of Linings Considered in the Trade Study

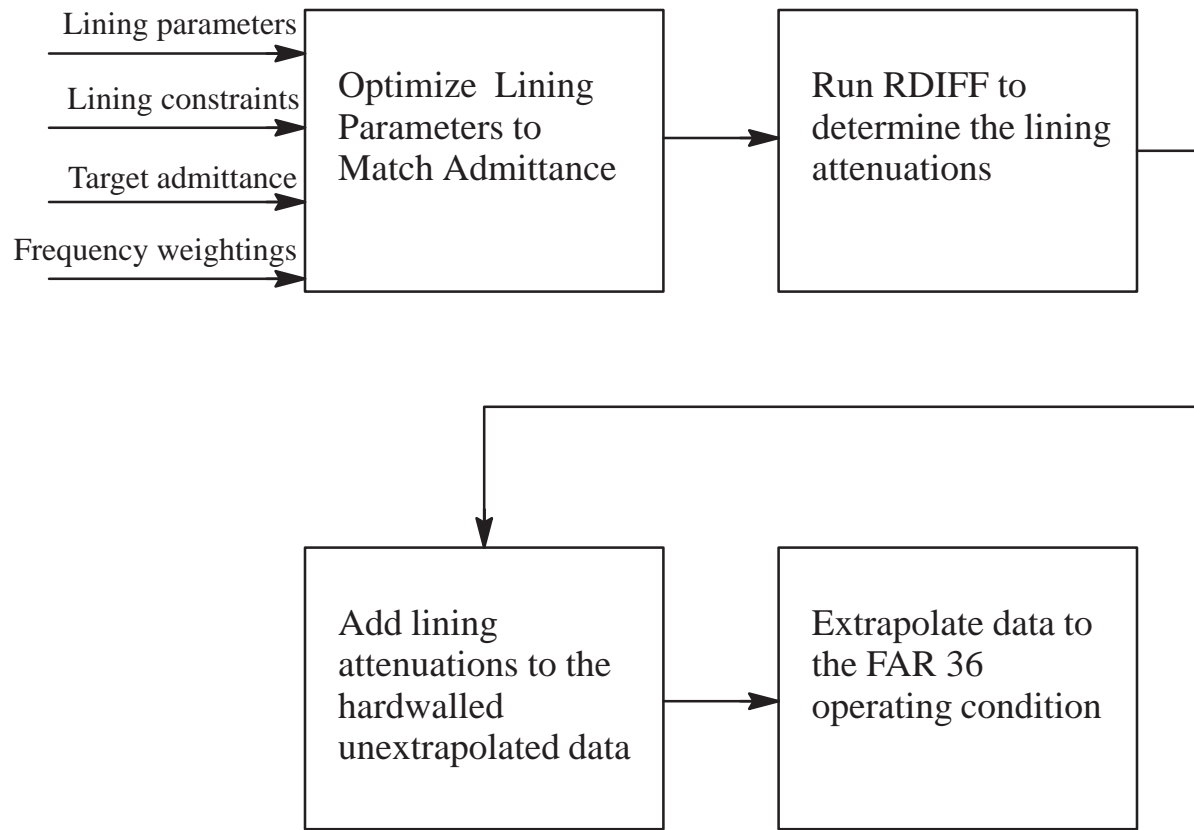


Figure 49: Block Diagram of the Evaluation Process for the Inlet

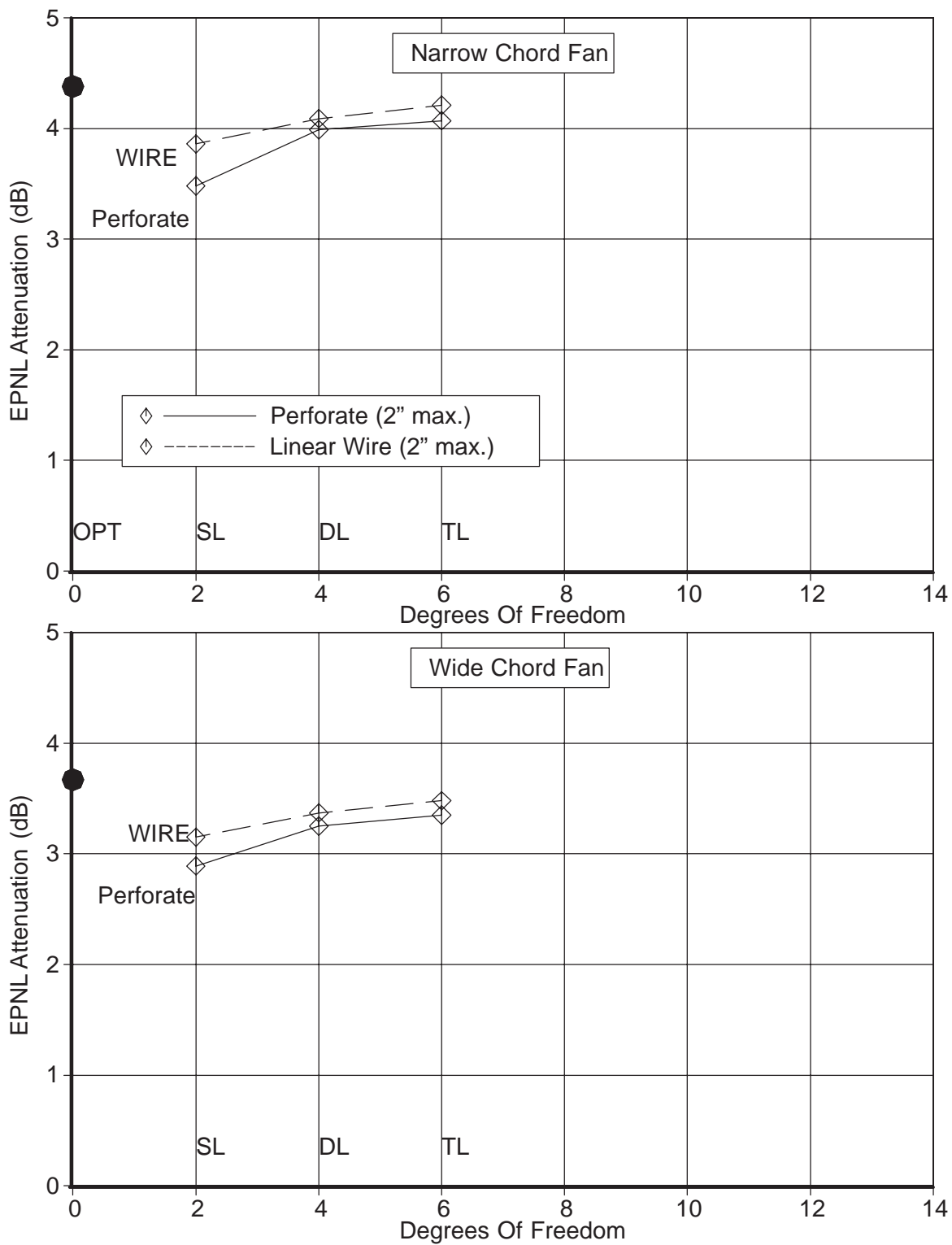


Figure 50: Results of the Impedance Study for the Inlet Component
(at the approach condition)

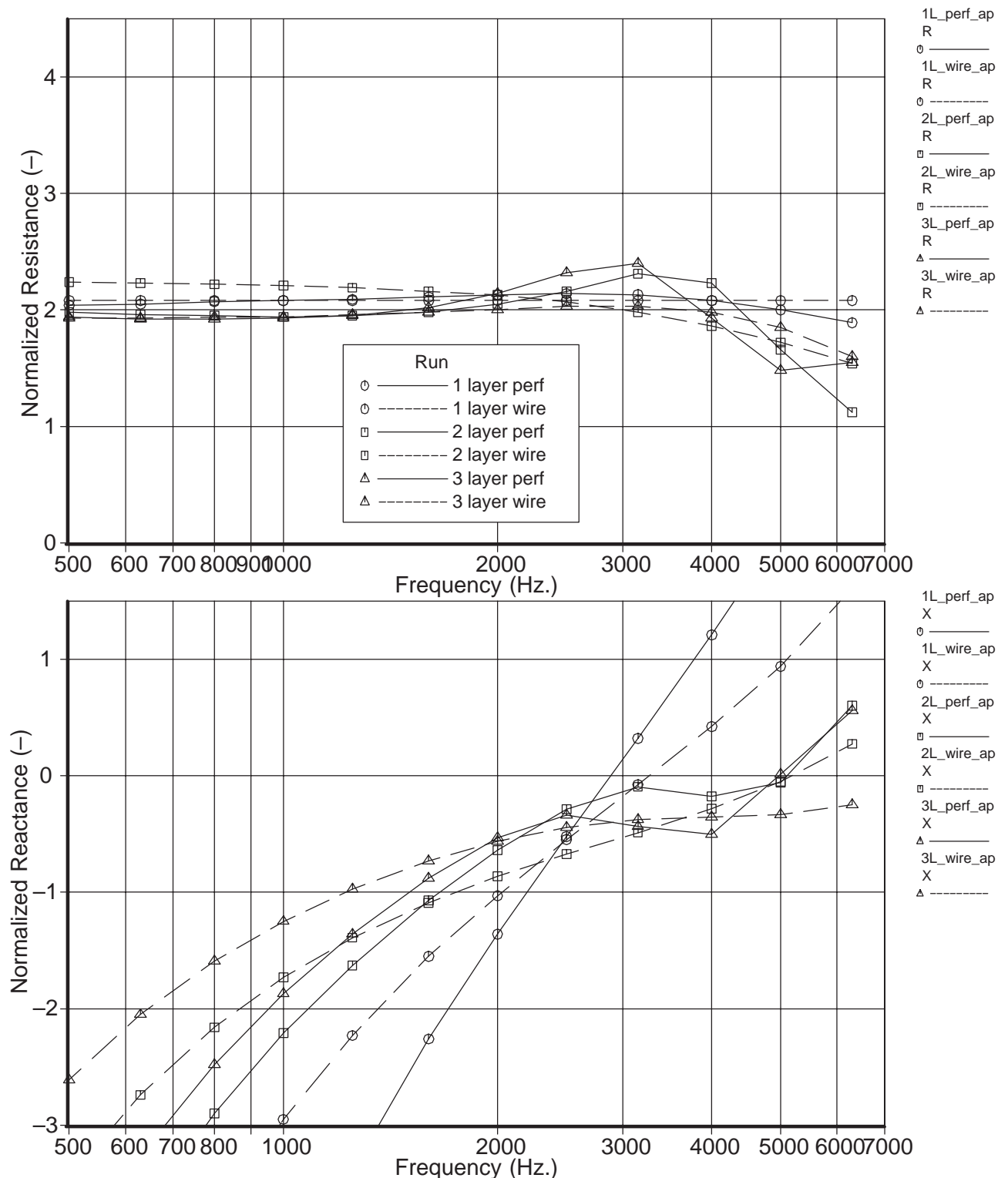
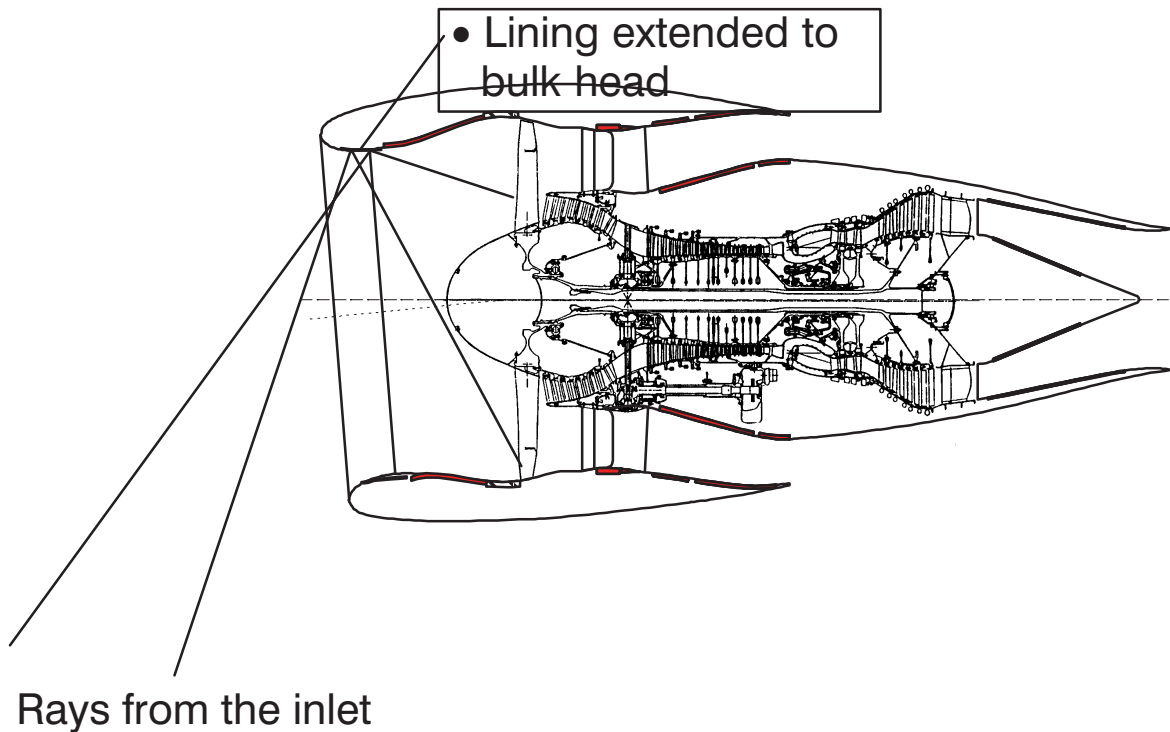


Figure 51: Impedance of the Inlet Liners
(at the approach condition)



Forward region in 1992 baseline sets floor on achievable lining improvement. The attenuations are controlled by the hardwalled areas not the lining panel attenuations. The options are:

- 1) Leave it and get 10–15% maximum improvement**
- 2) Extend treatment forward for 30–80% improvement**
- 3) Change the radiation directivity by scarfing the inlet**

Figure 52: Ray Acoustic Argument for Low Inlet Attenuations

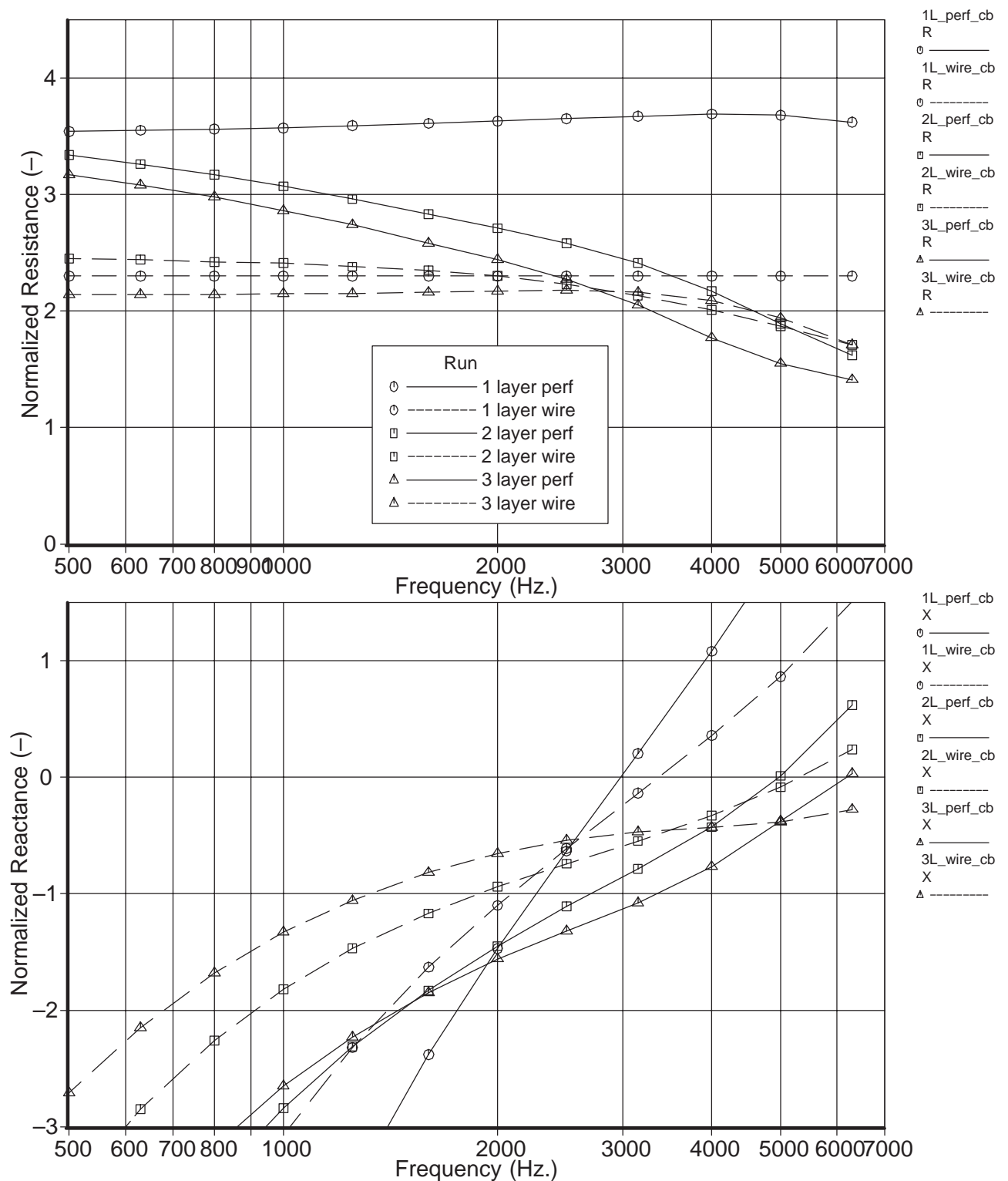
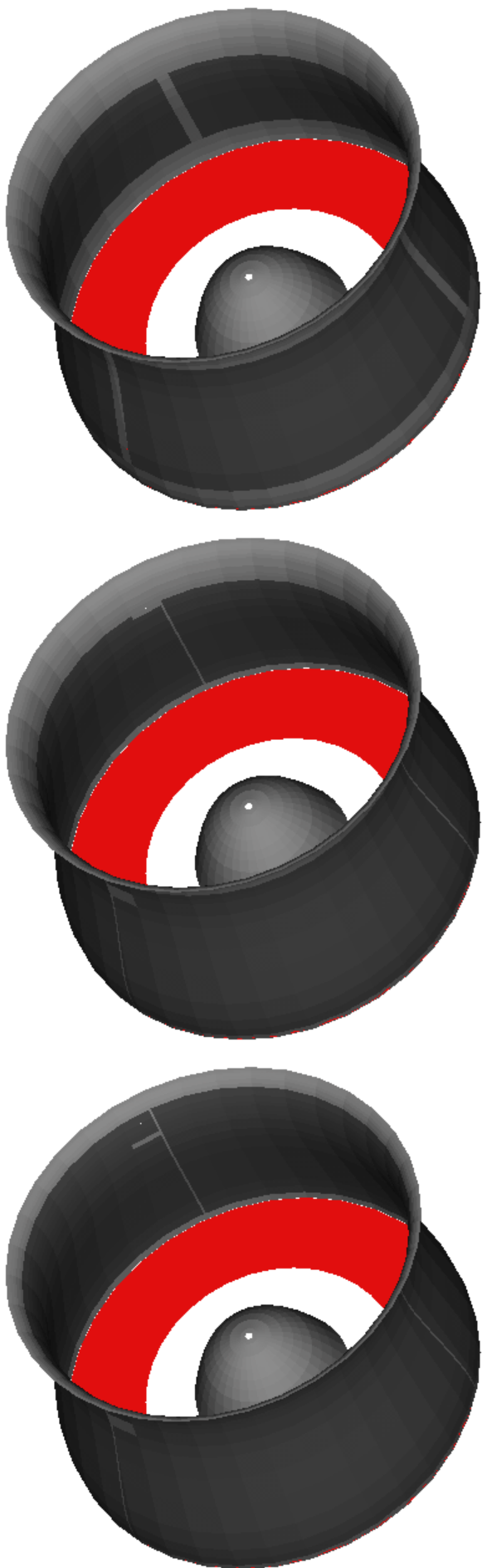


Figure 53: Impedance of the Inlet Liners
(at the cutback condition)

Figure 54: Comparison of Lining Area Technologies

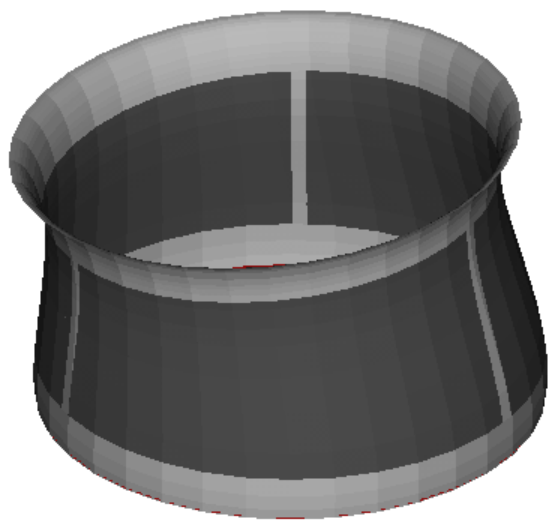


Conventional

AMAX technologies

AMAX & bulkhead lining

Conventional



Scarf

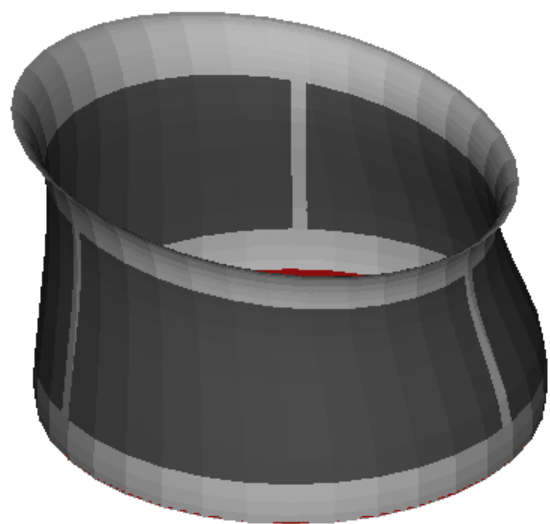


Figure 55: Conventional and Scarf Inlets

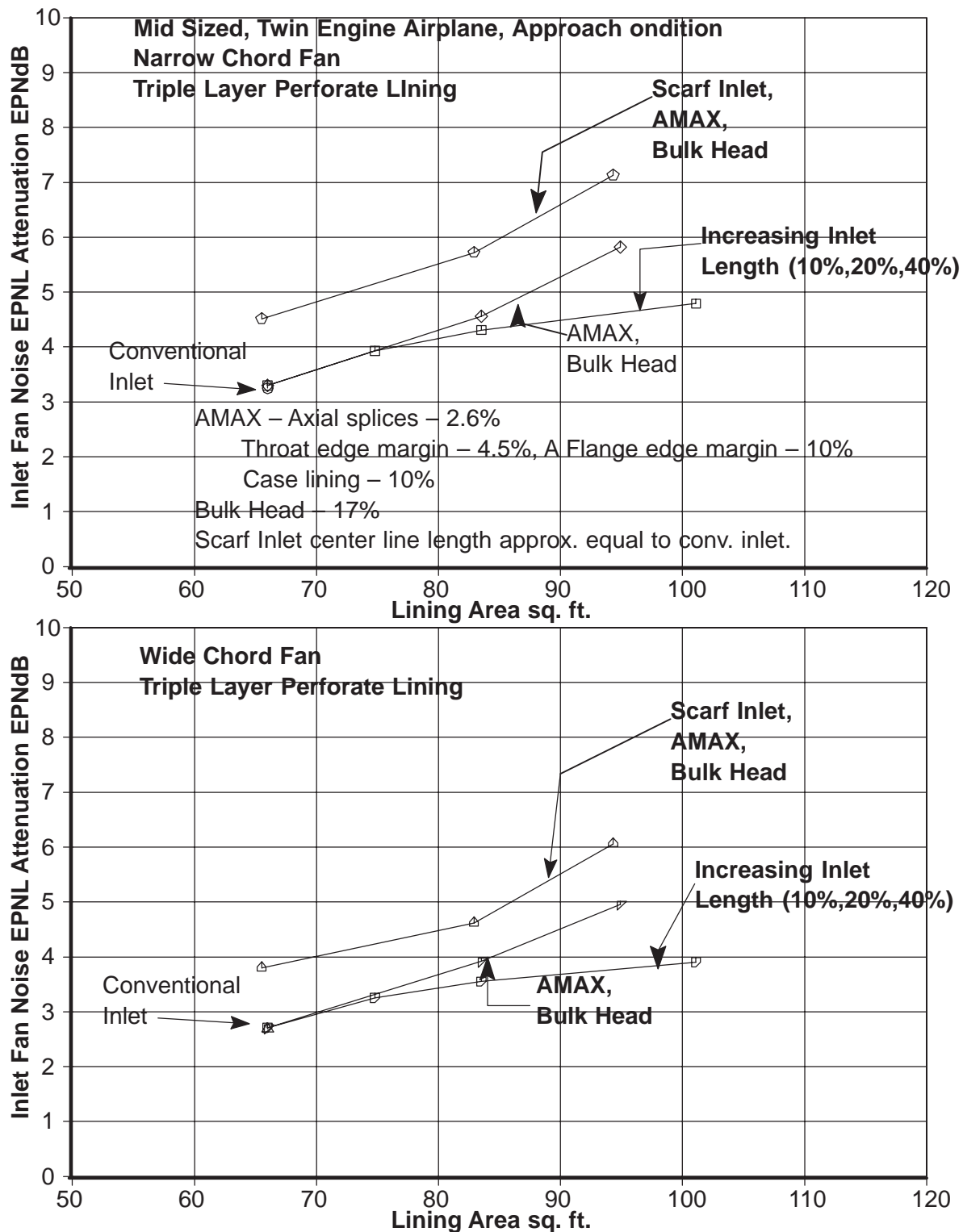


Figure 56: Inlet Lining Area and Configuration Study

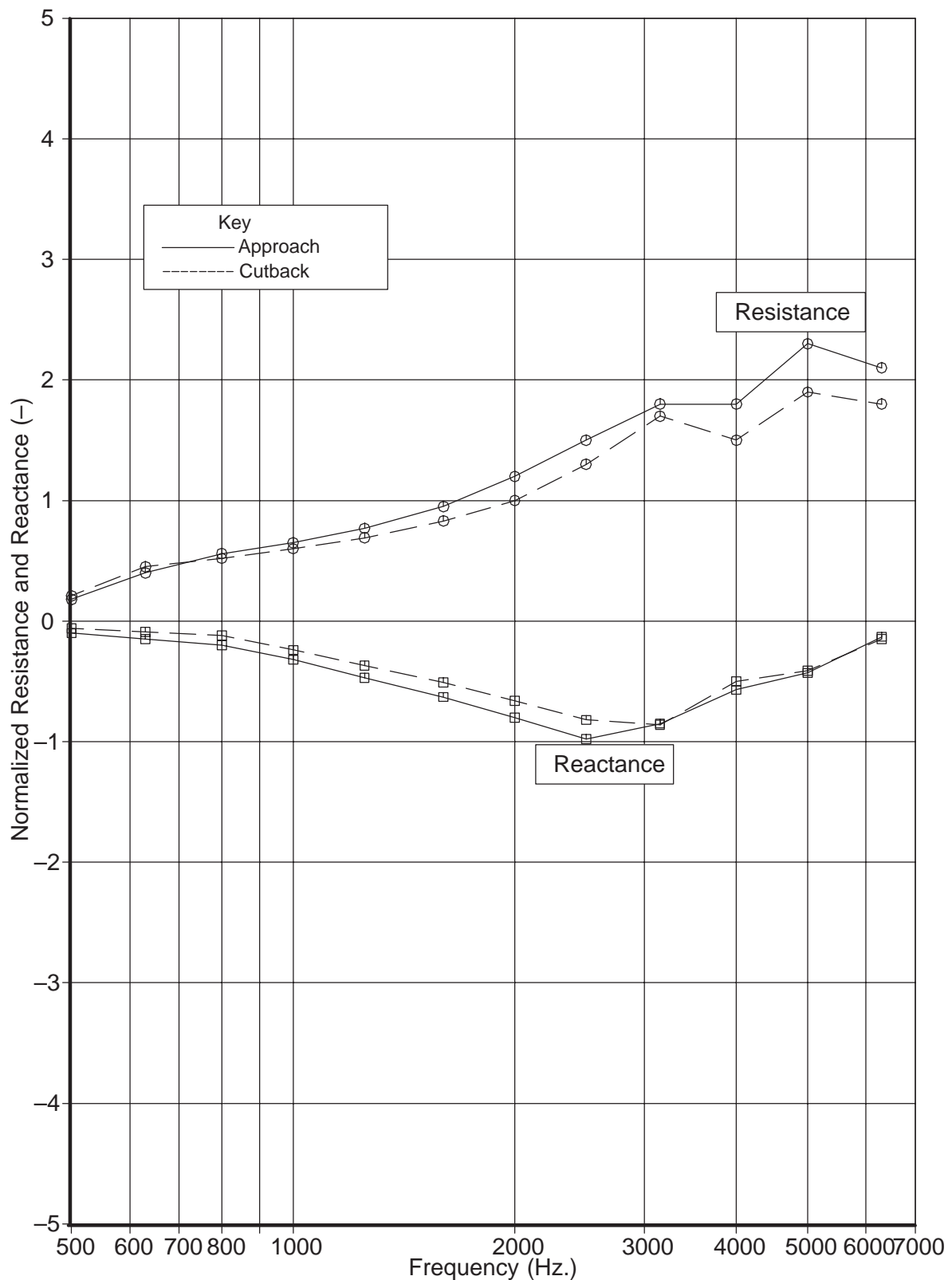


Figure 57: MELO Predicted Ideal Impedances
(for the approach and cutback conditions)

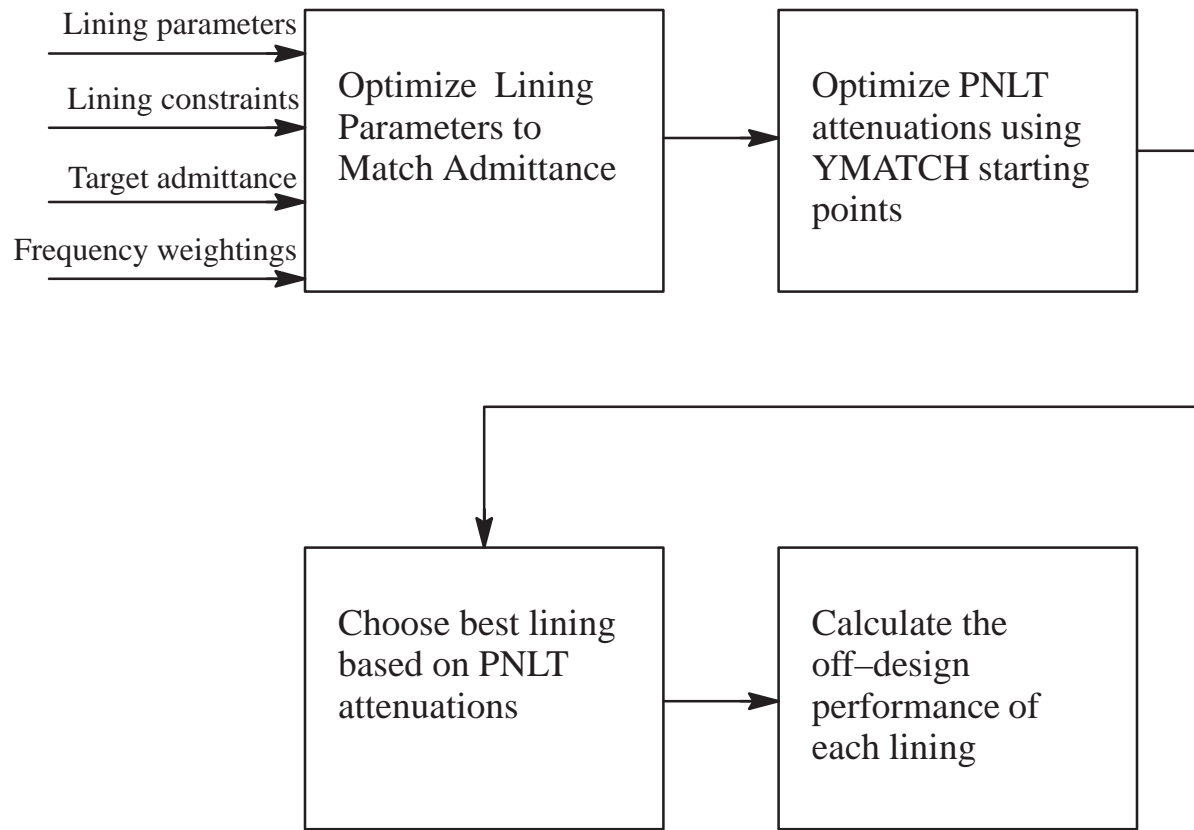


Figure 58: Block Diagram of the Evaluation Process for the Aft Duct

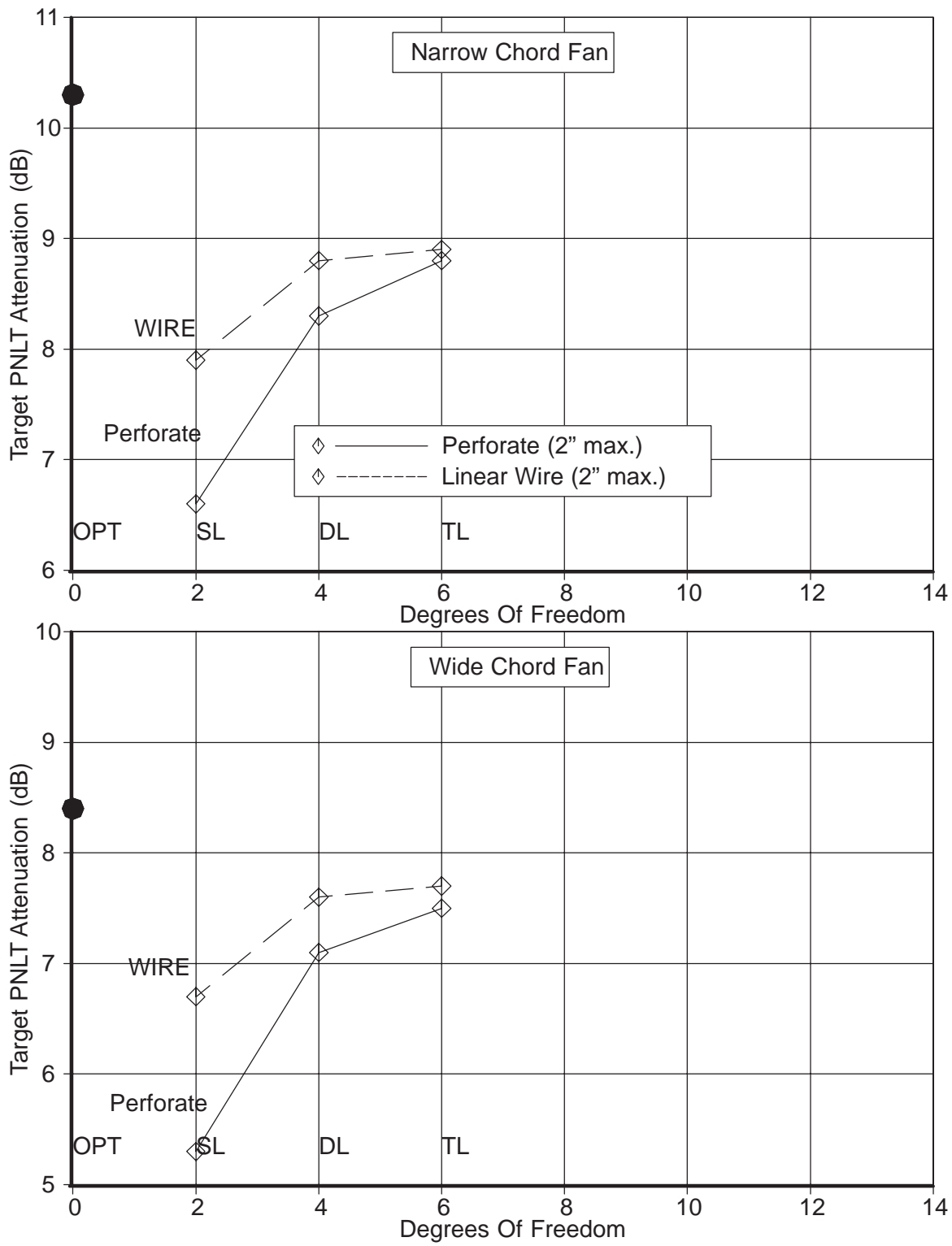


Figure 59: Comparison of Aftfan PNLT Attenuations at Approach

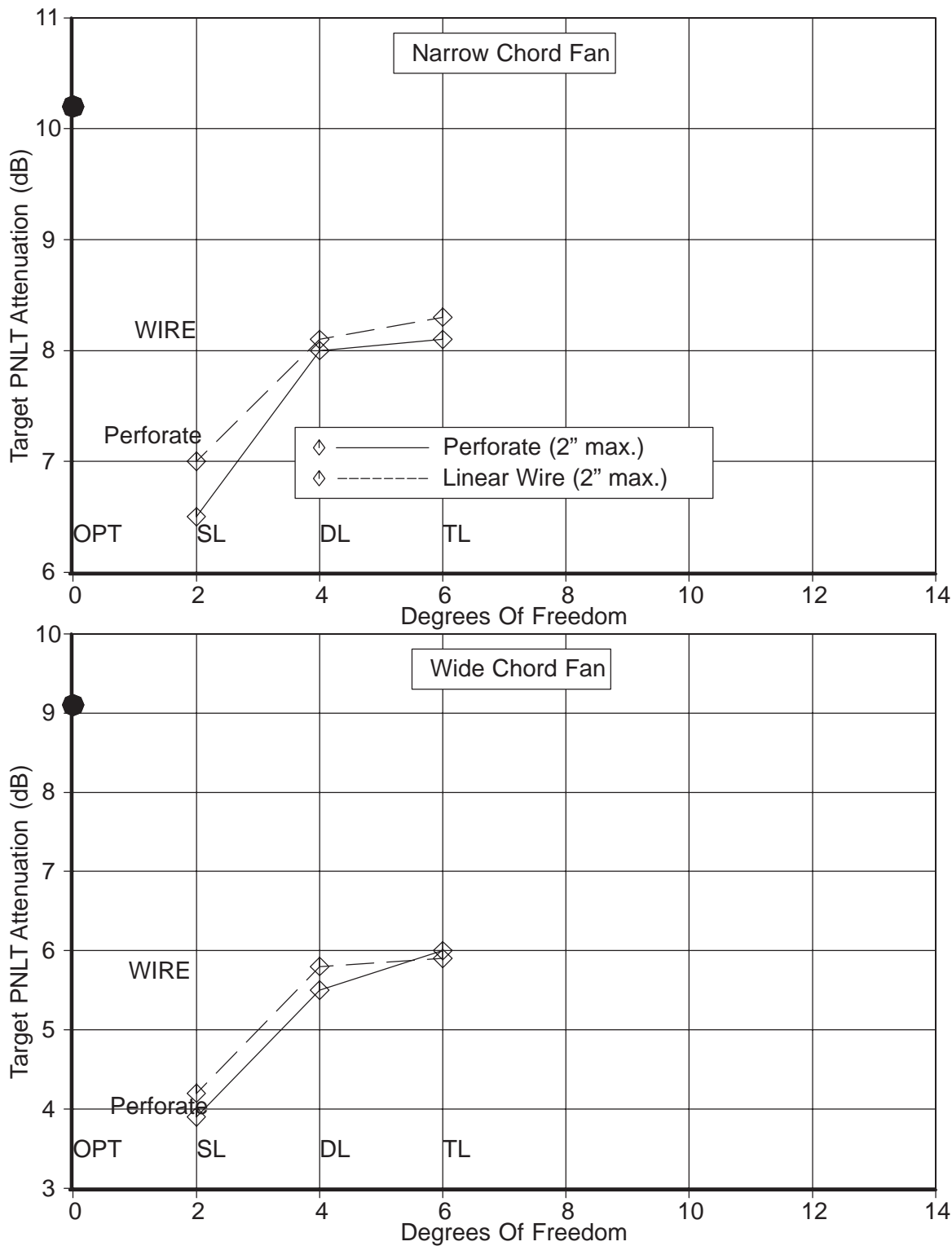


Figure 60: Comparison of Aftfan PNLT Attenuations at Cutback

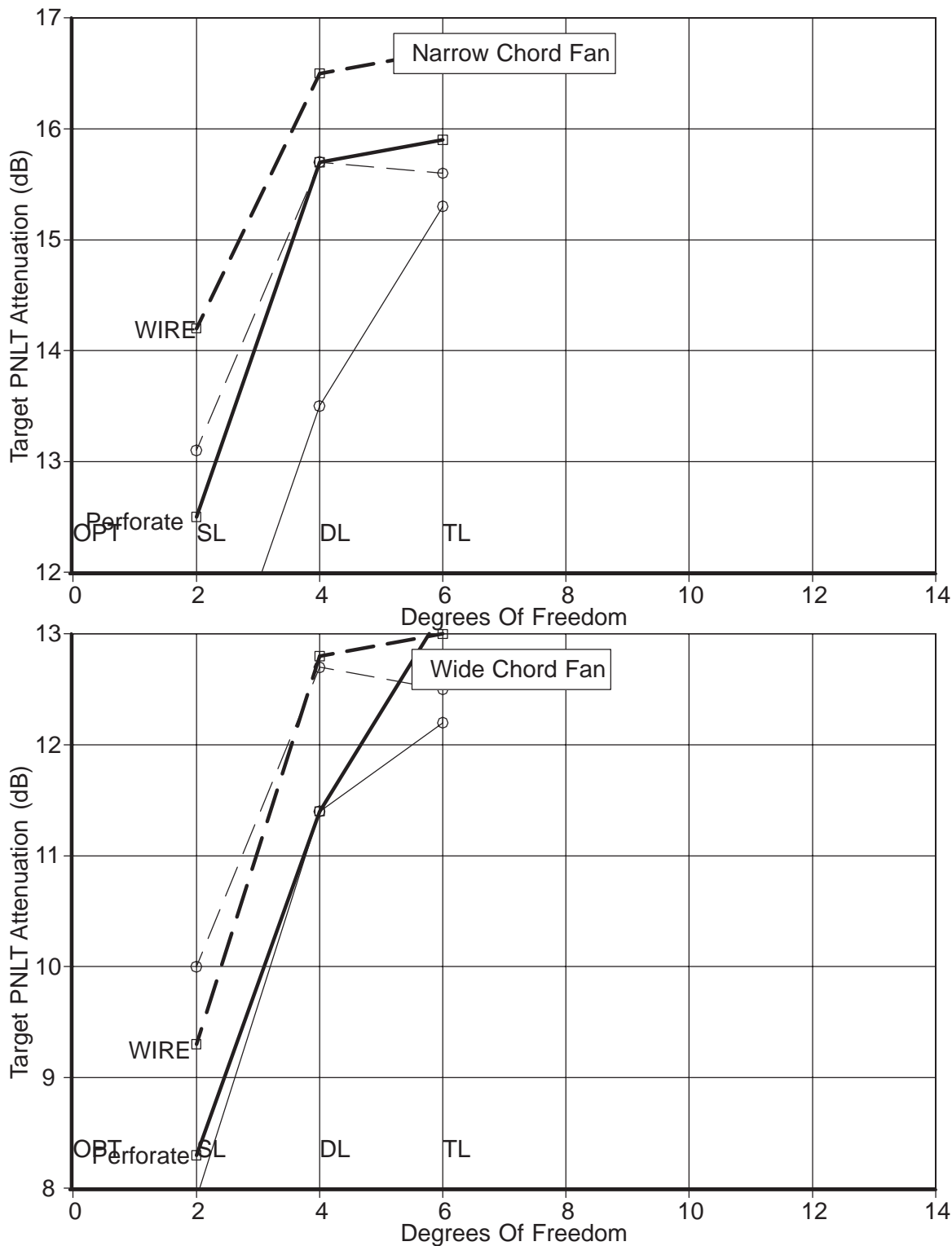


Figure 61: Comparison of Aftfan PNLT Attenuations
(summed approach and cutback conditions)

Appendices:

A1. "Theory And Design Of Helmholtz Resonators Constructed With Slot Perforates"
Allen Hersh and Bruce Walker

A2. "Theory And Design Of Helmholtz Resonators To Suppress Aircraft Engine Noise"
Allen Hersh and Bruce Walker

A3. "Theory And Design Of Helmholtz Resonators Constructed With Micro-Diameter Perforates"
Allen Hersh, Joseph Celano and Bruce Walker

A4. Impedance Models.

The following are the references for the impedance models incorporated into the Boeing lumped element impedance model library as a result of work on this contract :

1. Small diameter cell (parallel cells) from empirical formulae in Tijdeman JSV Vol.39, No.1, 1975, p1–33.
2. Perforated plate face sheet using a discharge coefficient formulation outlined in "Fluid Mechanical Model of the Acoustic Impedance of Small Orifices ", Hersh & Rogers, AIAA 75–495.
3. Bulk absorber model from empirical formulae presented in Voronina, Soviet Phys. Acoust. 29(5) Sept. – Oct. 1983
4. Perforated Plate – Uses code from Appendix 2.

| REPORT DOCUMENTATION PAGE | | | Form Approved OMB No. 0704-0188 |
|--|--|---|------------------------------------|
| <p>Public reporting burden for this collection of information is estimated to average 1 hour per response, including the time for reviewing instructions, searching existing data sources, gathering and maintaining the data needed, and completing and reviewing the collection of information. Send comments regarding this burden estimate or any other aspect of this collection of information, including suggestions for reducing this burden, to Washington Headquarters Services, Directorate for Information Operations and Reports, 1215 Jefferson Davis Highway, Suite 1204, Arlington, VA 22202-4302, and to the Office of Management and Budget, Paperwork Reduction Project (0704-0188), Washington, DC 20503.</p> | | | |
| 1. AGENCY USE ONLY (Leave blank) | 2. REPORT DATE | 3. REPORT TYPE AND DATES COVERED | |
| | February 1999 | Contractor Report | |
| 4. TITLE AND SUBTITLE | | 5. FUNDING NUMBERS | |
| Advanced Turbofan Duct Liner Concepts | | C NAS1-20090 | |
| 6. AUTHOR(S) | | WU 538-03-12-02 | |
| Gerald W. Bielak, John W. Premo, and Alan S. Hersh | | | |
| 7. PERFORMING ORGANIZATION NAME(S) AND ADDRESS(ES) | | 8. PERFORMING ORGANIZATION REPORT NUMBER | |
| Boeing Commercial Airplane Group MS 67-MK; P.O. Box 3707 Seattle, WA 98124-2207 | | Hersh Acoustical Engineering, Inc. 780 Lakefield Rd., Unit G Westlake Village, CA 91361 | |
| 9. SPONSORING/MONITORING AGENCY NAME(S) AND ADDRESS(ES) | | 10. SPONSORING/MONITORING AGENCY REPORT NUMBER | |
| National Aeronautics and Space Administration Langley Research Center Hampton, VA 23681-2199 | | NASA/CR-1999-209002 | |
| 11. SUPPLEMENTARY NOTES | | | |
| Bielak and Premo: Boeing Commercial Airplane Group; Hersh: Hersh Acoustical Engineering, Inc. Langley Technical Monitor: Tony L. Parrott | | | |
| 12a. DISTRIBUTION/AVAILABILITY STATEMENT | | 12b. DISTRIBUTION CODE | |
| Unclassified-Unlimited Subject Category 71 Availability: NASA CASI (301) 621-0390 | | | |
| 13. ABSTRACT (Maximum 200 words) | | | |
| <p>The Advanced Subsonic Technology Noise Reduction Program goal is to reduce aircraft noise by 10 EPNdB by the year 2000, relative to 1992 technology. The improvement goal for nacelle attenuation is 25% relative to 1992 technology by 1997 and 50% by 2000. The Advanced Turbofan Duct Liner Concepts Task work by Boeing presented in this document was in support of these goals. The basis for the technical approach was a Boeing study conducted in 1993-94 under NASA/FAA contract NAS1-19349, Task 6, investigating broadband acoustic liner concepts. As a result of this work, it was recommended that linear double layer, linear and perforate triple layer, parallel element, and bulk absorber liners be further investigated to improve nacelle attenuations. NASA LaRC also suggested that "adaptive" liner concepts that would allow "in-situ" acoustic impedance control also be considered. As a result, bias flow and high-temperature liner concepts were also added to the investigation. The major conclusion from the above studies is that improvements in nacelle liner average acoustic impedance characteristics alone will not result in 25% increased nacelle noise reduction relative to 1992 technology. Nacelle design advancements currently being developed by Boeing are expected to add 20-40% more acoustic lining to hardwall regions in current inlets, which is predicted to result in an additional 40-80% attenuation improvement. Similar advancements are expected to allow 10-30% more acoustic lining in current fan ducts with 10-30% more attenuation expected. In addition, Boeing is currently developing a scarf inlet concept which is expected to give an additional 40-80% attenuation improvement for equivalent lining areas.</p> | | | |
| 14. SUBJECT TERMS | | 15. NUMBER OF PAGES | |
| Noise; Duct linings; Turbofan engines | | 235 | |
| | | 16. PRICE CODE | |
| | | A11 | |
| 17. SECURITY CLASSIFICATION OF REPORT | 18. SECURITY CLASSIFICATION OF THIS PAGE | 19. SECURITY CLASSIFICATION OF ABSTRACT | 20. LIMITATION OF ABSTRACT |
| Unclassified | Unclassified | Unclassified | UL |